A GEOLOGICAL MODEL OF THE HIBERNIA FORMATION IN THE VICINITY OF THE TERRA NOVA AND HEBRON/BEN NEVIS OIL FIELDS, JEANNE D'ARC BASIN, OFFSHORE NEWFOUNDLAND

GRANT DAVID LETHBRIDGE

A GEOLOGICAL MODEL OF THE HIBERNIA FORMATION IN THE VICINITY OF THE TERRA NOVA AND HEBRON/BEN NEVIS OIL FIELDS, JEANNE D'ARC BASIN, OFFSHORE NEWFOUNDLAND

by

© Grant David Lethbridge, B.Sc. (Honours)

A thesis submitted to the School of Graduate Studies in partial fulfillment of the requirements for the degree of
Masters of Science

Department of Earth Sciences
Memorial University of Newfoundland
January 2012

St. John's Newfoundland and Labrador

ABSTRACT

The Hibernia Formation is a stacked siliciclastic sequence of interbedded sandstone and shale up to one kilometer thick that was deposited across the Jeanne d'Arc Basin. It represents coarse-grained progradation into the Jeanne d'Arc Basin during the second half of east-west oriented extension of the North Atlantic Rifting phase. Published literature regarding deposition of the Hibernia Formation has been focused on the Hibernia oil field, located along the western basin margin, or as broad, generalized regional studies across the entire Jeanne d'Arc Basin. No publications exist regarding the depositional environment of the Hibernia Formation along the eastern basin margin in the vicinity of the Terra Nova, Hebron, and Ben Nevis oil fields. This thesis presents the available data in the region surrounding the Terra Nova oil field and aims to refine the depositional model of the Hibernia Formation.

Three dimensional seismic data and fifty-one wells compose the raw data used in this study. Three wells have recovered core, totaling 150 meters over three zones, however these wells are all located in the northern half of the study area. Together the geophysical and geological data were combined to vertically subdivide the Hibernia Formation into ten depositional intervals that can be correlated across the study area. These depositional units record variations in rate of sedimentation and depositional direction as well as fluctuations between progradational and retrogradational trends. The Hibernia Formation is finally summarized as a series of block diagrams illustrating changes between successive units and overall evolution of the Hibernia Formation.

ACKNOWLEDGEMENTS

I would like to thank Petro-Canada and the National Science and Engineering Research Council (NSERC) for co-funding this Masters of Science thesis through an Industrial Post-Secondary research grant. Thanks to Petro-Canada for providing a workspace in the St. John's office and access to the geophysical and geological data. Without these tools and funds, this thesis would not have been possible. I would also like to extend my gratitude to Geoff Minielly and Irene Kelly for setting up this project and supervising me through this thesis while at Petro-Canada.

I would like to extend many thanks to Chuck Hurich and Rudi Meyers for supervising me through this thesis and having the patience to read through my thesis multiple times. I truly appreciate it. Thanks for answering my numerous emails while I was in Calgary and helping me put the finishing touches on this thesis. I know this took longer than expected but alas it has finally been compiled into a document.

Thanks to Dave Mills for keeping my sanity in check while I interpreted core data at C-NLOPB's core lab. Our many conversations definitely made it easier to get through the core descriptions and many laughs were had.

Finally I would like to say thanks to my wife, Michelle, for providing constant support and motivation to get through the writing of my thesis. Without her constant reminders to work on it I'm sure it would still be a pile of papers and maps on my desk waiting to be put into a legible document. Thank you!

Thanks to everyone else who has helped or encouraged me along the way, I am forever in debt to you all.

TABLE OF CONTENTS

Title Page i
Abstract ii
Acknowledgements iii
List of Figures vi
List of Tables xviii

Chapter 1: Introduction
1.1 Scope and Purpose 1
1.2 Location 2
1.3 Data Availability 5
1.4 Summary 7

Chapter 2: Methodology
2.1 Scope and Purpose 8
2.2 Three-Dimensional Seismic Dataset 10
2.3 Core Data 15
2.4 Petrophysical Well Data 16

Chapter 3: Structure and Stratigraphy
3.1 Introduction 26
3.2 Tectonic Evolution 27
3.2.1 Present-day Tectonic Setting 27
3.2.2 Tectonic and Stratigraphic History 27
3.2.2.1 Tethys Rifting Phase 28
3.2.2.2 North Atlantic Rifting Phase 31
3.2.2.3 Labrador Rifting Phase 32
3.3 Fault Classification 34
3.3.1 Basement Involved Faults 35
3.3.2 Cretaceous Basin Bounding Faults 36
3.3.3 Major Sedimentary Faults 37
3.3.4 Secondary Sedimentary Faults 38
3.4 Distinction of Faults within the Study Area 39
3.5 Summary 46

Chapter 4: Three-Dimensional Seismic Dataset
4.1 Scope and Purpose 48
4.2 Seismic Marker Definition 49
4.2.1 Base of Hibernia Formation 49
4.2.2 Mid-Hibernia Formation 63
4.2.3 Top of Hibernia Formation 76
4.3 Unit Definition and Description 88
4.3.1 Unit Definition 88

4.3.2 Unit Description 91
4.4 Conclusions 94

Chapter 5: Core Descriptions
5.1 Scope and Purpose 95
5.2 Amoco et al. West Bonne Bay (C-23) 97
5.2.1 Core Description 98
5.2.2 Depositional Environment 99
5.3 Mobil et al. Hebron (I-13) 108
5.3.1 Core Description 109
5.3.2 Depositional Environment 119
5.4 Chevron et al. Hebron (M-04) 121
5.4.1 Core Description 122
5.4.2 Depositional Environment 134
5.5 Conclusion 138

Chapter 6: Petrophysical Log Data
6.1 Scope and Purpose 141
6.2 Unit Definition 142
6.2.1 Lower Hibernia Member 142
6.2.1.1 Lower Hibernia Member sub-unit 306 146
6.2.1.2 Lower Hibernia Member sub-unit 308 150
6.2.1.3 Lower Hibernia Member sub-unit 310 154
6.2.1.4 Lower Hibernia Member sub-unit 312 158
6.2.1.5 Lower Hibernia Member sub-unit 320 162
6.2.2 Upper Hibernia Member 166
6.2.2.1 Upper Hibernia Member sub-unit 322 170
6.2.2.2 Upper Hibernia Member sub-unit 324 174
6.2.2.3 Upper Hibernia Member sub-unit 326 178
6.2.2.4 Upper Hibernia Member sub-unit 328 182
6.2.2.5 Upper Hibernia Member sub-unit 330 186
6.3 Discussion 190
6.4 Conclusion 199

Chapter 7: Concluding Summary
7.1 Geological Model 200
7.2 Future Work 209

References 211

Appendices
Appendix A: Detailed Core Log and Core Photos - Amoco et al. West Bonne Bay C-23 Well A-1
Appendix B: Detailed Core Log and Core Photos - Mobil et al. Hebron I-13 Well B-1
Appendix C: Detailed Core Log and Core Photos - Chevron et al. Hebron M-04 Well C-1

LIST OF FIGURES

1.1 Map of Atlantic Canada illustrating the location of the Mesozoic and Paleozoic Basins. Note the black outline indicating the approximate location of Figure 1.2 over the Jeanne d'Arc Basin. Modified after C-NLOPB (2005), Geological Survey of Canada and Enachescu (2004). 3

1.2 Structural features of the Jeanne d'Arc Basin including the locations of any significant petroleum discoveries. Modified after C-NLOPB (2005), Grant et al. (1986) and Enachescu (1988). 4

1.3 Map highlighting data availability for the study area. Seismic boundaries are indicated by the green polygon. Location of the fifty-one (51) exploration, delineation and development wells are shown in black, with a legend showing the well names on the right. The three wells that have Hibernia Formation core are circled in red. Location of the study area is highlighted in Figure 1.2. 6

2.1 Map highlighting data availability for the study area. Seismic boundaries are indicated by the green polygon. Location of the fifty-one (51) exploration, delineation and development wells are shown in black, with a legend showing the well names on the right. The three wells that have Hibernia Formation core are circled in red. Location of the study area is highlighted in Figure 1.2. 9

2.2 Seismic wavelet extractions over the Hibernia Formation at the King's Cove A-26 well (top) and the Ben Nevis I-45 well (bottom). The seismic wavelet is in the left panel; note resemblance to the Ricker wavelet of Figure 2.3. The top-right panel is the frequency spectrum for the wavelet with the amplitude in percentage. Note that peak frequency at the King's Cove A-26 well is twenty-two hertz and maximum frequency is approximately sixty hertz, while peak frequency at the Ben Nevis I-45 well is eighteen hertz and maximum frequency is approximately fifty hertz. The bottom-right panel is the phase spectrum for the wavelet; note how both wells illustrate the near zero-phase character of the seismic wavelet (within thirty degrees). 12

2.3 Ricker wavelet with dominant frequency of twenty-two hertz and onset time of twenty milliseconds. 13

2.4 Example of the details recorded for the core descriptions. Gamma ray log is taken from petrophysical well data. 15

2.5 Well header used to label petrophysical logs. Gamma ray log is filled with lithology interpretation where yellow is sandstone, orange is siltstone, brown is shale, and blue is carbonate or carbonate-cemented interval. 17

2.6 Representative well (Terra Nova L-98_5) indicating the ten sub-units that comprise the Hibernia Formation. 20

2.7 Generalized stratigraphic panel of the Hibernia Formation within the study area based on the wells used in this thesis. Sandstone is yellow and shale is brown. 21

2.8 True vertical depth below sea-level map of the top of the Hibernia Formation. Contour interval is 100 meters with every 500 meters in bold lines. Locations of the five main faults are highlighted with blue dotted lines. 25

3.1 Tectono-stratigraphic chart for the Jeanne d'Arc Basin illustrating the timing of the tectonic stages, significant orogenic events, and the dominant subsidence or deformation styles. Modified after C-NLOPB (2005), Sinclair (1993) and Sinclair *et al.* (2005). 29

3.2 Simplified geological cross-section of basement involved faults. Take note of their relation to the basin-bounding fault. After Enachescu (1987). 36

3.3 Simplified geological cross-section of a Cretaceous basin-bounding fault (Voyager Fault System). Also shown in the figure is a major sedimentary fault. Note how the major sedimentary fault soles out above the basement block, while the Voyager Fault System pierces the basement rock and shows significant growth in the Cretaceous sediments. After Enachescu (1987). 38

3.4 Simplified geological cross-section illustrating the relationship of minor sedimentary faults to a major sedimentary fault (MSF). Note the antithetic and synthetic geometry of the minor faults and how the major fault soles along a salt surface. After Enachescu (1987). 39

3.5 True vertical depth below sea level map of the top of the Hibernia Formation. The various oil and gas fields that the study area covers area labeled in the white boxes. The Trans Basin Fault Zone is also labeled as the trend of northwest-southeast trending faults that mark the area north of the Terra Nova oil field. The Trinity Fault family is the first set of faults in the Trans Basin Fault Zone that marks the northern boundary of the Terra Nova oil field. The Voyager Fault is in the southeastern corner of the study area and essentially marks the southeastern depositional or erosional limit of the Hibernia Formation. 42

3.6 North-south seismic section (crossline 942) from the eastern area of the study area. Location is shown on inset map of Top of Hibernia Formation. Top figure is the uninterpreted seismic line. Bottom figure has the faults interpreted in yellow. The base Cenomanian Unconformity is in brown; note how faults generally do not penetrate this horizon. The Top, Mid- and Base Hibernia Formation are shown in orange, purple, and green, respectively. Note the growth across the Voyager Fault System (Cretaceous basin-bounding fault) of the Hibernia Formation. Three major sedimentary faults are also highlighted in the Jeanne d'Arc Basin as well as one over the Central Ridge Complex. 43

3.7 West-east seismic section (inline 790) from the northern area of the study area. Location is shown on inset map of Top of Hibernia Formation. Top figure is the uninterpreted seismic line. Bottom figure has the faults interpreted in yellow with the distinction between major and minor sedimentary faults. The base Cenomanian Unconformity is in brown; note how faults generally do not penetrate this horizon. The Top, Mid- and Base Hibernia Formation are shown in orange, purple, and green, respectively. 44

3.8 North-south seismic section (crossline 462) from the western area of the study area. Location is shown on inset map of Top of Hibernia Formation. Top figure is the uninterpreted seismic line. Bottom figure has the faults interpreted in yellow. The base Cenomanian Unconformity is in brown; note how faults generally do not penetrate this horizon. The Top, Mid- and Base Hibernia Formation are shown in orange, purple, and green, respectively. The minor sedimentary faults presented here are due to syn-sedimentary accommodation and later Labrador Rift extension. Notice the significant growth to the north, towards the basin depocentre. 45

4.1 Petrophysical log at the Terra Nova G-90_5Z well over the depth interval: 2887-3007 meters TVDSS. Displayed well boundary (GDL_300) marks the base of the Hibernia Formation. It is characterized as the subtle, yet often sharp, increase in velocity with depth creating a moderate seismic peak signature. The velocity change also correlates well with a sharp change in the Uranium spectral gamma ray signature between basal shales of the Hibernia Formation and underlying Fortune Bay Formation shales. 50

4.2 True vertical depth below sea-level map of the base of the Hibernia Formation. Contour interval is 100 meters with every 500 meters in bold lines. Note the easterly dip in the western and southern areas with the transition to a northerly dip within the Trans Basin Fault Zone. 53

4.3 Seismic coherency map of the base of the Hibernia Formation. The scale bar is opposite to natural instinct, in which correlative events are displayed as lows and non-correlative events are displayed as highs. Overall, the base of the Hibernia Formation appears to be coherent near Hebron and progressively less coherent in the south. The thin zones of incoherency that mimic the overlain fault trends most likely represent the fault zone, where an abundance of seismically invisible faults are likely to exist. 54

4.4 Reflection strength map of the base of the Hibernia Formation. Note the distinct increase in reflection strength to the north. Several zones of high reflection strength exist in the southern region and are likely due to local changes (ie. increased sandstone thickness above the basal boundary) rather than the larger scale northern transition. 55

4.5 Instantaneous frequency map of the base of the Hibernia Formation. The Trinity Fault transition zone further illustrates the seismic character change to the north. The southern area is dominated by higher frequencies and is markedly different than the northern, lower frequencies. The overall decrease to the north, however, may be due to the attenuation with depth of the seismic frequency spectrum. 56

4.6 Petrophysical signature of the base Hibernia Formation boundary (represented as well pick GDL_300) at the King's Cove A-26, Terra Nova K-17 and Terra Nova K-18 wells. Locations of these wells can be seen in Figures 4.2 – 4.5. Deposition of sandstone and siltstone beds in the upper Fortune Bay Formation provide a sharp contrast with the base Hibernia Formation shales and provide a good source for strong reflections. Absence of these beds at the Terra Nova K-17 well explains the low reflection strength visible in the synthetic seismogram. Gamma ray log is filled with CanStrat® lithology interpretation where yellow=sandstone, orange=siltstone, brown=shale, and blue=carbonates or carbonate-cemented intervals. 60

4.7 Petrophysical signature of the base Hibernia Formation boundary (represented as well pick GDL_300) at the Terra Nova F-88_3, Terra Nova G-90_5Z and Terra Nova C-69_3 wells. Locations of these wells can be seen in Figures 4.2 - 4.5. These three wells highlight the consistency of the base Hibernia Formation. The base Hibernia Formation boundary is indicated by the minor decrease-upwards in the gamma ray as well as the increase-upwards in sonic. There is no significant change, in general, in the density log, however there is occasional increase in density with depth. Gamma ray log is filled with CanStrat® lithology interpretation where yellow=sandstone, orange=siltstone, brown=shale, and blue=carbonates or carbonate-cemented intervals. 61

4.8 Petrophysical signature of the base Hibernia Formation boundary (represented as well pick GDL_300) at the Hebron I-13, West Ben Nevis B-75 and West Bonne Bay C-23 wells. Locations of these wells can be seen in Figures 4.2 – 4.5. The distal location of these three wells in comparison to the previous six wells is shown through the higher deposition of shale at the base of the Hibernia Formation as well as the lack of thin sandstone and siltstone beds in the upper Fortune Bay Formation. The nature of the base Hibernia Formation boundary is not clearly identified in the petrophysical logs. Lower frequency seen in seismic attribute mapping is likely due to the thick shale above and below the boundary, creating a thick seismic response interval. The source of high reflection strength is not obvious through the study of the petrophysical parameters and may be due to visible seismic velocity contrasts being clearly imaged through absence of thin bed "noise". Gamma ray log is filled with CanStrat® lithology interpretation where yellow=sandstone, orange=siltstone, brown=shale, and blue=carbonates or carbonate-cemented intervals. 62

4.9 Petrophysical log at the Terra Nova G-90_5Z well over the depth interval: 2575-2695 meters TVDSS. The displayed well pick (GDL_320) marks the mid-Hibernia Formation. It is characterized by the high bulk density and increase in velocity with depth creating a moderate seismic peak signature. It is also constrained as the flooding surface that can be seen in the gamma ray log. 64

4.10 True vertical depth below sea-level map of the mid-Hibernia Formation. Contour interval is 100 meters with every 500 meters in bold lines. Note the easterly dip in the western and southern areas with the transition to a northerly dip within the Trans Basin Fault Zone. 66

4.11 Seismic coherency map of the mid-Hibernia Formation. The scale bar is opposite to natural instinct, in which correlative events are displayed as lows and non-correlative events are displayed as highs. Overall, the mid-Hibernia Formation appears to be rather uniform and no distinct zoning is distinguishable, except for the very correlative region in the northeast. The thin zones of incoherency that mimic the overlain fault trends most likely represent the fault zone, where an abundance of seismically invisible faults exist. 67

4.12 Reflection strength map of the mid-Hibernia Formation. Note the distinct increase in reflection strength in the northeast region, as well as the moderate reflection strength region in the west. Overall the mid-Hibernia Formation is of relatively weak reflection strength, except for several small, localized zones of high reflection strength. The dashed orange lines on the map highlight the two broader zones. 68

4.13 Instantaneous frequency map of the mid-Hibernia Formation. The southern region is dominated by the highest frequencies and the region in the northwest has moderately high frequencies as well. There is a zone of moderate frequencies in the central west region and a zone of low frequencies in the northeast region. The dashed orange lines on the map highlight these zones. 69

4.14 Petrophysical signature of the mid-Hibernia Formation boundary (represented as well pick GDL_320) at the King's Cove A-26, Terra Nova K-17 and Terra Nova K-18 wells. Locations of these wells can be seen in Figures 4.10 – 4.13. Abundance of sandstone and shale interbeds surrounding the mid-Hibernia Formation flooding surface is likely the source of low reflection strength at the King's Cove A-26 and Terra Nova K-17 wells. Reduced presence of sandstone beds above the flooding surface at Terra Nova K-18 provides greater contrast above and below the boundary to produce a higher reflection strength. Gamma ray log is filled with CanStrat® lithology interpretation where yellow=sandstone, orange=siltstone, brown=shale, and blue=carbonates or carbonate-cemented intervals. 73

4.15 Petrophysical signature of the mid-Hibernia Formation boundary (represented as well pick GDL_320) at the Terra Nova F-88_3, Terra Nova F-100_2 and Terra Nova C-69_3 wells. Locations of these wells can be seen in Figures 4.10 – 4.13. All three wells have similar sandstone and shale content above and below the mid-Hibernia Formation boundary resulting in low to moderate reflection strength. Gamma ray log is filled with CanStrat® lithology interpretation where yellow=sandstone, orange=siltstone, brown=shale, and blue=carbonates or carbonate-cemented intervals. 74

4.16 Petrophysical signature of the mid-Hibernia Formation boundary (represented as well pick GDL_320) at the Hebron I-13, West Ben Nevis B-75 and West Bonne Bay C-23 wells. Locations of these wells can be seen in Figures 4.10 – 4.13. Low reflection strength at Hebron I-13 is shown by the abundance sandstone above the boundary providing minimal contrast with the underlying sandstone. Conversely, the high shale content above the boundary provides good contrast with the underlying thick sandstone at West Ben Nevis B-75 and West Bonne Bay C-23 to produce a strong, near single boundary response. Gamma ray log is filled with CanStrat® lithology interpretation where yellow=sandstone, orange=siltstone, brown=shale, and blue=carbonates or carbonate-cemented intervals. 75

4.17 Petrophysical log at the Terra Nova G-90_5Z well over the depth interval: 2329-2449 meters TVDSS. Displayed well pick (GDL_330) marks the top of the Hibernia Formation. It is characterized by changes in the sonic and bulk density logs that create a strong seismic trough signature. It is also characterized by a distinct resistivity decrease from the 'B' Marker limestone (low porosity) to the Hibernia Formation sandstones (high porosity). 77

4.18 True vertical depth below sea-level map of the top of the Hibernia Formation. Contour interval is 100 meters with every 500 meters in bold lines. Note the easterly dip in the western and southern areas with the transition to a northerly dip within the Trans Basin Fault Zone. 79

4.19 Seismic coherency map of the top of the Hibernia Formation. The scale bar is opposite to natural instinct, in which correlative events are displayed as lows and non-correlative events are displayed as highs. Overall, the top of the Hibernia Formation appears to be rather uniform and very coherent with no distinct zoning. The thin zones of incoherency that mimic the overlain fault trends most likely represent the fault zone, where an abundance of seismically invisible faults exist. 80

4.20 Reflection strength map of the top of the Hibernia Formation. Note the distinct increase in reflection strength to the north. Overall the top of the Hibernia Formation has a very high reflection strength in the north and has a moderate reflection strength along the southern region. The black lines on the map highlight the low reflection strength zone. 81

4.21 Instantaneous frequency map of the top of the Hibernia Formation. The southern region is dominated by the highest frequencies. Two regions of low frequencies are found in the northwest and northeast. The black lines on the map highlight these zones. 82

4.22 Petrophysical signature of the top Hibernia Formation boundary (represented as well pick GDL_330) at the King's Cove A-26, Terra Nova K-17 and Terra Nova K-18 wells. Locations of these wells can be seen in Figures 4.18 – 4.21. These three wells highlight consistency of the top of the Hibernia Formation. Thick carbonates of the 'B' Marker limestone overlying thick sandstones of the Upper Hibernia Formation provide excellent contrast and produce a strong seismic reflection. The north-trending corridor of low reflection strength in the west is not clearly evident from the petrophysical logs. Gamma ray log is filled with CanStrat® lithology interpretation where yellow=sandstone, orange=siltstone, brown=shale, and blue=carbonates or carbonate-cemented intervals. 85

4.23 Petrophysical signature of the top Hibernia Formation boundary (represented as well pick GDL_330) at the Terra Nova F-88_3, Terra Nova G-90_5Z and Terra Nova C-69_3 wells. Locations of these wells can be seen in Figures 4.18 – 4.21. Consistency of the top of the Hibernia Formation is further illustrated through these wells. Deposition of fine-grained sediments is seen at the Terra Nova G-90_5Z and Terra Nova C-69_3 wells via the presence of thin shale beds and coarsening-upwards gamma ray signatures, respectively. The high reflection strength observed in seismic attribute mapping is explained through the sharp contact. Gamma ray log is filled with CanStrat® lithology interpretation where yellow=sandstone, orange=siltstone, brown=shale, and blue=carbonates or carbonate-cemented intervals. 86

4.24 Petrophysical signature of the top Hibernia Formation boundary (represented as well pick GDL_330) at the Hebron I-13, West Ben Nevis B-75 and Ben Nevis I-45 wells. Locations of these wells can be seen in Figures 4.18 – 4.21. All three wells have high reflection strength, which is evident through the distinct change from carbonates to siliciclastics. Gamma ray log is filled with CanStrat® lithology interpretation where yellow=sandstone, orange=siltstone, brown=shale, and blue=carbonates or carbonate-cemented intervals. 87

4.25 Thickness map of the Lower Hibernia Member. Overall the Lower Hibernia Member thickens to the north and northeast but has local variations that trend across multiple fault blocks, suggesting they are depositional in nature. 89

4.26 Thickness map of the Upper Hibernia Member. Overall the Upper Hibernia Member thickens rather uniformly to the north and northeast. Notice the southern step-back of thickening compared to the Lower Hibernia Member in the region south of Ben Nevis. 90

4.27 Seismic section illustrating the correlation of the well logs to the seismic dataset. Location of seismic section is shown in upper left corner. The upper panel is the uninterpreted section and the lower panel is the interpreted section. The yellow lines represent the interpreted faults. The three displayed horizons are the base Hibernia Formation (dark purple), the mid-Hibernia Formation (light purple), and the top Hibernia Formation (orange). The displayed wells are shown in red with their corresponding gamma ray logs (blue and green curves). The displayed wells, from north to south, are Hebron M-04, Hebron I-13, Terra Nova C-09, Terra Nova K-08, Terra Nova K-07, and Beothuk M-05. This section highlights the significant growth seen in the Lower Hibernia Member between the Hebron M-04 and Hebron I-13 wells and overall thickening of the Hibernia Formation to the north. 92

4.28 Seismic attribute extractions along the seismic section shown in Panel A. Panel B is the seismic coherency, Panel C is the reflection strength, and Panel D is the instantaneous frequency. For each section, the yellow lines represent faults. The four displayed horizons on each panel represent the base Hibernia Formation (dark purple), mid-Hibernia Formation (light purple), top Hibernia Formation (orange), and base Tertiary Unconformity (brown). The vertical scale for each panel is two-way travel time. The horizontal scale is traces with large divisions of 50 traces. Traces are at a 25 meter spacing. 93

5.1 Location of the fifty-one (51) exploration, delineation and development wells used in this study. The three wells used in the core evaluation are circled in red. 96

5.2 Petrophysical log for the West Bonne Bay C-23 well over the depth interval 3774 – 3826 meters MD. Orange highlighted regions represent cored intervals. Core 1 is the top thinner interval and Core 2 is the lower thicker interval. The displayed depth interval is located within the Lower Hibernia Member (sub-unit 308). 97

5.3 Extensively bioturbated sandstone (**F1**) found in the C-23 well (Core 2, Box 10). Examples of *Ophiomorpha isp* and *Skolithos isp* are shown with green and blue arrows, respectively. Black arrow shows a small patch of calcite cement at the top. Note absence of preserved sedimentary structures. 100

5.4 Example of coarse-grained sandstone (**F2**) separating intervals of **F1** in the C-23 well (Core 2, Box 11). Orange marker highlights erosive boundary that separates lag deposits of **F2** (above) from **F1** (below). Red arrow shows position of thin, wispy, left-dipping laminations of carbonaceous clay material within an interval of overall right-dipping laminations. Black arrows indicate the edge of a calcite cemented zone. 101

5.5 Laminated sandstone (**F2**) found in the C-23 well (Core 2, Box 9). A large *Skolithos isp* trace fossil is shown by blue arrow; however it is possibly the vertical shaft of an *Ophiomorpha isp* trace fossil. Orange and red arrows indicate locations of planar and arcuate carbonaceous laminations, respectively, that are present throughout the facies. 102

5.6 Organic matter layer from the C-23 well (Core 2, Box 4). Yellow arrow indicates location of ~1 centimeter thick organic matter layer. Rusty red-brown discoloration surrounding organic matter highlights sideritization zone. Black arrows indicate edges of the calcite cement nodule that is present at this depth. Grey discoloration differentiates calcite cement from light brown uncemented sandstone. 103

5.7 **F1** located with the **F2** of the C-23 well (Core 2, Box 2). Trace fossils identifiable include: *Ophiomorpha isp* (green arrow), *Paleophycus isp* (red arrow), *Planolites isp* (purple arrow), and *Skolithos isp* (blue arrow). The upward-increase in cementation abundance is visible through the transition to the light grey coloration from the light brown sandstone. The sharp contact above the bioturbated interval is indicated by the orange coloured marker, where **F1** was overlain by **F2**. 104

5.8 Petrophysical log for the Hebron I-13 well over the depth interval 2924 – 2976 meters MD. Orange highlighted region represents cored interval (Core 4). Displayed depth interval is located within the Upper Hibernia Member (sub-unit 328). 108

5.9 Extensively bioturbated sandstone (**F1**) found in the I-13 well (Core 4, Box 13). Identified trace fossils include *Asterosoma isp* (light blue arrows), *Chondrites isp* (orange arrows), and *Chondrites isp* in longitudinal section (dark blue arrow). Shell fragments are common (purple arrow). 110

5.10 Calcareous serpulid tube fossils (blue arrows) commonly found in **F1** of the I-13 well (Top image: Core 4, Box 13; Bottom image: Core 4, Box 12. Shell fragment is shown by purple arrow. Organic matter lamination/fragment is shown by yellow arrow. 111

5.11 Grainstone (**F3**) found in the I-13 well (Core 4, Box 12). The orange line highlights irregular base of **F3** overlying **F1**. Note abundant carbonate material and shell fragments of **F3**. 112

5.12 **F2** sharply truncating underlying **F1** in the I-13 well (Core 4, Box 11). Erosive base of **F2** is shown by orange line. Green line highlights one of the low-angle laminations. A cluster of shell fragments is indicated by purple arrow. 113

5.13 Transition to **F1** deposition from **F2** below in the I-13 well (Core 4, Box 10). Areas that are light brown highlight original laminated sandstone while light and dark grey areas highlight bioturbated portions of the sandstone. Light blue arrow identifies an *Asterosoma isp.* Red arrows identify *Teichichnus isp.* 114

5.14 Fining-upwards, irregularly based **F3** overlying **F1** in the I-13 well (Core 4, Box 7). Erosive to irregular base of **F3** is highlighted by orange line. 116

5.15 Low-angle cross-laminated sandstone (**F2**) found in the I-13 well (Core 4, Box 7). Red lines highlight four visible laminations with different dip directions. 117

5.16 Heavily sideritized organic matter laminations contained within a grainstone bed (**F3**) in the I-13 well (Core 4, Box4). Yellow arrow marks location of organic matter laminations. 118

5.17 Petrophysical log for the Hebron M-04 well over the depth interval 2974 – 3101 meters MD. Orange highlighted region represents cored interval (Core 3). The displayed depth interval is located within the Upper Hibernia Member (sub-units 328 and 330) and the "B"-Marker limestone. 121

5.18 Basal carbonate-rich lag deposit found in the M-04 well (Core 3, Box 82). Purple arrows show locations of large shell fragments. Orange arrow shows location of a thin organic matter fragment. Green arrow shows location of overlying mud-clasts. 123

5.19 Low-angle laminated sandstone (**F2**) found in the M-04 well (Core 3, Box 84). Note abundant carbonaceous material and small lithic fragments that highlight laminations. 124

5.20 Burrowed sandstone (**F1**) found in the M-04 well (Core 3, Box 87). Green and red arrows show locations of *Ophiomorpha isp* and *Paleophycus isp* trace fossils, respectively. 125

5.21 Thick grainstone deposit (**F3**) found in the M-04 well (Core 3, Boxes 71 & 72). Base of cored section is in lower left corner and top is in upper right corner. 1: Matrix-supported shell fragments and carbonate clasts overly **F1**. 2: Fully clast-supported grainstone with minimal muddy matrix. 3: Approximately 4-5 centimeter thick laminated fine-grained sandstone lens (**F2**). 4: Top of fully clast-supported grainstone, above which carbonate fragments become matrix-supported and increasingly absent in overlying two meters. **F1** overlies uppermost carbonate-rich interval. 127

5.22 Massive shale deposit (**F4**) containing an interval of red shale found in the M-04 well (Core 3, Boxes 53 & 54). Full length of core boxes is not shown so displayed intervals do not stack directly together to form a continuous zone. Left grey shale contains minimal identifiable trace fossils and grades upwards into ~15 centimeter thick red shale. Gradationally above the red shale, the grey shale was re-established and contains minimal trace fossils. *Note: As shown, the core quality is the lowest of the recovered core and the shale is fairly broken up. The shale also swells when wet, so identifying trace fossils and cleaning the core samples are difficult tasks.* 128

5.23 Rudstone (**F5**) found in the M-04 well (Core 3, Box 52). Note large size and sub-angular nature of clasts, as well as abundance of muddy matrix that supports some clasts. 130

5.24 Fining-upwards succession of sandstone found in the M-04 well (Core 3, Box 38). The base is coarse-grained sandstone with no distinguishable internal character (**F2**) that fines-upwards into **F1**. 131

5.25 Grainstone (**F3**) found in the M-04 well (Core 3, Box 22). **F3** is rich in shell fragments and has no distinguishable internal structure. There are faint low-angle laminations in the upper section. Green arrows indicate two trace fossils that resemble *Ophiomorpha isp* in cross-section of a horizontal burrow (left arrow) and a vertical shaft (right arrow). 133

6.1 Gross thickness maps of the Lower Hibernia Member. Top map shows contouring without the influence of faulting. Bottom map shows contouring with the influence of faulting. Purple dotted lines show locations of Plate 1 (S-N/NE) and Plate 2 (W-E). 143

6.2 Percent-sandstone maps of the Lower Hibernia Member. Top map shows contouring without the influence of faulting. Bottom map shows contouring with the influence of faulting. Purple dotted lines show locations of Plate 1 (S-N/NE) and Plate 2 (W-E). 144

6.3 Type-sections of Lower Hibernia Member sub-unit 306. 147

6.4 Gross thickness maps of Lower Hibernia Member sub-unit 306. Top map shows contouring without the influence of faulting. Bottom map shows contouring with the influence of faulting. Purple dotted lines show locations of Plate 1 (S-N/NE) and Plate 2 (W-E). 148

6.5 Percent-sandstone maps of Lower Hibernia Member sub-unit 306. Top map shows contouring without the influence of faulting. Bottom map shows contouring with the influence of faulting. Purple dotted lines show locations of Plate 1 (S-N/NE) and Plate 2 (W-E). 149

6.6 Type-sections of the Lower Hibernia Member sub-unit 308. 151

6.7 Gross thickness maps of Lower Hibernia Member sub-unit 308. Top map shows contouring without the influence of faulting. Bottom map shows contouring with the influence of faulting. Black line represents the division between northern and southern depositional character. Purple dotted lines show locations of Plate 1 (S-N/NE) and Plate 2 (W-E). 152

6.8 Percent-sandstone maps of Lower Hibernia Member sub-unit 308. Top map shows contouring without the influence of faulting. Bottom map shows contouring with the influence of faulting. Purple dotted lines show locations of Plate 1 (S-N/NE) and Plate 2 (W-E). 153

6.9 Type-sections of the Lower Hibernia Member sub-unit 310. 155

6.10 Gross thickness maps of Lower Hibernia Member sub-unit 310. Top map shows contouring without the influence of faulting. Bottom map shows contouring with the influence of faulting. Purple dotted lines show locations of Plate 1 (S-N/NE) and Plate 2 (W-E). 156

6.11 Percent-sandstone maps of Lower Hibernia Member sub-unit 310. Top map shows contouring without the influence of faulting. Bottom map shows contouring with the influence of faulting. Purple dotted lines show locations of Plate 1 (S-N/NE) and Plate 2 (W-E). 157

6.12 Type-sections of the Lower Hibernia Member sub-unit 312. 158

6.13 Gross thickness maps of Lower Hibernia Member sub-unit 312. Top map shows contouring without the influence of faulting. Bottom map shows contouring with the influence of faulting. Purple dotted lines show locations of Plate 1 (S-N/NE) and Plate 2 (W-E). 160

6.14 Percent-sandstone maps of Lower Hibernia Member sub-unit 312. Top map shows contouring without the influence of faulting. Bottom map shows contouring with the influence of faulting. Purple dotted lines show locations of Plate 1 (S-N/NE) and Plate 2 (W-E). 161

6.15 Type-sections of the Lower Hibernia Member sub-unit 320. 163

6.16 Gross thickness maps of Lower Hibernia Member sub-unit 320. Top map shows contouring without the influence of faulting. Bottom map shows contouring with the influence of faulting. Purple dotted lines show locations of Plate 1 (S-N/NE) and Plate 2 (W-E). 164

6.17 Percent-sandstone maps of Lower Hibernia Member sub-unit 320. Top map shows contouring without the influence of faulting. Bottom map shows contouring with the influence of faulting. Purple dotted lines show locations of Plate 1 (S-N/NE) and Plate 2 (W-E). 165

6.18 Gross thickness maps of the Upper Hibernia Member. Top map shows contouring without the influence of faulting. Bottom map shows contouring with the influence of faulting. Purple dotted lines show locations of Plate 3 (S-N/NE) and Plate 4 (W-E). 168

6.19 Percent-sandstone maps of the Upper Hibernia Member. Top map shows contouring without the influence of faulting. Bottom map shows contouring with the influence of faulting. Purple dotted lines show locations of Plate 3 (S-N/NE) and Plate 4 (W-E). 169

6.20 Type-section of the Upper Hibernia Member sub-unit 322. 171

6.21 Gross thickness maps of Upper Hibernia Member sub-unit 322. Top map shows contouring without the influence of faulting. Bottom map shows contouring with the influence of faulting. Purple dotted lines show locations of Plate 3 (S-N/NE) and Plate 4 (W-E). 172

6.22 Percent-sandstone maps of Upper Hibernia Member sub-unit 322. Top map shows contouring without the influence of faulting. Bottom map shows contouring with the influence of faulting. Purple dotted lines show locations of Plate 3 (S-N/NE) and Plate 4 (W-E). 173

6.23 Type-section of the Upper Hibernia Member sub-unit 324. 175

6.24 Gross thickness maps of Upper Hibernia Member sub-unit 324. Top map shows contouring without the influence of faulting. Bottom map shows contouring with the influence of faulting. Purple dotted lines show locations of Plate 3 (S-N/NE) and Plate 4 (W-E). 176

6.25 Percent-sandstone maps of Upper Hibernia Member sub-unit 324. Top map shows contouring without the influence of faulting. Bottom map shows contouring with the influence of faulting. Purple dotted lines show locations of Plate 3 (S-N/NE) and Plate 4 (W-E). 177

6.26 Type-section of the Upper Hibernia Member sub-unit 326. 179

6.27 Gross thickness maps of Upper Hibernia Member sub-unit 326. Top map shows contouring without the influence of faulting. Bottom map shows contouring with the influence of faulting. Purple dotted lines show locations of Plate 3 (S-N/NE) and Plate 4 (W-E). 180

6.28 Percent-sandstone maps of Upper Hibernia Member sub-unit 326. Top map shows contouring without the influence of faulting. Bottom map shows contouring with the influence of faulting. Purple dotted lines show locations of Plate 3 (S-N/NE) and Plate 4 (W-E). 181

6.29 Type-section of the Upper Hibernia Member sub-unit 328. 183

6.30 Gross thickness maps of Upper Hibernia Member sub-unit 328. Top map shows contouring without the influence of faulting. Bottom map shows contouring with the influence of faulting. Purple dotted lines show locations of Plate 3 (S-N/NE) and Plate 4 (W-E). 184

6.31 Percent-sandstone maps of Upper Hibernia Member sub-unit 328. Top map shows contouring without the influence of faulting. Bottom map shows contouring with the influence of faulting. Purple dotted lines show locations of Plate 3 (S-N/NE) and Plate 4 (W-E). 185

6.32 Type-section of the Upper Hibernia Member sub-unit 330. 186

6.33 Gross thickness maps of Upper Hibernia Member sub-unit 330. Top map shows contouring without the influence of faulting. Bottom map shows contouring with the influence of faulting. Purple dotted lines show locations of Plate 3 (S-N/NE) and Plate 4 (W-E). 188

6.34 Percent-sandstone maps of Upper Hibernia Member sub-unit 330. Top map shows contouring without the influence of faulting. Bottom map shows contouring with the influence of faulting. Purple dotted lines show locations of Plate 3 (S-N/NE) and Plate 4 (W-E). 189

6.35 Series of simplified percent sandstone maps with key contours shown for each unit to illustrate relative shifts in the paleo-shoreline of the Lower Hibernia Member. Blue contours represent the younger sub-unit, while red contours represent the older sub-unit. Arrows illustrate lateral migration trends of the paleo-shoreline between successive sub-units (red to blue contours). 192

6.36 Series of simplified percent sandstone maps with key contours shown for each unit to illustrate relative shifts in the paleo-shoreline of the Upper Hibernia Member. Blue contours represent the younger sub-unit, while red contours represent the older sub-unit. Arrows illustrate lateral migration trends of the paleo-shoreline between successive sub-units (red to blue contours). 196

7.1 Schematic model of the Hibernia Formation. The yellow areas represent the delta plain to delta front facies of the Hibernia Formation (characterized by >70% sandstone deposition). The orange areas represent the upper- to mid-shoreface facies of the Hibernia Formation (characterized by 20-70% sandstone). The brown areas represent the lower shoreface to marine facies of the Hibernia Formation (characterized by 0-20% sandstone). Figure 7.1 consists of ten images progressing from A illustrating the depositional setting of the Lower Hibernia Member sub-unit 306 through the depositional history to J illustrating the depositional setting of the Upper Hibernia Member sub-unit 330. 201

LIST OF TABLES

2.1 Thickness of missing stratigraphy in wells due to faulting. Orange highlights wells with 50-100 meters of missing section. Blue highlights wells with >100 meters of missing section and subsequently wells that had minimal influence on interpretation and correlations. 18

CHAPTER 1 – INTRODUCTION

1.1 SCOPE AND PURPOSE

When the Terra Nova oil field was discovered in 1984, attention was focused on the Jeanne d'Arc Formation since it was the primary oil-bearing reservoir. However, with maturation of the Terra Nova oil field, consideration is being placed on secondary reservoirs and smaller satellite fields. The neighbouring Hebron/Ben Nevis oil field to the north was discovered between 1980 and 1984, and one of the primary reservoirs is the Berriasian to Valanginian-aged Hibernia Formation. To aid in the understanding of the petroleum system, a depositional model of the Hibernia Formation is required to ultimately derive petroleum migration pathways of that reservoir and understand why the Hibernia Formation is oil-bearing within the Hebron oil field while the area within the Terra Nova oil field is limited to minor oil shows and oil-staining.

In the last twenty years, the Hibernia Formation has been ignored in publications in both the Terra Nova and Hebron/Ben Nevis oil fields. Most recent publications on the Hibernia Formation have been either basin-wide scale studies of general depositional environments or localized studies within the Hibernia oil field of Hibernia Formation reservoir properties (Brown, 1985; Fitzgerald, 1987; Gower, 1988). This thesis incorporates geophysical and geological data to produce a depositional model of the Hibernia Formation over the Terra Nova and Hebron/Ben Nevis oil fields. Using available geological and geophysical data, a definition for the top, middle and base Hibernia Formation is proposed as a framework for future developments. As oil fields are discovered, investigated, and developed, more detailed depositional models are essential for accurate and efficient petroleum location and extraction. Clearly, re-

evaluation of a depositional model is important as new data are made available. During aforementioned studies, only fourteen wells were available for incorporation into the depositional model, in comparison to fifty-one wells that are integrated into this study, over the region covering the Terra Nova and Hebron/Ben Nevis oil fields.

This thesis is proposed as a working model and does not adhere to the accepted North American Stratigraphic Code (NACSN, 2005) or the stratigraphic nomenclature available at the Canada-Newfoundland and Labrador Offshore Petroleum Board. The interpretation presented in this thesis is based solely on the data and geological boundaries within the study area. The stratigraphic boundaries proposed are not necessarily part of the generally accepted stratigraphic column of McAlpine (1990). Stratigraphic tops are informal and used solely to develop the working model within the study area. Formal modification to the stratigraphic column of McAlpine (1990) is beyond the scope of this thesis.

1.2 LOCATION

The Jeanne d'Arc Basin is located 300 kilometers east of St. John's, Newfoundland along the eastern edge of the Grand Banks (Figure 1.1). The basin is bounded to the north by the Cumberland Belt Transform Zone (CBTZ) and the Phoenix Sub-Basin, to the west by the Bonavista Platform (via the Murre Fault and Mercury Fault Systems), to the south by the Egret Fault (south of which the basin is referred to as the South Jeanne d'Arc Basin) and to the east by the Ridge Complex (via the Voyager Fault System). The study area is situated along the southeastern edge of the basin, at the intersection of the Trans-Basin Fault Zone (TBFZ) and the Voyager Fault System (Figure 1.2). The location of the study area at the intersection of major fault systems resulted in structural

complexity that formed significant traps and the juxtaposition along the major basin-bounding Voyager Fault System controlled the supply of coarse-grained siliciclastic sediments from the paleo-platform to the southeast and east.

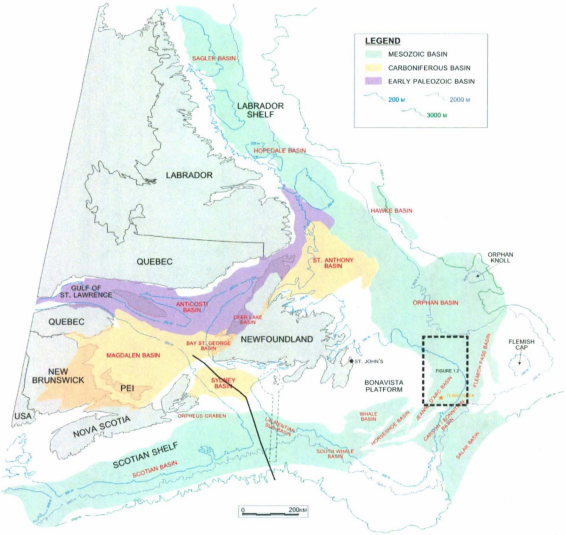


Figure 1.1: Map of Atlantic Canada illustrating the location of the Mesozoic and Paleozoic Basins. Note the black outline indicating the approximate location of Figure 1.2 over the Jeanne d'Arc Basin. Modified after C-NLOPB (2005), Geological Survey of Canada and Enachescu and Fagan (2004).

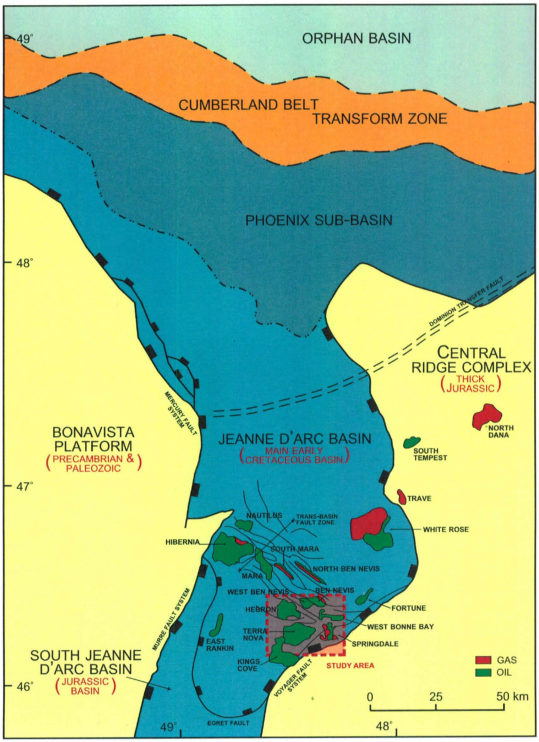


Figure 1.2: Structural features of the Jeanne d'Arc Basin including the locations of any significant petroleum discoveries. Modified after C-NLOPB (2005), Grant *et al.* (1986) and Enachescu (1988).

1.3 Data Availability

This thesis combined geophysical and geological data to produce a fully integrated model of the Hibernia Formation. Figure 1.3 illustrates the location of available data within the study area. It incorporated 675 km^2 of a three-dimensional seismic dataset over the study area as well as a suite of petrophysical well logs from fifty-one exploration, delineation, and production wells. The seismic dataset is privately owned and therefore confidential; however, through the Canada-Newfoundland and Labrador Offshore Petroleum Board (C-NLOPB) select lines are available in paper format. A complete list of publicly available seismic lines can be obtained through the C-NLOPB. Only three of the fifty-one wells contain core, totaling approximately 150 meters of recovered core within the Hibernia Formation. Seismic data provide large-scale structural information needed to develop structural aspects of the depositional model, while well data provides information needed for sedimentological and stratigraphic components of the model. Core data provide distinct control points for interpretation of depositional environments through facies description and analysis and provided limited aid to define the major stratigraphic boundaries of the Hibernia Formation. Together, geophysical and geological data allowed a better understanding of the reservoir distribution and general nature of associated stratigraphic and structural traps.

The depositional model was constrained by parameters that were defined using the three-dimensional seismic dataset and petrophysical well data. Parameters derived from petrophysical well data are gross interval thickness, net sandstone, sandstone to shale ratio, and petrophysical signature. Core data provide more specific information regarding sedimentary structures and presence of trace fossils to help differentiate between possible depositional environments. For illustration purposes in this thesis, the

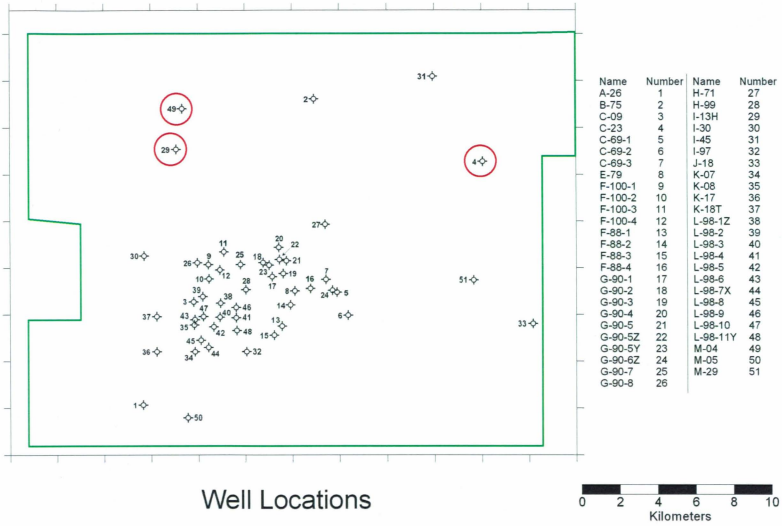


Figure 1.3: Map highlighting data availability for the study area. Seismic boundaries are indicated by the green polygon. Location of the fifty-one (51) exploration, delineation and development wells are shown in black, with a legend showing the well names on the right. The three wells that have Hibernia Formation core are circled in red. Location of study area is highlighted in Figure 1.2.

depositional model is presented as a series of maps of parameters used to define the depositional model, as well as several schematic block diagrams illustrating interpreted depositional environments of the Hibernia Formation. This depositional model illustrates the extent and connectivity of informal units within the Hibernia Formation as well as environments of deposition.

1.4 SUMMARY

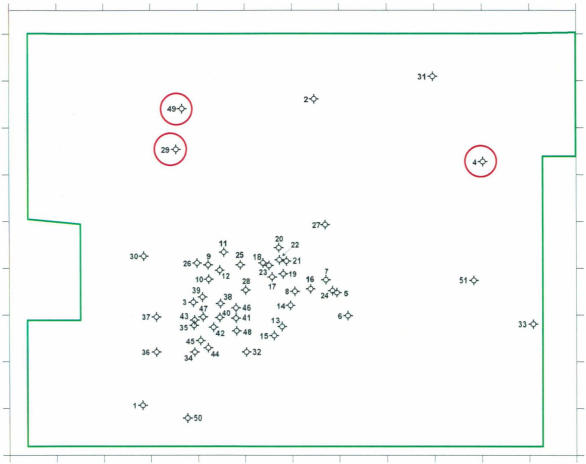
This thesis incorporates data available from the interpretation of a three-dimensional seismic dataset covering an area of 675 km^2, a total of fifty-one exploration, delineation, and production wells, and a total of approximately 150 meters of recovered core from three wells. The primary objective of this thesis was to develop a seismo-stratigraphic framework of the Hibernia Formation over the region surrounding the Terra Nova and Hebron/Ben Nevis oil fields. This model consists of a series of maps of defining parameters and schematic diagrams illustrating the succession of interpreted depositional environments. These maps show the distribution of various informal units within the Hibernia Formation, which may ultimately provide the framework for the interpretation of petroleum traps and accumulations (not covered as part of this thesis). Integration of available geological and geophysical data has allowed a seismic-scaled depositional model of the Hibernia Formation to be proposed. This model consists of multiple intervals that correspond to correlative events identified in seismic and well data and were attributed to distinct depositional intervals. Sequential layering of these correlative events allowed development of a depositional history.

CHAPTER 2 – METHODOLOGY

2.1 SCOPE AND PURPOSE

This chapter outlines the methodology used to interpret the various types of data presented in this thesis. It discusses techniques used to map faults and various seismic markers across the study area using the three-dimensional seismic dataset, as well as definitions for various lithofacies identified in the examined core. It also outlines the parameters and assumptions used in the correlation of the petrophysical well data across the study area. Since all three types of data (seismic, well data, and core) are used together to help interpret each data-type as a whole, all parameters used in the interpretation are presented in this chapter.

The study area is shown in Figure 2.1, illustrating the locations of all wells used in this thesis and is entirely covered by the three-dimensional seismic dataset. Please note that all coordinates have been removed from the map because seismic data ownership is private and all presented seismic sections are taken from a limited list of seismic data that is publicly available through the Canada-Newfoundland and Labrador Offshore Petroleum Board (C-NLOPB).



Name	Number	Name	Number
A-26	1	H-71	27
B-75	2	H-99	28
C-09	3	I-13H	29
C-23	4	I-30	30
C-69-1	5	I-45	31
C-69-2	6	I-97	32
C-69-3	7	J-18	33
E-79	8	K-07	34
F-100-1	9	K-08	35
F-100-2	10	K-17	36
F-100-3	11	K-18T	37
F-100-4	12	L-98-1Z	38
F-88-1	13	L-98-2	39
F-88-2	14	L-98-3	40
F-88-3	15	L-98-4	41
F-88-4	16	L-98-5	42
G-90-1	17	L-98-6	43
G-90-2	18	L-98-7X	44
G-90-3	19	L-98-8	45
G-90-4	20	L-98-9	46
G-90-5	21	L-98-10	47
G-90-5Z	22	L-98-11Y	48
G-90-5Y	23	M-04	49
G-90-6Z	24	M-05	50
G-90-7	25	M-29	51
G-90-8	26		

Figure 2.1: Map highlighting data availability for the study area. Seismic boundaries are indicated by the green polygon. Location of the fifty-one (51) exploration, delineation and development wells are shown in black, with a legend showing the well names on the right. The three wells that have Hibernia Formation core are circled in red. Location of study area is highlighted in Figure 1.2.

2.2 THREE-DIMENSIONAL SEISMIC DATASET

The three-dimensional seismic dataset over the study area was recorded in 1997 and covers 749 square kilometers. The mapped portion of the seismic dataset used in this thesis approximately corresponds to the southern 650 square kilometers with the northern extent of the study area being seismic inline 910. The seismic dataset is available through the Canada-Newfoundland and Labrador Offshore Petroleum Board (C-NLOPB) under program numbers 8924-P028-004E and 8924-P028-005E. Recorded seismic data resulted in a Common Mid-Point (CMP) spacing of fifty meters which was interpolated to twenty-five meter spacing. Close lateral spacing of seismic data provides very detailed information about the lateral distribution of the Hibernia Formation. However, vertical resolution is limited at the level of the Hibernia Formation, where peak seismic frequencies are approximately 18-22 Hz (~50-65 meters based on quarter-wavelength calculations using a velocity of ~4500 m/s) with a maximum frequency of approximately 50-60 Hz (~20-25 meters). This relatively low vertical resolution level of the seismic dataset allows distinction of major boundaries but blurs the signature of minor, thinner beds. Vertical resolution of the Hibernia Formation is better preserved in the petrophysical well data (discussed in Chapter 6).

Interpretation of the three-dimensional seismic dataset was done using Landmark's SeisWorks® and SynTool® applications. SynTool® was used to construct synthetic seismograms in order to correlate well data to seismic data. Figure 2.2 illustrates two seismic wavelet extractions from seismic data at the King's Cove A-26 and Ben Nevis I-45 wells over the Hibernia Formation (see Figure 2.1 for well locations). Also shown in Figure 2.2 are the frequency and phase spectra of the extracted wavelet. Note the lower peak frequency of eighteen hertz at the Ben Nevis I-45 well compared to

twenty-two hertz at the King's Cove A-26 well, generally due to the increased depth of the Hibernia Formation at I-45. The phase spectrum is fairly smooth and approximately zero-phase (within thirty degrees) across the dominant frequency range. Finally, note the approximately twenty millisecond delay of the seismic wavelet shown in the time series panel of Figure 2.2. Based on these extracted wavelets, a Ricker wavelet with a peak frequency of twenty-two hertz was used in the generation of synthetic seismograms for remaining wells. A Ricker wavelet is a zero-phase seismic wavelet, a second-derivative of the idealized Gaussian wavelet, which is uniquely defined by its dominant frequency and amplitude (Ricker, 1953). Figure 2.3 illustrates a Ricker wavelet with a peak frequency of twenty-two hertz and an onset time of twenty milliseconds. Note the similarity of the extracted wavelets of Figure 2.2 and the Ricker wavelet of Figure 2.3.

Three stratigraphic tops were correlated to the seismic dataset: i) base of Hibernia Formation, ii) mid-Hibernia Formation, and iii) top of Hibernia Formation. Parameters used to identify these seismic markers are discussed in detail in Chapter 4 and further in Chapter 6. Once synthetic seismograms were constructed for all wells, it was possible to tie well signatures to the seismic dataset using SeisWorks®. Seismic marker and fault interpretations were both done using SeisWorks®.

Before seismic marker interpretation could commence, however, the complex distribution of faults in the study area had to be understood. Seismic interpretation began by coarsely mapping faults as a suite of fault picks every eight inlines and crosslines. This allowed a very good understanding of the general abundance of faults present and the relationship of various faults with one another. It was also possible to recognize the main structure-forming faults as well as secondary faults. Several

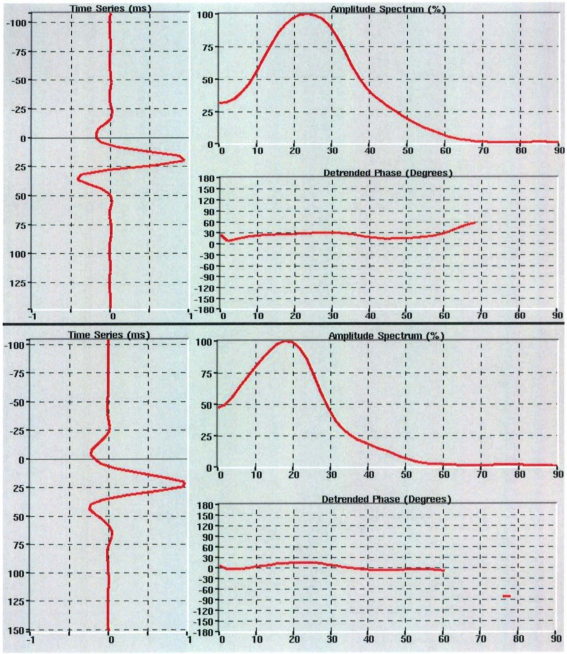


Figure 2.2: Seismic wavelet extractions over the Hibernia Formation at the King's Cove A-26 well (top) and the Ben Nevis I-45 well (bottom). The seismic wavelet is in the left panel; note resemblance to the Ricker wavelet of Figure 2.3. The top-right panel is the frequency spectrum for the wavelet with the amplitude in percentage. Note that peak frequency at the King's Cove A-26 well is twenty-two hertz and maximum frequency is approximately sixty hertz, while peak frequency at the Ben Nevis I-45 well is eighteen hertz and maximum frequency is approximately fifty hertz. The bottom-right panel is the phase spectrum for the wavelet; note how both wells illustrate the near zero-phase character of the seismic wavelet (within thirty degrees).

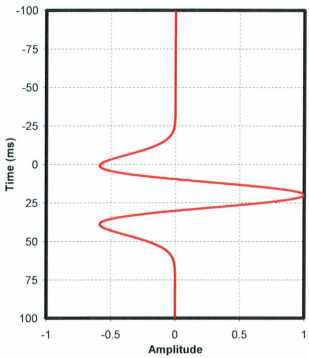


Figure 2.3: Ricker wavelet with dominant frequency of twenty-two hertz and onset time of twenty milliseconds.

iterations of cycling between inline and crossline directions were done to determine the cross-cutting nature of the faults. This allowed relationships of major faults to minor faults to be determined and allowed classification of various fault structures (shown in Chapter 3). Once fault relationships were confidently defined, individual fault picks were correlated with each other and triangulated to define individual fault planes in three dimensions. Triangulation was the final step in fault interpretation since it took individual fault segments on the inlines and crosslines and transformed them into a continuous fault plane for each fault.

After fault interpretation was complete it was possible to more accurately interpret the seismic stratigraphy of the Hibernia Formation. Seismic marker

interpretation began by manually constructing a coarse grid over the study area using synthetic well ties created in SynTool®. The coarse grid was loop-tied to surrounding well locations in a radially-outward direction. Once loop-ties were completed, the seismic marker interpretation began by interpreting areas inside the well-controlled grid first and then expanding outwards away from control points. As each seismic marker was completed, it was re-checked against synthetic seismogram well ties, as well as correcting any misties between inlines and crosslines.

Interpretation of faults and seismic markers allowed a detailed picture of the structure and stratigraphy of the Hibernia Formation within the study area. However, further analysis of seismic attributes of the Hibernia Formation allowed detailed characterization and subdivision into different seismic facies. These attributes consist of reflection strength, coherency, and instantaneous frequency. Changes in seismic attributes help locate lateral facies boundaries as well as characterize the changing nature of a particular seismic marker. Seismic attribute extractions were done for individual seismic markers mapped for the Hibernia Formation.

2.3 CORE DATA

Core for each well was laid-out in the core examination room of the Canada-Newfoundland and Labrador Offshore Petroleum Board (C-NLOPB) Core Storage and Research Centre located on 30-32 Duffy Place, St. John's, Newfoundland. The core was examined and described from base to top. For the purpose of this thesis, the following parameters were compiled from the core: i) graphic log, ii) cement abundance, iii) sandstone-to-shale ratio, iv) bioturbation intensity, v) grain size, and vi) remarks of distinct features or trace fossils visible in the core. A sample of a core description log can be seen in Figure 2.4.

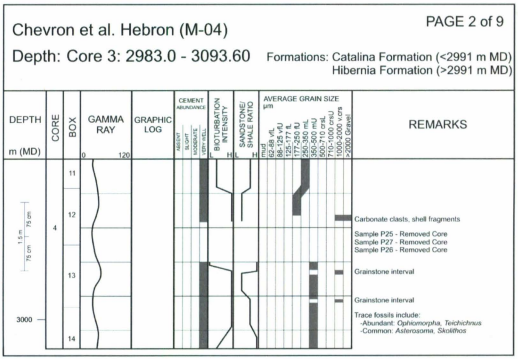


Figure 2.4: Example of the details recorded for the core descriptions. Gamma ray log is taken from petrophysical well data.

Core intervals were then subdivided into broadly distinguishable lithofacies to establish common vertical stacking patterns as well as facies associations. Definition of lithofacies was based on depositional characteristics including grain size, current structures and presence of traces (bioturbation and specific burrow types). Although a number of multi-scale lithofacies are present, principal facies can be summarized as the following: *i)* extensively bioturbated sandstones (**F1**) possibly deposited in mid- to lower shoreface setting; *ii)* low-angle to horizontally laminated sandstones (**F2**) possibly deposited in a foreshore to upper shoreface setting; *iii)* medium- to coarse-grained grainstones (**F3**) possibly the result of episodic storm events; *iv)* thick massive shales (**F4**) possibly deposited in a fully marine setting; and *v)* erosively based, conglomeratic rudstone to grainstone (**F5**) possibly the result of episodic storm events.

2.4 PETROPHYSICAL WELL DATA

The fifty-one (51) exploration, delineation and development wells all contain some degree of petrophysical well data in the form of wireline logs. The following logs were used to define the characteristics of the Hibernia Formation: i) Gamma Ray, ii) Spectral Gamma Ray components (Potassium, Thorium, and Uranium), iii) Resistivity, iv) Neutron Density (estimate of porosity), v) Sonic (compressional and shear sonic, where available), and vi) Bulk Density. Borehole caliper was used as quality control for other petrophysical logs to locate zones of washout and cave-in. Lithology-fill displayed with the Gamma Ray logs is based on drill cuttings descriptions from the wellsite geologist for individual wells; yellow represents sandstone, orange represents siltstone, brown represents shale, and blue represents carbonates or carbonate-cemented intervals. Bulk density and sonic logs were used to construct synthetic seismograms for

each well in order to tie petrophysical data to seismic data (refer to Chapter 4). An example of the well header used in figures involving wells can be seen in Figure 2.5. Locations of the fifty-one wells used in this study can be found in Figure 2.1.

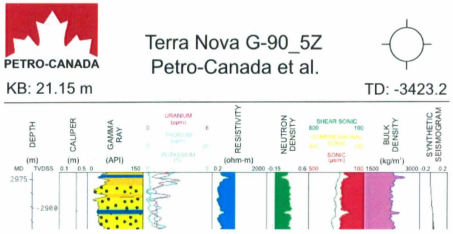


Figure 2.5: Well header used to label petrophysical logs. Gamma ray log is filled with lithology interpretation where yellow is sandstone, orange is siltstone, brown is shale, and blue is carbonate or carbonate-cemented interval.

The first step in well correlations was to determine the top, middle and base of the Hibernia Formation (picks GDL_330, GDL_320, and GDL_300, respectively). The base of the Hibernia Formation is marked by the onset of coarse-grained siliciclastic input into the study area above the Fortune Bay Formation marine shales. This change is often gradual and is predominantly marked by a steady decrease in gamma ray intensity upwards. The middle of the Hibernia Formation is a laterally continuous maximum flooding surface (maximum gamma ray deflection) that overlies a distinct low gamma ray package. Above the maximum flooding surface the Hibernia Formation seems to coarsen-upwards overall (upward decrease of gamma ray). The top of the Hibernia Formation is marked by the sharp transition into the overlying 'B' Marker limestone and is characterized by a distinct change in resistivity and matrix density

across the boundary as deposition changes from siliciclastic to carbonate lithology. Parameters used to define major boundaries within the Hibernia Formation are presented in detail in Chapter 6.

Using the above petrophysical logs for available wells, wells were subdivided into groups based on the amount of Hibernia Formation that had been removed from the well location due to normal faulting (Table 2.1). Faults were determined by observing the well location in seismic data and noting the approximate intersection of faults with the well track. Depth of the intersection point was transferred to borehole caliper and the

Well Name	Well Number	Missing Section (meters)	Well Name	Well Number	Missing Section (meters)
King's Cove	A-26	0	North Trinity	H-71	~60
West Ben Nevis	B-75	0	Terra Nova	H-99	~130
Terra Nova	C-09	~20	Hebron	I-13H	0
West Bonne Bay	C-23	0	Brent's Cove	I-30	~80
Terra Nova	C-69-1	~260	Ben Nevis	I-45	0
Terra Nova	C-69-2	~25	Terra Nova	I-97	~70
Terra Nova	C-69-3	0	Voyager	J-18	0
Terra Nova	E-79	~300	Terra Nova	K-07	~20
Terra Nova	F-100-1	~140	Terra Nova	K-08	0
Terra Nova	F-100-2	0	Terra Nova	K-17	0
Terra Nova	F-100-3	~70	Terra Nova	K-18T	0
Terra Nova	F-100-4	~100	Terra Nova	L-98-1Z	0
Terra Nova	F-88-1	~50	Terra Nova	L-98-2	~30
Terra Nova	F-88-2	~120	Terra Nova	L-98-3	0
Terra Nova	F-88-3	0	Terra Nova	L-98-4	~200
Terra Nova	F-88-4	~260	Terra Nova	L-98-5	0
Terra Nova	G-90-1	~70	Terra Nova	L-98-6	0
Terra Nova	G-90-2	0	Terra Nova	L-98-7X	0
Terra Nova	G-90-3	~65	Terra Nova	L-98-8	~20
Terra Nova	G-90-4	0	Terra Nova	L-98-9	~180
Terra Nova	G-90-5	0	Terra Nova	L-98-10	0
Terra Nova	G-90-5Z	0	Terra Nova	L-98-11Y	~210
Terra Nova	G-90-5Y	0	Hebron	M-04	0
Terra Nova	G-90-6Z	~230	Beothuk	M-05	0
Terra Nova	G-90-7	0	Springdale	M-29	0
Terra Nova	G-90-8	~245			

Table 2.1: Thickness of missing stratigraphy in wells due to faulting. Orange highlights wells with 50-100 meters of missing section. Blue highlights wells with >100 meters of missing section and subsequently wells that had minimal influence on interpretation and correlations.

maximum deflection point in borehole caliper near the approximate depth of intersection was defined as the fault location. Wells that did not encounter significant faults (less than 25 meters of missing section) were used for primary well correlations. Fault offsets were estimated using seismic data and preserved section in offsetting wells. Once the top, middle and base of the Hibernia Formation were confidently correlated on non-faulted wells, faulted wells were introduced to the correlations. Furthermore, based on well correlations (discussed in Chapter 6) it is possible to subdivide the Hibernia Formation into two distinct prograding packages separated by a widespread possible flooding surface that is present in every well within the study area. Based on these packages, it is proposed herein that the Hibernia Formation be informally sub-divided into the Upper and Lower Hibernia Members. The Upper and Lower Hibernia Members were then further subdivided into five sub-units each. The Lower Hibernia Member is composed of sub-units 306 to 320, while the Upper Hibernia Member is composed of sub-units 322 to 330. These subdivisions are based on qualitative log response patterns that appear to be the predominant lithologic signature across multiple wells. These patterns were then subsequently correlated across the study area first using non-faulted wells, followed by incorporation of faulted wells. This resulted in the lithostratigraphic correlation of ten sub-units within the Hibernia Formation across the study area. A representative well is shown in Figure 2.6, illustrating the typical petrophysical character of the Hibernia Formation and subdivision into ten sub-units (discussed in greater detail in Chapter 6). A generalized stratigraphic panel of the Hibernia Formation is illustrated in Figure 2.7 illustrating the lateral continuity of individual sub-units. It is possible that several small hiatuses separate successive sub-units; however chronostratigraphic relationships between sub-units are beyond the scope of this thesis.

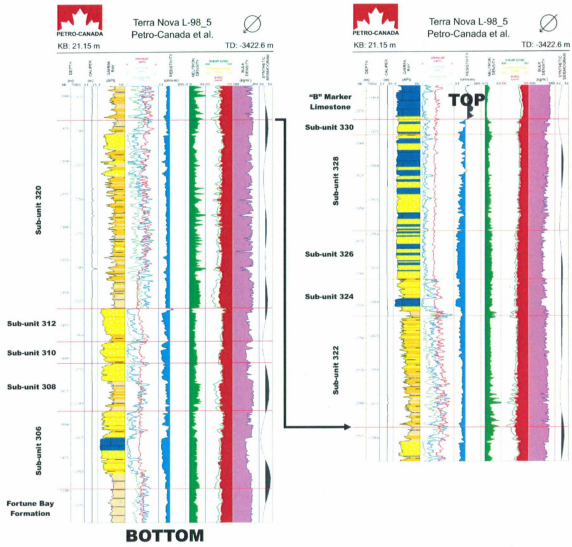


Figure 2.6: Representative well (Terra Nova L-98_5) indicating the ten sub-units that comprise the Hibernia Formation.

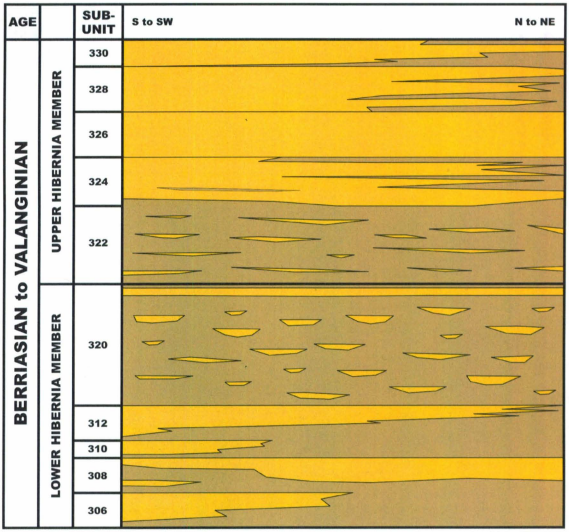


Figure 2.7: Generalized stratigraphic panel of the Hibernia Formation within the study area based on the wells used in this thesis. Sandstone is yellow and shale is brown.

Using the ten sub-units of the Hibernia Formation, thickness and percent-sandstone of each zone was mapped across the study area and were contoured with and without the influence of the main faults on contour patterns. Fault locations are indicated on the maps; however they do not extend into the northern half of the study area due to the lack of well control for contouring. Percent-sandstone was calculated for each well by determining a sandstone/shale cutoff based on the gamma ray. Gamma

ray was suitable to differentiate lithologies since sandstones are predominantly quartz arenites (low gamma ray), while shales are composed of radioactive clays (high gamma ray), as determined using the core data (Chapter 5). The actual gamma ray cutoff number varied between wells due to differences in the calibration of well logging tools between individual wells. However, the cutoff generally remained the same throughout any given well since the Hibernia Formation was typically completely logged in one wireline run and the lithologic composition appears to be relatively homogeneous. When logging runs ended and commenced within the Hibernia Formation, the cutoff was re-calculated. The cutoff was calculated using the following formula:

Cutoff = [Maximum Value – Minimum Value] x 0.7 + Minimum Value

which I determined as a basis to distinguish sand-dominated from shale-dominated lithologies. It is important to note that sandstone and carbonate lithologies were not differentiated when using the Gamma Ray cutoff. Sandstones are typically clean quartz arenites and possess a very similar low gamma ray log character to known limestone deposits. This was deemed to be insignificant for the purpose of this thesis since limestone cores recovered within the Hibernia Formation are not *in situ* deposits and contain mixed siliciclastic and carbonate lithologies, thereby obscuring the petrophysical signature of the deposits (refer to Chapter 5).. Proper calibration of carbonate beds (as highlighted in the gamma ray fill) to core data could be accomplished with the use of a photoelectric absorption (PE) log. The PE log would be able to distinguish low gamma ray sandstones from low gamma ray carbonates since sandstones have a low photoelectric absorption and carbonates have a high

photoelectric absorption. Well characterization produced a gross thickness and sandstone ratio map for each of the ten sub-units to provide a detailed understanding of the shift in depositional trends throughout the history of the Hibernia Formation. All of the percent-sandstone maps are displayed using the same scale (0 to 100 percent) to ease comparisons and highlight changes between subsequent zones.

To accommodate differences in lateral resolution between petrophysical data and seismic data, only major faults were used in compiling petrophysical thickness and percent-sandstone maps. Smaller faults were not used in the preparation of the maps to avoid the representation of fault blocks without well penetrations, and because the maps are intended to reflect large-scale, general trends across the study area. For the purpose of this thesis, the following main faults are defined:

- Jinker Fault: east-dipping extensional fault separating West Flank and Graben
- Mauzy Fault: west-dipping extensional fault separating Graben and East Flank
- Prise Fault: east-dipping extensional fault separating East Flank and Far East
- Doter Fault: west dipping extensional fault separating Far East and Terrace
- Voyager Fault: northwest-dipping, basin-bounding extensional fault

The Jinker, Mauzy, Prise, and Doter faults are names chosen for this thesis; however, the Voyager Fault is a well known feature that is discussed in many other studies as it is one of the Jeanne d'Arc basin-bounding faults (such as Enachescu, 1987 and 1988; Enachescu and Fagan, 2004; Grant and Mc Alpine, 1990; McAlpine, 1990; Tankard and Welsink, 1987 and 1988). Locations of these faults are shown in Figure 2.8. Further complexity of the system of faults is discussed in Chapters 3 and 4. Unit thickness variations across faults highlight those faults that experienced displacement during deposition of given units. Increased fault activity is assumed to have created

accommodation space and increased the depositional slope during sedimentation of the Hibernia Formation. Therefore, as sediment was deposited in topographic lows, depositional slopes were again reduced, barring additional fault activity. Once depositional slopes were reduced, loci of sandstone deposition must have bypassed to more distal locations, including outside of the study area. Although the above fault-depositional model is not unique and in turn dependent on depositional settings, these concepts of depositional response to faulting are used to provide a consistent approach to describe relationships between fault activity, depositional thickness, depositional slope, and percent-sandstone. Consideration of additional and variable fault response models is clearly not warranted given the scale of the study area and sparsity of core data available to derive more specific depositional conditions.

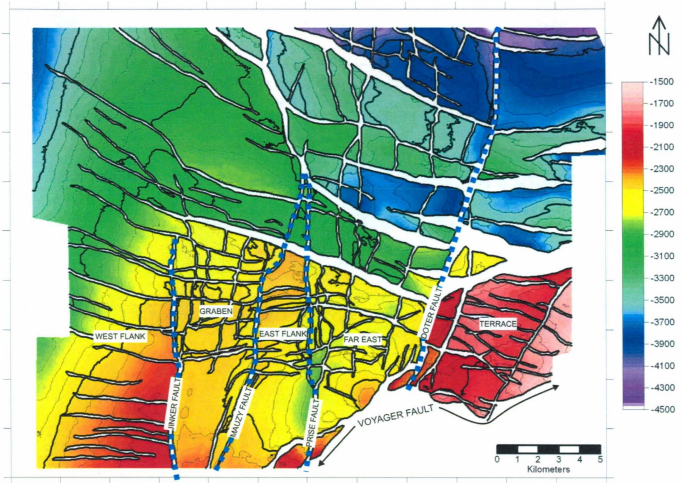


Figure 2.8: True vertical depth below sea-level map of the top of the Hibernia Formation. Contour interval is 100 meters with every 500 meters in bold lines. Locations of the five main faults are highlights with blue dotted lines.

CHAPTER 3 – STRUCTURE AND STRATIGRAPHY

3.1 INTRODUCTION

The tectonic evolution of the Jeanne d'Arc Basin is critical to an understanding of the evolution of depositional environments during the basin's history. By recording the orientation of faults that displayed syn-sedimentary growth across the Hibernia Formation, faults that were active during this time are identified and the dominant direction of extension during deposition of the Hibernia Formation can be determined. This also allowed areas of potential sediment accommodation, as well as areas of siliciclastic sediment sources, to be inferred. Structural highs provided the source of siliciclastic sediments and structural lows provided potential sediment accommodation zones. In conjunction with sea level fluctuations, the structural setting during the Berriasian to Valanginian was a key factor that controlled the sediments that compose the Hibernia Formation.

This chapter focuses on the tectonic evolution of the Jeanne d'Arc Basin and influence of the evolving extensional regime on structural and stratigraphic compartmentalization of the Hibernia Formation. The extensional history of the basin is first summarized, followed by representative fault families that are present in the study area. Emphasis is placed on the North Atlantic Rifting Phase of extension since it is the active phase during deposition of the Hibernia Formation. Stratigraphy of the Jeanne d'Arc Basin is also summarized and correlated with corresponding stages of basin evolution.

3.2 TECTONIC EVOLUTION

3.2.1 PRESENT-DAY TECTONIC SETTING

The Jeanne d'Arc Basin is a fault-bounded Mesozoic basin located in the area of the Grand Banks, offshore Newfoundland. The north-south trending basin is bounded by the stable Bonavista Platform to the west, composed of metamorphosed Precambrian and Paleozoic rocks (Enachescu, 1992). The boundary between the Bonavista Platform and the Jeanne d'Arc Basin is marked by the Murre and Mercury faults systems. The basin is bounded to the east by the Central Ridge Complex, composed of highly faulted Early Mesozoic sediments (McAlpine, 1990). The boundary between the Central Ridge Complex and the Jeanne d'Arc Basin is marked by the Voyager Fault System. The basin extends north to the Phoenix Sub-Basin and Cumberland Belt Transform Zone and its southern extent is marked by the Egret Fault, which separates the Jeanne d'Arc Basin from the South Jeanne d'Arc Basin (Figure 1.2).

3.2.2 TECTONIC AND STRATIGRAPHIC HISTORY

Grant *et al.* (1986), Enachescu (1987), Tankard and Welsink (1987), Sinclair (1988), Tankard and Welsink (1988), , McAlpine (1990), Tankard (1990), Williamson (1992), and Sinclair (1995 a,b) extensively discuss the tectonic history and stratigraphy of the Jeanne d'Arc Basin. This section and subsequent three sub-sections are a condensed summary of the main stages in the tectonic evolution of the Jeanne d'Arc Basin taken from the above list of references, unless otherwise noted. Figure 3.1 is a representative tectono-stratigraphic chart for the Jeanne d'Arc Basin illustrating times of significant tectonic events and dominant subsidence styles.

The Jeanne d'Arc Basin has experienced three distinct episodes of extension and subsequent episodes of thermal subsidence, resulting in a detailed record of the break-up of Pangaea and opening of the North Atlantic Ocean. Initial northwest-southeast oriented extension began in the Late Triassic during the Tethys rifting phase. Extension was re-oriented in a west-east direction in the Late Jurassic during the North Atlantic rifting phase. Final Jeanne d'Arc Basin extension was oriented northeast-southwest during the Labrador rifting phase. Each episode of extension was followed by a period of prolonged post-rift subsidence. The Jeanne d'Arc Basin is a failed rift basin since no oceanic crust was created (Enachescu, 1987). Oceanic crust creation was established further east of the Jeanne d'Arc Basin along the eastern margin of the Central Ridge Complex via the Carson-Bonnition and Salar basins and to the north via the Orphan Basin (Enachescu, 1992).

3.2.2.1 TETHYS RIFTING PHASE

Initial rifting began in the Late Triassic (Early Carnian) to Early Jurassic (Mid-Pliensbachian) as a vast rift system was established between the North America-Greenland and Europe-Africa continental plates. Extension was in a northwest-southeast direction. Initial rift sediments, which thicken across faults, were deposited on the pre-Mesozoic basement composed of Precambrian metamorphic and Paleozoic metasedimentary and igneous rocks. Initial rift sediments were conglomerates and siliciclastic red beds of the Eurydice Formation that filled newly created valleys under arid continental conditions. Gradual marine flooding of rift valleys by the Tethys Sea resulted in widespread evaporite deposits in restricted basins forming the Argo Formation. Thin subaerial basalt flows of the Spoonbill Formation were emplaced during

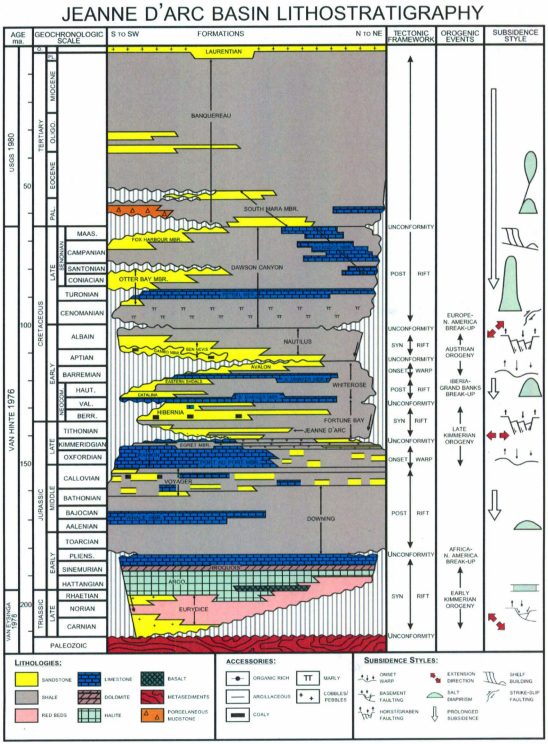


Figure 3.1: Tectono-stratigraphic chart for the Jeanne d'Arc Basin illustrating the timing of the tectonic stages, significant orogenic events, and the dominant subsidence or deformation styles. Modified after C-NLOPB (2005), Sinclair (1993) and Sinclair *et al.* (2005).

a widespread igneous event associated with the initial stage of North Atlantic rifting (Jansa and Pe-Piper, 1986). Marine limestones of the Iroquois Formation were deposited over the halite beds as more marine conditions were developed as coastal sabkhas and restricted lagoons within a warm shallow sea.

The end of the first episode of rifting is marked by development of a broad epeiric sea from Mid-Pliensbachian to Late Jurassic (Kimmeridgian). During this time plate movement was accommodated along the Newfoundland Fracture Zone via transform motion and rifting ceased to the north. This marks the first period of thermal sag in the Jeanne d'Arc Basin and a hiatus in continental crust extension. Initiation of thermal subsidence is recorded by the Downing Formation shales and limestones that reflect the depositional environment of a low-energy, shallow epicontinental sea. Fine-grained sandstones, shales and oolitic limestones of the Voyager Formation suggest infilling of the sea through deltaic nearshore to marginal-marine environments. The Rankin Formation is dominated by very shallow water limestones and minor fine-grained sandstones in the southern portion of the Jeanne d'Arc Basin but north of the Trans-Basin Fault Zone the Rankin Formation consists of fine-grained siliciclastics deposited in a deeper marine environment. The Early Kimmeridgian Egret Member is a distinctive, organic-rich shale that represents the major oil source for the Jeanne d'Arc Basin. Its interpreted depositional environment is that of a restricted, anoxic basin with high planktonic productivity (Williamson, 1992).

3.2.2.2 North Atlantic Rifting Phase

Prior to the Late Jurassic (Tithonian), extension was renewed and re-oriented in a west-east direction. The Avalon Uplift region as well as uplift and consequent erosion of the rift shoulders provided significant amounts of clastic debris into rejuvenated grabens. The Avalon Uplift is the region south of the Jeanne d'Arc Basin which experienced regional doming following the Tethys Rifting Phase, recorded by the Avalon Unconformity between deformed Jurassic and older rocks and undeformed Cretaceous sediment (Enachescu, 1987, 1992; Tankard and Welsink, 1987; Brown *et al.*, 1989; Grant and McAlpine, 1990). The term "uplift" is loosely used to refer to structural highs (relative footwall uplift) and footwall "rebound" in response to tectonic faulting in an extensional regime (Ma and Kusznir, 1993; Walsh and Watterson, 1988; and Watterson, 1986). Potential siliciclastic source areas for the Jeanne d'Arc Basin are the Avalon Uplift, south of the Egret Fault, the Bonavista Platform to the west and the Central Ridge Complex to the east. Coarse clastics of the Jeanne d'Arc Formation were deposited during the Tithonian within incised valleys, cut and filled by fluvial erosion/deposits, as well as basin-margin fluvial fans and fan-deltas. Overlying shales of the Fortune Bay Formation were deposited in a marginal marine to neritic environment and provide a good seal for the Jeanne d'Arc Formation sandstone reservoirs. Hibernia Formation sandstones are part of a northward prograding fluvial-deltaic system of medium- to coarse-grained sandstones and alternating shales and siltstones that was developed during the Early Cretaceous (Berriasian to Valanginian). The North Atlantic Rifting package is characterized by syn-tectonic structures related to synchronous basement extension, formation of salt diapirs and syn-sedimentary faulting.

A second period of basin stability was established after deposition of the Hibernia Formation reflected by deposition of the widespread "B" Marker limestone in the Late Valanginian. It is an excellent regional stratigraphic and seismic marker. A return to a nearshore marine environment is recorded by fine sandstones, siltstones, shales and minor limestones of the overlying Catalina Formation. Partially equivalent thick silty shales of the Whiterose Formation were deposited subsequently, with northward distal thickening. The "A" Marker, another laterally persistent limestone, lies above the Whiterose Formation in the Hibernia and Whiterose oilfields but grades to oolitic and bioclastic-rich sandstones in the central and southern portions of the Jeanne d'Arc Basin where it is referred to as the Eastern Shoals Formation. The end of the second thermal sag period was marked by deposition of the Avalon Formation during the Early Cretaceous (Barremian to Aptian) and the separation of the east Grand Banks from Iberia. The Avalon Formation is a coarsening-upward marine sandstone that represents regressive basin infilling (Pemberton *et al.*, 2001) that may be due to renewed tectonic activity in the Avalon Uplift area to the south.

3.2.2.3 Labrador Rifting Phase

During the Aptian-Albian, a final episode of large-scale, widespread extension and structural deformation occurred within the Jeanne d'Arc Basin. Extension was primarily in a northeast-southwest direction and is recorded in the Trans-Basin Fault Zone (Figure 1.2) as a series of northwest-southeast trending faults. There has been considerable debate on the driving mechanism for these faults (see review in Sinclair, 1993); however, the Labrador Rifting Phase is interpreted as the final episode of rifting to affect continental crust of the northern Grand Banks. For the purpose of this study, this

period of time is important because it reactivated older faults and further compartmentalized the Hibernia Formation through the introduction of northwest-southeast trending faults. Northeast-southwest extension could have also introduced a component of strike-slip movement along older, oblique faults, further complicating fault juxtapositions and reconstructions of faults that were active during Hibernia Formation deposition. Salt diapirism is also thought to be significant during this period resulting in the formation of salt ridges and pillars. Increased fault activity greatly increased accommodation space, halted the regression of the Avalon Formation, and began long-term transgression of the Ben Nevis Formation across the mid-Aptian angular unconformity. High volumes of siliciclastic sediments shed off the raised rift margins combined with high accommodation space allowed deposition of coastal plain strata buried by marginal to shallow marine sandstones of the Ben Nevis Formation. The Ben Nevis Formation grades laterally and vertically into partially time-equivalent distal shales of the Nautilus Formation. The late-Albian unconformity marks the end of the final rifting episode and separation of the northern Grand Banks from Europe along the Orphan Basin.

During the Cenomanian, the Jeanne d'Arc Basin flooded and became starved of clastic sediment leading to deposition of widespread Petrel Member lime mudstone. Two shelf building events occurred during the Late Cretaceous at the leading edges of the Otter Bay Member sandstones and the Fox Harbour Member sandstones. Prograding clinoforms observed on seismic lines indicate sediment influx from the west forming a clastic wedge. Equivalent sediments in the basin depocentre are chalky, outer neritic limestones of the Wyandot Member. Encompassing the aforementioned members are transgressive marine shales of the Dawson Canyon Formation. The top of

the Dawson Canyon Formation is marked by a regional unconformity (base Tertiary Unconformity) that exhibits channeling and canyons along the shelf edge margins. This indicates a marked drop in relative sea level, which resulted in deposition of delta front sandstones, submarine fans, and prodelta turbidites of the Paleocene South Mara Member. Throughout the Tertiary, the depositional setting over the Grand Banks is an established passive margin flanking the spreading Atlantic Ocean. Low sediment influx, long term thermal subsidence, and seaward tilting led to deposition of the structurally undisturbed marine succession of the Banquereau Formation. This marine succession consists of deep neritic shales and minor chalks, siliceous mudstones, and rare sandstone-siltstone beds. In the Oligocene, a change from deep neritic and bathyal deposition to shallow neritic environments is recorded in two regressive sandstone units. Most recent deposition was by paralic glacial deposits that were eroded and displaced by shield ice masses during the Quaternary.

3.3 FAULT CLASSIFICATION

The complex faulting history of the Jeanne d'Arc Basin has led to development of several different types of faults and interaction of these different fault types. The dominant basin-bounding faults of the Murre-Mercury Fault System are listric in nature and developed as part of the Tethys Rift episode, accommodating the majority of crustal extension. There is no direct evidence of transfer faults in the study area; however, they do exist within the Jeanne d'Arc Basin (e.g. Dominion Transfer Fault, Figure 1.2). For the purpose of this study, the term "basement" refers to Pre-Mesozoic rocks found in the study area. For example, a basement-involved fault will penetrate the underlying Pre-Mesozoic rocks. Conversely, the term "sedimentary faults" refers to syn-sedimentary

faults that do not penetrate basement rocks. Faults found in the study area can be distinguished as basement involved faults, Cretaceous basin-bounding faults, major sedimentary faults and secondary sedimentary faults.

3.3.1 Basement Involved Faults

Basement involved faults penetrate Pre-Mesozoic basement and create major crustal structural units by breaking-up the downthrown, hanging-wall block of basin-bounding faults. These divide the extended basement into: i) asymmetrical grabens that are filled with sediments and ii) horsts that are exposed or covered by a thin sedimentary layer; Figure 3.2 (after Enachescu, 1987). Basement involved faults that developed in response to basin-bounding faults are of two types: i) antithetic faults; those faults that have an opposite sense of dip to the basin-bounding fault and ii) synthetic faults; those faults that have a similar sense of dip to the basin-bounding fault. Wernicke (1981), Gibbs (1983, 1984), and Angelier (1985) discussed how basement involved faults play an important role in increasing the complexity of a rift system. These faults border either side of the Central Ridge Complex and are responsible for providing the main building blocks of the Beothuk Knoll, Flemish Cap, and other major tectonic elements found throughout the Jeanne d'Arc Basin.

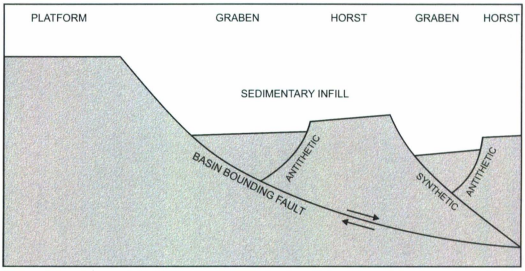


Figure 3.2: Simplified geological cross-section of basement involved faults. Take note of their relation to the basin-bounding fault. After Enachescu (1987).

3.3.2 CRETACEOUS BASIN-BOUNDING FAULTS

Cretaceous basin-bounding faults are the result of renewed extension during the Late Jurassic-Early Cretaceous North Atlantic Rift episode. These faults are basement involved faults that pierce pre-Cretaceous sediments and provide accommodation space for the Cretaceous sedimentary fill (Figure 3.3; Enachescu, 1987). They are particularly important because they were active during deposition of the Hibernia Formation and thus have a direct influence on the distribution of Cretaceous sediments. The Voyager fault system is made of Cretaceous basin-bounding faults that make-up the eastern boundary of the Jeanne d'Arc Basin and reflects the west-east extension experienced during the North Atlantic rift episode. However, subordinate north-northeast to south-southwest extension is recorded by the Cretaceous Egret Fault as there is over one kilometer of sedimentary growth across this fault (Enachescu, 1987). Similar growth magnitude is observed across the Voyager Fault System. The Egret Fault is the

southern boundary of the Jeanne d'Arc Basin and connects the Murre and Voyager fault systems. The Voyager Fault System separates the Jeanne d'Arc Basin from the Central Ridge Complex to the east. These faults were reactivated in the subsequent thermal sag and Labrador Rift episodes providing additional accommodation space at later times, as well as introducing further structural complexity.

3.3.3 MAJOR SEDIMENTARY FAULTS

Major sedimentary faults found in the Jeanne d'Arc Basin generally sole deeply and at a low angle into basin-bounding faults, top basement surfaces, or along salt contacts (Enachescu, 1987). They can be the source of additional horsts and grabens away from the basin margins. Significant rollover structures are often associated with these faults and can be amplified by the existence of a salt core. Figure 3.3 illustrates a major sedimentary fault that soles along a Triassic salt structure above the underlying basement block. A rollover structure in the Jurassic and Cretaceous sediments, cored by Triassic salt, is shown to accompany the fault. These faults play an important role in controlling the depositional loci of reservoir rocks, formation of hydrocarbon traps, and migration of hydrocarbons due to their large displacement and often repeated growth and reactivation during subsequent rifting episodes.

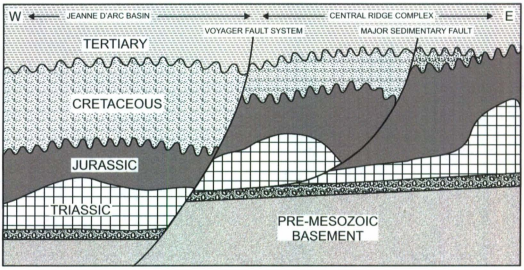


Figure 3.3: Simplified geological cross-section of a Cretaceous basin-bounding fault (Voyager Fault System). Also shown in the figure is a major sedimentary fault. Note how the major sedimentary fault soles out above the basement block, while the Voyager Fault System pierces the basement rock and shows significant growth in the Cretaceous sediments. After Enachescu (1987).

3.3.4 Secondary Sedimentary Faults

Secondary, or minor, sedimentary faults are high angle, listric, antithetic and synthetic faults that accompany a major sedimentary fault or salt structure (Enachescu, 1987), and provide additional sedimentary accommodation space. They form local grabens, horsts, tilted blocks, and local rollovers that have proven to be excellent hydrocarbon traps in the Jeanne d'Arc Basin through discoveries of the Hibernia, Terra Nova, and White Rose oil fields. Salt piercement and collapse structures are also related to the formation of a series of secondary faults. Intersecting fault families can be observed in three dimensional seismic datasets, where one set exhibits subsequent fault plane faulting. The Trans Basin Fault Zone is composed of a series of major and minor sedimentary faults that connect the Hibernia oil field to the northern edge of the Terra Nova oil field. Figure 3.4 illustrates the distinction and relationship of minor sedimentary faults with major sedimentary faults.

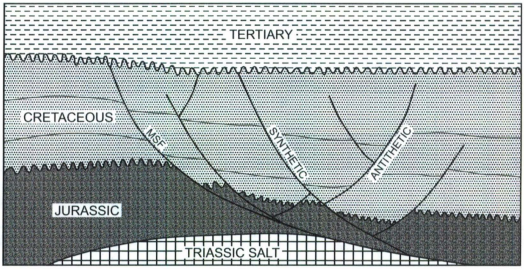


Figure 3.4: Simplified geological cross-section illustrating the relationship of minor sedimentary faults to a major sedimentary fault (MSF). Note the antithetic and synthetic geometry of the minor faults and how the major fault soles along a salt surface. After Enachescu (1987).

3.4 DISTINCTION OF FAULTS WITHIN THE STUDY AREA

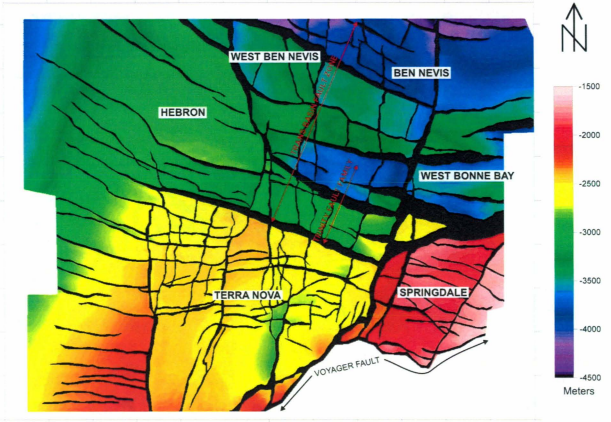
The focus area of this thesis is delineated by the three-dimensional seismic dataset that covers the Terra Nova, Hebron, Ben Nevis, West Ben Nevis, West Bonne Bay, and Springdale oil and gas fields (Figure 3.5). The Terra Nova oil field is the only field currently under development; remaining fields are part of significant discovery licenses and signify the future potential of the Jeanne d'Arc Basin with recent emphasis on the Hebron – Ben Nevis oil fields. For this reason the study area is often referred to as the Terra Nova to Hebron-Ben Nevis area. As shown in Figure 3.5, the Voyager Fault System lies in the southeastern corner of the study area and trends approximately northeast-southwest.

The Terra Nova to Hebron-Ben Nevis study area of this thesis contains a record of three distinct rift episodes that have affected the Jeanne d'Arc Basin. The Tethys rift

episode is not as recognizable as the North Atlantic and Labrador rift episodes, but is recorded through identifiable basement involved faults that formed the basin margin (Figure 3.6). Generally, however, the three dimensional seismic dataset was not recorded deep enough to sufficiently image the basement, thus it is only visible in the southeastern corner of the study area where basement rocks are closer to the surface within the Central Ridge Complex.

The North Atlantic rift episode is extensively recorded across the study area as it was one of two main extensional periods of the Jeanne d'Arc Basin during which widespread reservoir-quality sediments were deposited. West-east extension formed north-south trending fault systems (Figure 3.5) that created a series of horsts and grabens across the entire study area. Figure 3.7 illustrates a major sedimentary fault and associated graben, formed via minor antithetic sedimentary faults, in the hanging wall. The graben provided accommodation space during deposition of the Hibernia Formation, as recorded by overall thickening of the Hibernia Formation across the graben structure (Figure 3.7). Small, discrete thickness changes are evident along the north-south faults when correlating individual seismic surfaces across the fault, suggesting gradual growth of the faults during deposition of the Hibernia Formation. The North Atlantic rift episode was also responsible for forming the Voyager Fault System, or the Cretaceous basin-bounding fault, which separates the Jeanne d'Arc Basin to the west and the Central Ridge Complex to the east (Figure 1.2). North-south trending faults also sub-divide the Terra Nova oil field into a series of horsts and grabens that acted as barriers or conduits for deposition of the clastic sediments from the southern Avalon Uplift source area (Figure 3.5).

The Labrador rift episode is also extensively recorded across the study area through major and minor sedimentary faults trending northwest-southeast to west-east. These faults further compartmentalized the Jeanne d'Arc Basin's reservoirs and formed the Trans Basin Fault Zone, which connects the Murre-Mercury Fault System to the Voyager Fault System across the Hibernia and Terra Nova oil fields. Compartmentalization of the Jeanne d'Arc Basin can be seen in Figures 3.5 and 3.8 through a series of west-east trending minor sedimentary faults. Major sedimentary faults labelled in Figure 3.6 are part of the Trinity Fault System. The Trinity Fault System is part of the Trans Basin Fault Zone and marks the northern boundary of the Terra Nova oil field and separates it from the Hebron-Ben Nevis oil field to the north. Some faults in the Trinity Fault System have offsets of more than one kilometer, acting as hydrocarbon traps for the Hebron-Ben Nevis oil field with the juxtaposition of Hibernia Formation reservoirs against older Fortune Bay Formation shales.



Top of Hibernia Formation - Depth TVDSS Map

Figure 3.5: True vertical depth below sea level map of the top of the Hibernia Formation. The various oil and gas fields that the study area covers are labeled in the white boxes. The Trans Basin Fault Zone is also labeled as the trend of northwest-southeast trending faults that mark the area north of the Terra Nova oil field. The Trinity Fault family is the first set of faults in the Trans Basin Fault Zone that marks the northern boundary of the Terra Nova oil field. The Voyager Fault is in the southeastern corner of the study area and essentially marks the southeastern depositional or erosional limit of the Hibernia Formation.

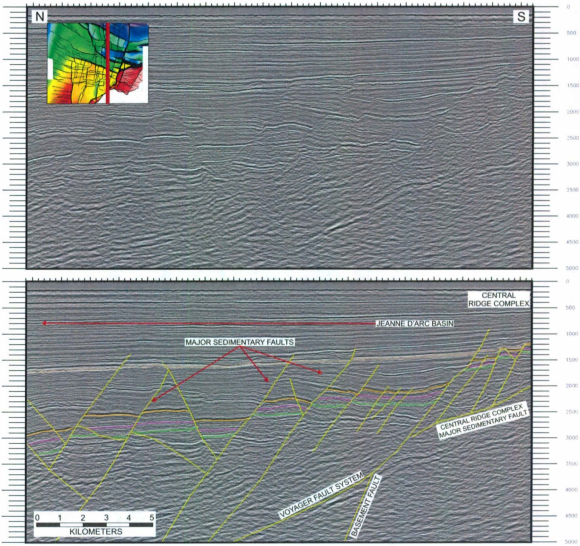


Figure 3.6: North-south seismic section (crossline 942) from the eastern area of the study area. Location is shown on inset structure map of Top of Hibernia Formation. Top figure is the uninterpreted seismic line. Bottom figure has the faults interpreted in yellow. The base Cenomanian Unconformity is in brown; note how faults generally do not penetrate this horizon. The Top, Mid- and Base Hibernia Formation are shown in orange, purple, and green, respectively. Note the growth across the Voyager Fault System (Cretaceous basin-bounding fault) of the Hibernia Formation. Three major sedimentary faults are also highlighted in the Jeanne d'Arc Basin as well as one over the Central Ridge Complex.

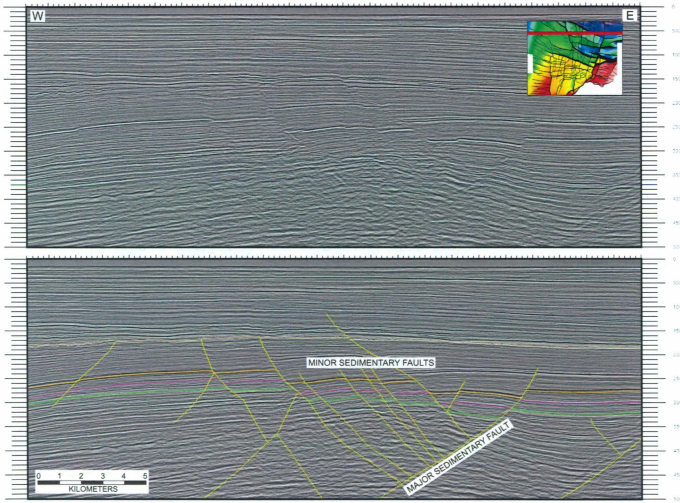


Figure 3.7: West-east seismic section (inline 790) from the northern area of the study area. Location is shown on inset structure map of Top of Hibernia Formation. Top figure is the uninterpreted seismic line. Bottom figure has the faults interpreted in yellow with the distinction between major and minor sedimentary faults. The base Cenomanian Unconformity is in brown; note how faults generally do not penetrate this horizon. The Top, Mid- and Base Hibernia Formation are shown in orange, purple, and green, respectively.

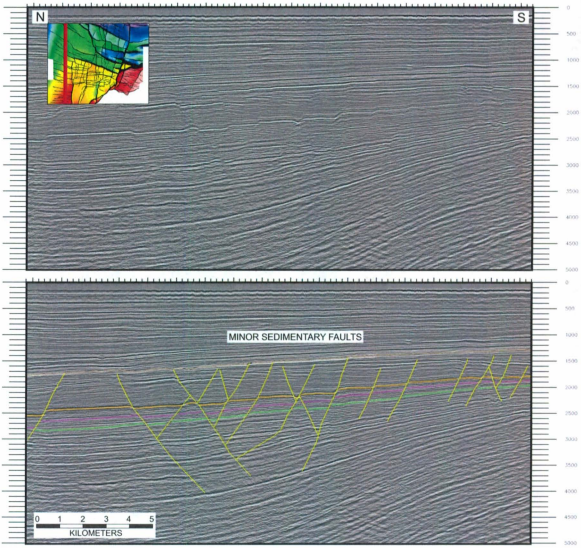


Figure 3.8: North-south seismic section (crossline 462) from the western area of the study area. Location is shown on inset structure map of Top of Hibernia Formation. Top figure is the uninterpreted seismic line. Bottom figure has the faults interpreted in yellow. The base Cenomanian Unconformity is in brown; note how faults generally do not penetrate this horizon. The Top, Mid- and Base Hibernia Formation are shown in orange, purple, and green, respectively. The minor sedimentary faults presented here are post-Hibernia Formation deposition as a result of the later Labrador Rift extension. Notice the significant overall sedimentary growth to the north, towards the basin depocentre.

The Hibernia Formation, the primary focus of this thesis, was deposited during the Berriasian to Valanginian. Faults that influenced deposition of the Hibernia Formation are the Voyager Fault System, which essentially marks the southeastern boundary, and north-south faults, which were main sources of accommodation space at the time. Most west-east trending faults were likely created during the Labrador rift episode. However, some may have formed during the North Atlantic rift episode as minor sedimentary faults cutting through the siliciclastic and carbonate wedge that formed across the hanging wall of the Voyager Fault System, extending towards the basin's depocentre. It is difficult to determine if these small faults were active during deposition of the Hibernia Formation since fault offset is generally low and seismic resolution is not high enough to measure significant thickness variations. Thickness variations are recorded in seismic sections and in well logs across larger offset north-south faults that subdivide the Terra Nova and Hebron-Ben Nevis oil fields. Thickness changes and variations of the Hibernia Formation will be discussed in greater detail in subsequent chapters dealing with the seismic dataset, petrophysical log data, and depositional environments.

3.5 SUMMARY

The Jeanne d'Arc Basin has experienced three episodes of rifting, the orientation of which rotated counterclockwise from northwest-southeast extension through west-east extension to the final northeast-southwest extension. The most significant episode of extension was during the Late Jurassic-Early Cretaceous, which caused development of the Avalon Uplift to the south and the eastern basin-bounding Voyager Fault System. This extension and associated uplift of the basin flanks led to an influx of siliciclastic

sediment towards the depocentre of the Jeanne d'Arc Basin resulting in deposition of the Hibernia Formation. West-east extension of the North Atlantic rifting episode formed a network of north-south trending normal faults that formed a series of horsts and grabens leading away from the southern source area. These grabens acted as conduits for sediment transport as the Hibernia Formation preferentially filled in topographic lows created by the grabens compared to being deposited overtop horst blocks. During the Late Valanginian, extension halted and a prolonged period of basin stability was maintained, which lead to deposition of a widespread limestone ("B" Marker Limestone) across the Jeanne d'Arc Basin, effectively capping the top of the Hibernia Formation. The final period of rifting was initiated in the Aptian-Albian through northeast-southwest extension that severely compartmentalized the Jeanne d'Arc Basin. The combination of significant fault offsets, forming lateral traps, and vertical sealing of reservoirs by overlying shales, created structures for entrapment of migrating hydrocarbons. Following chapters of this thesis deal with seismic, petrophysical log and core interpretations, which have been combined to develop an integrative description of the Hibernia Formation across the study area. A depositional model has been developed using interpretations derived from seismic, well and core data, providing a framework for the prediction of petroleum reservoir locations.

CHAPTER 4 – THREE-DIMENSIONAL SEISMIC DATASET

4.1 SCOPE AND PURPOSE

Three-dimensional seismic data are a very useful tool for understanding the complex structural architecture of the subsurface, especially in a highly faulted rift basin where a high density of data points are necessary to fully capture the basin's complexity. The seismic dataset allowed mapping of the main stratigraphic boundaries of the Hibernia Formation over the study area. As discussed in Chapter 3, the seismic data also allowed mapping of numerous seismically-visible extensional faults that exist in the study area. The primary focus of seismic mapping was to characterize the Hibernia Formation at high lateral resolution and to correlate seismic facies changes using seismic attributes. The seismic data also provided gross thickness variations, which in turn reflect the activity of faults during deposition.

The seismic dataset was interpreted in two parts. First, the seismic response was determined for three key surfaces within the Hibernia Formation; top, middle and base Hibernia Formation. These surfaces were subsequently mapped across the study area and seismic attributes were extracted from the seismic dataset along the mapped surfaces. Based on seismic attributes, several distinct regions were identified for each surface. These regions were further compared to several well log responses to derive the overall lithologies corresponding to the seismically defined regions. Second, seismic attributes were investigated in three dimensions focusing on two intervals, the Upper and Lower Hibernia Members, defined by the three key seismic surfaces. Anomalies that were identified in plan view for each key surface were further investigated in three dimensions to aid understanding the cause of the seismic anomalies.

Seismic data interpretation is less reliable without well ties to correlate seismic response to petrophysical response. Synthetic seismograms (discussed in Chapter 2) were first constructed for wells so the well stratigraphy could be correlated to the seismic markers. This chapter primarily focuses on the seismic aspect of the project and briefly introduces petrophysical well data. Well correlations and descriptions are discussed in greater detail in Chapter 6 and further compared to the seismic data in Chapter 7.

4.2 Seismic Marker Definition

4.2.1 Base of Hibernia Formation

The base of the Hibernia Formation is defined as the distinct change from underlying marine Fortune Bay Formation shales to overlying coarser clastic sediments associated with progradation of the Lower Hibernia Member. This change is gradual but yet still distinct enough to be identified in both the petrophysical well logs and seismic dataset. Figure 4.1 illustrates the basal boundary of the Hibernia Formation (represented as well pick GDL_300) at the Petro-Canada et al. Terra Nova G-90_5Z well (refer to Figure 2.1 for well location). As shown, the contact is within a thick package of shale but at distinct changes seen in the logs. Transition from marine to fluvial deposition is marked by gradual reduction upwards of the total gamma ray log but more distinctly by the sharp reduction upwards of Uranium response on the spectral gamma ray log (SGR) in the Lower Hibernia Member. Relative to high $GR_{Uranium}$ content of organic-bearing marine shales, much less U is adsorbed onto carbonaceous organic matter of terrestrial origin (Rider, 1996). Hence, decreased Uranium signatures are often used to distinguish shales of continental origin from marine shales (Adams & Weaver, 1958). In this case, increased continental input due to the onset of deposition of the

Hibernia Formation may have reduced the fixation of Uranium compared to the underlying Fortune Bay Formation marine shales. Shales overlying the basal contact are also slightly seismically slower than underlying shales resulting in a seismic response, which can be correlated to a peak in the synthetic seismogram. Bulk density has minimal fluctuation across the boundary. The subtle nature of the seismic marker makes it quite difficult to correlate in the seismic data; however, moving basinward this seismic marker becomes increasingly more pronounced, especially away from highly faulted areas of the southeastern region of the study area. One of the main reasons why

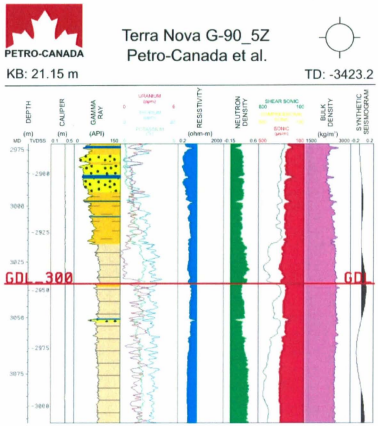


Figure 4.1: Petrophysical log at the Terra Nova G-90_5Z well over the depth interval: 2887-3007 meters TVDSS. Displayed well pick (GDL_300) marks the base of the Hibernia Formation. It is characterized as the subtle, yet often sharp, increase in velocity with depth creating a moderate seismic peak signature. The velocity change also correlates well with a sharp change in the Uranium spectral gamma ray signature between basal shales of the Hibernia Formation and underlying Fortune Bay Formation shales.

fault-density affects the seismic signature of this boundary is that minor sedimentary faults often sole out within the thick shale package of the Fortune Bay Formation. Another reason for the increasing basinward prominence of the basal Hibernia Formation seismic marker might be decreased coarse-grained siliciclastic content of the underlying Fortune Bay Formation leading to greater acoustic contrast.

The base of the Hibernia Formation ranges in depth from 1800 meters to 5400 meters below sea level (Figure 4.2). It has a gentle westward dip in southern and western regions of the study area but in the northeast corner it has an abrupt change to a northerly dip due to post-depositional faulting and subsequent block rotation along the Trans Basin Fault Zone. Figure 4.3 displays seismic coherency and narrow trends of relatively low values typically highlight fault zones, which can be seen as non-coherent areas that parallel fault planes. Overall, the seismic marker seems to be fairly incoherent in the region surrounding the Terra Nova oil field and becomes increasingly more coherent north of the Trinity Fault. This is probably due to two factors: i) fault density is higher in the southern region, close to the Voyager Fault System and ii) possibly prodeltaic, basal shales are thicker in the north providing a consistent contrast with the underlying Fortune Bay Formation (discussed in Chapter 6). Figure 4.4 represents seismic reflection strength and further illustrates this south-to-north change in seismic response. The southern area is dominated by fairly low reflection strength, whereas north of the Trinity Fault there is a distinct increase in reflection strength. Again, this is likely due to increased thickness of basal prodelta shales above the base of the Hibernia Formation boundary, providing a clear response that can be resolved in seismic data. There are also several zones of high reflection strength in the southern region that do not appear to be correlative to fault trends and may be representative of

local incision of the overlying Hibernia Formation into the Fortune Bay Formation. Figure 4.5 represents instantaneous seismic frequency and illustrates a decrease in frequency towards the northeast. Within the Terra Nova oil field, seismic frequency is fairly high, averaging 45 Hz or more. North of the Trinity Fault, however, there is a distinct decrease in dominant frequency to 30-40 Hz in the west and 20-35 Hz in the east. This is probably due to two factors: i) attenuation of higher frequencies with depth due to the effect of the series of down-to-the-north large offset normal faults making-up the Trans Basin Fault Zone, and; ii) thickness of the seismic response boundary.

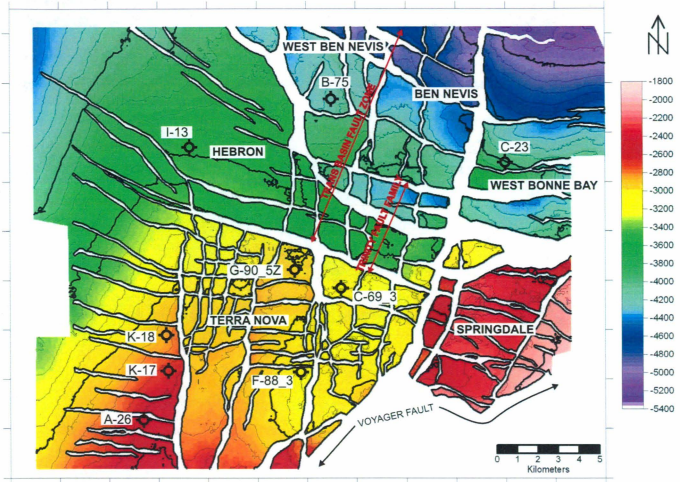


Figure 4.2: True vertical depth below sea-level map of the base of the Hibernia Formation. Contour interval is 100 meters with every 500 meters in bold lines. Note the easterly dip in the western and southern areas with the transition to a northerly dip within the Trans Basin Fault Zone.

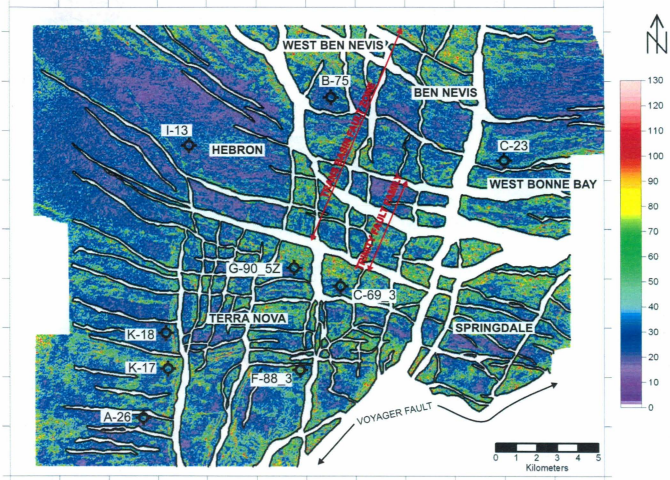


Figure 4.3: Seismic coherency map of the base of the Hibernia Formation. The scale bar is opposite to natural instinct, in which correlative events are displayed as lows and non-correlative events are displayed as highs. Overall, the base of the Hibernia Formation appears to be coherent near Hebron and progressively less coherent in the south. The thin zones of incoherency that mimic the overlain fault trends most likely represent the fault zone, where an abundance of seismically invisible faults/fractures are likely to exist.

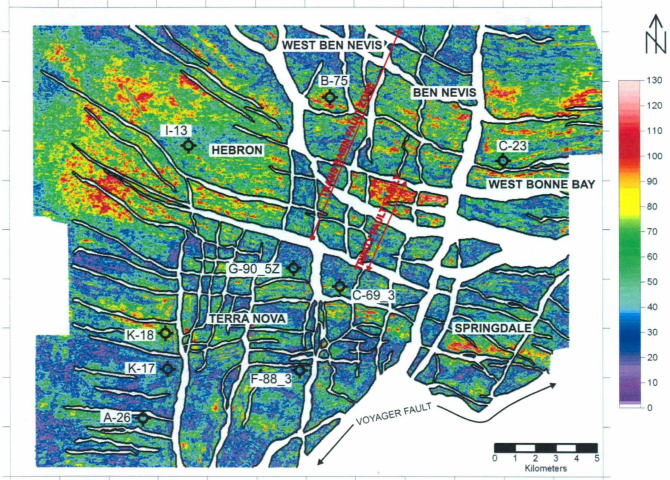


Figure 4.4: Reflection strength map of the base of the Hibernia Formation. Note the distinct increase in reflection strength to the north. Several zones of high reflection strength exist in the southern region and are likely due to local changes (ie. increased sandstone thickness above the basal boundary) rather than the larger scale northern transition.

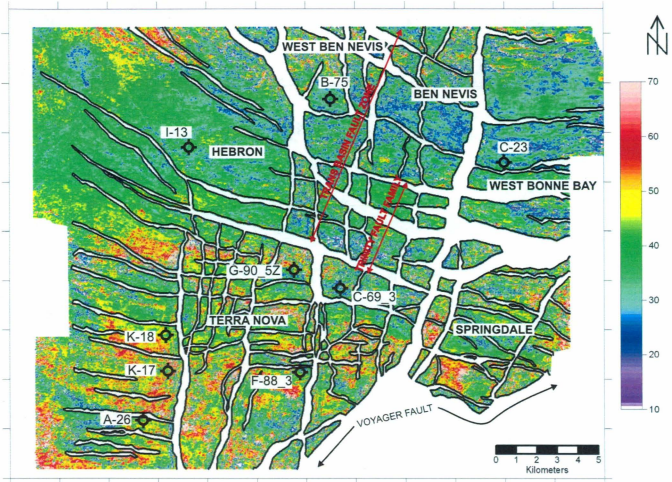


Figure 4.5: Instantaneous frequency map of the base of the Hibernia Formation. The Trinity Fault transition zone further illustrates the seismic character change to the north. The southern area is dominated by higher frequencies and is markedly different than the northern, lower frequencies. The overall decrease to the north, however, may be due to the attenuation with depth of the seismic frequency spectrum.

Variations in petrophysical character can be seen in Figures 4.6 – 4.8 and will be discussed in greater detail in Chapter 6. Figures 4.6 – 4.8 display a fifty meter zone above and below the base Hibernia Formation boundary on nine selected wells; well locations are displayed on the maps of Figures 4.2 – 4.5. Beginning in the southwest with the King's Cove A-26, Terra Nova K-17, and Terra Nova K-18 wells the contrast across the boundary can be clearly seen (Figure 4.6). The King's Cove A-26 well shows deposition of thin sandstone beds near the top of the Fortune Bay Formation overlain by a thick package of basal shale of the Hibernia Formation. This provides sharp contrast that can be seen in gamma ray, sonic and density logs and is clearly imaged in seismic data. Similarly, the Terra Nova K-17 well shows deposition of thin sandstone beds, although significantly less than King's Cove A-26, near the top of the Fortune Bay Formation. However, basal shales of the Hibernia Formation are significantly thinner. The synthetic seismogram shows a weak response that is likely due to noisy sonic and density logs due to poor well bore conditions, which can be identified by increased caliper over this basal interval. Sharp reduction of $GR_{Uranium}$ in shales above the base Hibernia Formation boundary clearly identifies the top of Fortune Bay shales. The Terra Nova K-18 well shows a mixed seismic response at the base of the Hibernia Formation. The top of the Fortune Bay Formation has few identifiable thin sandstone beds but appears to contain intervals of significant siltstone content. Approximately twenty-five meters below the base Hibernia Formation boundary there is another boundary that displays an increase in seismic velocity and bulk density creating another seismic peak in the synthetic seismogram. These two boundaries are close enough together such that the synthetic seismogram does not fully resolve either response, which results in two incomplete seismic peaks combining to form one duplex seismic peak.

Further east, at the centre of the Terra Nova oil field are the locations of the Terra Nova F-88_3, Terra Nova G-90_5Z, and Terra Nova C-69_3 wells (Figure 4.7). These three wells highlight the relative consistency of the seismic response of the base Hibernia Formation boundary throughout this region. Basal shales of the Hibernia Formation are clearly distinguishable from underlying Fortune Bay Formation shales through slight deflection in the gamma ray logs as well as lower seismic velocity (higher sonic) in the Hibernia Formation (more pronounced in shear sonic logs when present). There is often no noticeable change in bulk density between the two shales. These characteristics combine to produce a moderately strong seismic response. Basal Hibernia Formation shale thickness may be a cause for changing instantaneous frequency of the seismic data along the base Hibernia Formation boundary, where the frequency is thought to be inversely proportional to the amount of shale deposited.

North of the Trinity Fault System, in the region dominated by high seismic reflection strength and low frequency, are the locations of the Hebron I-13, West Ben Nevis B-75, and West Bonne Bay C-23 wells (Figure 4.8). These wells are located in more distal positions in comparison to the previous six wells and show an increase in shale thickness. High reflection strength seen in the seismic attribute mapping is not clearly identifiable through the petrophysical log data. The seismic signature still appears to be caused by a velocity increase across the base Hibernia Formation boundary; however, it seems to be gradual except for an approximately ten-meter thick low velocity zone that can be seen at the Hebron I-13 well. This zone would be a cause of stronger amplitudes (due to the greater reflection coefficients) and possibly a higher frequency response (due to its thin nature). Absence of significant sharp contrasts at the West Ben Nevis B-75 and West Bonne Bay C-23 wells should generate lower reflection

strength and lower frequency due to a thick seismic response zone. Therefore, the northern petrophysical well data do not fully coincide with the seismic response that is seen in seismic attribute maps. However, in part this is likely due to missing petrophysical data introducing errors in the synthetic seismogram. For example, note the truncation of neutron density and bulk density logs in the West Bonne Bay C-23.

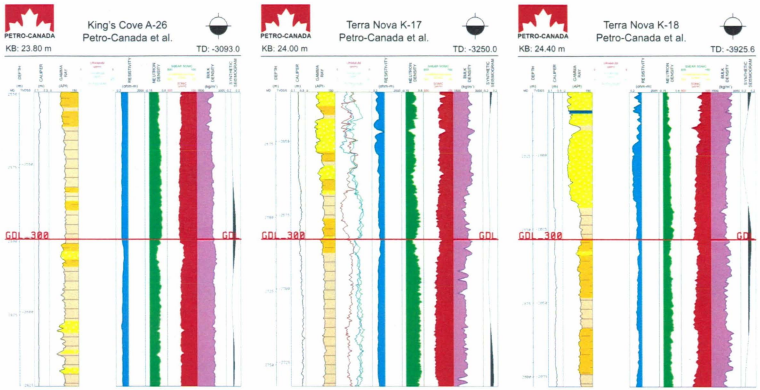


Figure 4.6: Petrophysical signature of the base Hibernia Formation boundary (represented as well pick GDL_300) at the King's Cove A-26, Terra Nova K-17 and Terra Nova K-18 wells. Locations of these wells can be seen in Figures 4.2 - 4.5. Deposition of sandstone and siltstone beds in the upper Fortune Bay Formation provide a sharp contrast with the base Hibernia Formation shales and provide a good source for strong reflections. Absence of these beds at the Terra Nova K-17 well explains the low reflection strength visible in the synthetic seismogram. Gamma ray log is filled with CanStrat® lithology interpretation where yellow=sandstone, orange=siltstone, brown=shale, and blue=carbonates or carbonate-cemented intervals.

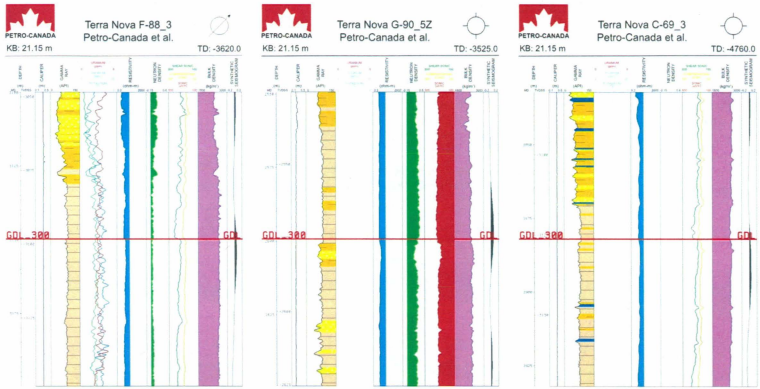


Figure 4.7: Petrophysical signature of the base Hibernia Formation boundary (represented as well pick GDL_300) at the Terra Nova F-88_3, Terra Nova G-90_5Z and Terra Nova C-69_3 wells. Locations of these wells can be seen in Figures 4.2 - 4.5. These three wells highlight the consistency of the seismic response of the base Hibernia Formation. The base Hibernia Formation boundary is indicated by the minor decrease-upwards in the gamma ray as well as the increase-upwards in sonic. There is no significant change, in general, in the density log, however there is occasional increase in density with depth. Gamma ray log is filled with CanStrat® lithology interpretation where yellow=sandstone, orange=siltstone, brown=shale, and blue=carbonates or carbonate-cemented intervals.

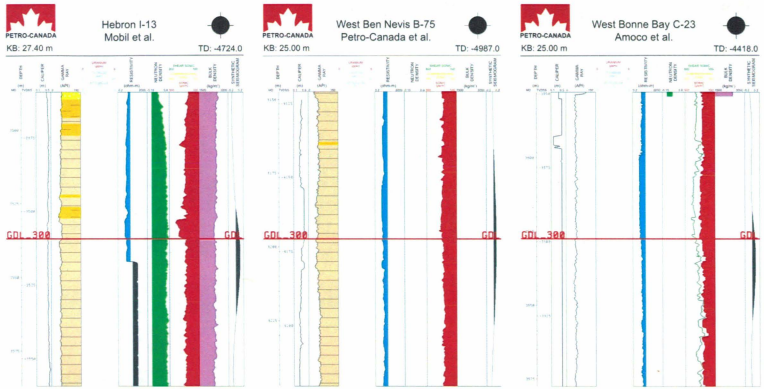


Figure 4.8: Petrophysical signature of the base Hibernia Formation boundary (represented as well pick GDL_300) at the Hebron I-13, West Ben Nevis B-75 and West Bonne Bay C-23 wells. Locations of these wells can be seen in Figures 4.2 - 4.5. The distal location of these three wells in comparison to the previous six wells is shown through the higher deposition of shale at the base of the Hibernia Formation as well as the lack of thin sandstone and siltstone beds in the upper Fortune Bay Formation. The nature of the base Hibernia Formation boundary is not clearly identified in the petrophysical logs. Lower frequency seen in seismic attribute mapping is likely due to the thick shale above and below the boundary, creating a thick seismic response interval. The source of high reflection strength is not obvious through the study of the petrophysical parameters and may be due to visible seismic velocity contrasts being clearly imaged through absence of thin bed "noise". Gamma ray log is filled with CanStrat® lithology interpretation where yellow=sandstone, orange=siltstone, brown=shale, and blue=carbonates or carbonate-cemented intervals.

4.2.2 MID-HIBERNIA FORMATION

The mid-Hibernia Formation seismic marker is a distinct widespread maximum flooding surface at the base of the Valanginian that separates the Upper and Lower Hibernia Member deltaic succession (see Chapters 6 and 7). For the purpose of this study, in the context of deltaic successions, a flooding surface marks the cessation of clastic input into a region, either by sea-level rise and/or lateral migration of the sediment source. Therefore, a maximum flooding surface would represent a large-scale or regional flooding event marked by a significant, overall shift from sandstone-dominated deposition to shale-dominated deposition. The position of the flooding surface within the thick package of interbedded sandstones, siltstones and shales makes it somewhat difficult to correlate throughout the highly faulted southeastern area of the study area. Figure 4.9 illustrates the petrophysical signature of the mid-Hibernia Formation boundary (represented as well pick GDL_320) at the Petro-Canada et al. Terra Nova G-90_5Z well (refer to Figure 2.1 for well location). The mid-Hibernia Formation horizon, picked as the highest Gamma Ray immediately above a laterally continuous sandstone package (~20 – 25 meters thick), is interpreted as a maximum flooding surface. It is important to recall that the peak frequency of the seismic dataset is approximately eighteen hertz (sixty-two meter quarter-wavelength) at this depth with a maximum frequency generally in the range of fifty hertz (twenty two meters quarter-wavelength). This frequency range prohibits imaging the rather thin beds found enveloping the mid-Hibernia Formation flooding surface, instead the seismic data are responding to larger scale trends seen in the sonic and bulk density logs. Note how the bulk density log records a thick block of dense sediments surrounding the flooding surface while the sonic logs display a pattern of increasing velocity with depth for the same interval. This signature results in the

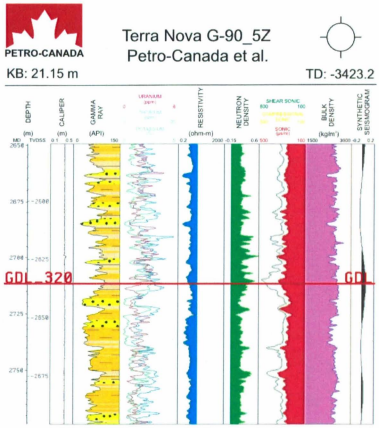


Figure 4.9: Petrophysical log at the Terra Nova G-90_5Z well over the depth interval: 2575-2695 meters TVDSS. The displayed well pick (GDL_320) marks the mid-Hibernia Formation. It is characterized by the high bulk density and increase in velocity with depth creating a moderate seismic peak signature. It is also constrained as the flooding surface that can be seen in the gamma ray log.

creation of a seismic peak across the depth interval encompassing the flooding surface.

The mid-Hibernia Formation surface has a similar structure to the base Hibernia Formation, as is expected since there are no major fault detachment surfaces located within the Hibernia Formation. The depth range of the mid-Hibernia Formation is from 1700 meters to 4900 meters below sea level (Figure 4.10). Figure 4.11 represents seismic coherency and illustrates the rather uniform and monotonous signature of the mid-Hibernia Formation marker. No distinctive features stand-out for this boundary, except for the correlative region in the northeast corner. The remainder of the seismic

marker appears to be a moderately correlative event with randomly fluctuating levels of coherency with no real distinct zonation. Figure 4.12 represents seismic reflection strength and illustrates several distinct zones of varying reflection strength. The mid-Hibernia Formation marker seems to have relatively low reflection strength throughout the study area except for the notable increase in the northeast region. An approximately west-east trend of higher reflection strength exists through the middle of the study area and connects to the high values seen in the northeast region. Figure 4.13 represents instantaneous seismic frequency and further subdivides the mid-Hibernia Formation seismic marker into various zones. The southern area of the region is dominated by very high frequencies and is sharply bounded to the north by mid-range frequencies that seem to follow the same west-east trend of high reflection strength seen in Figure 4.12. The northwest region of the study area is dominantly high frequencies but slightly lower than the southern region, possibly due to greater depths to the north that might be attenuating higher frequencies. The northeast region shows the lowest frequencies, which are similar to the west-east trend. Again, greater depth to the northeast likely attenuates some higher frequencies.

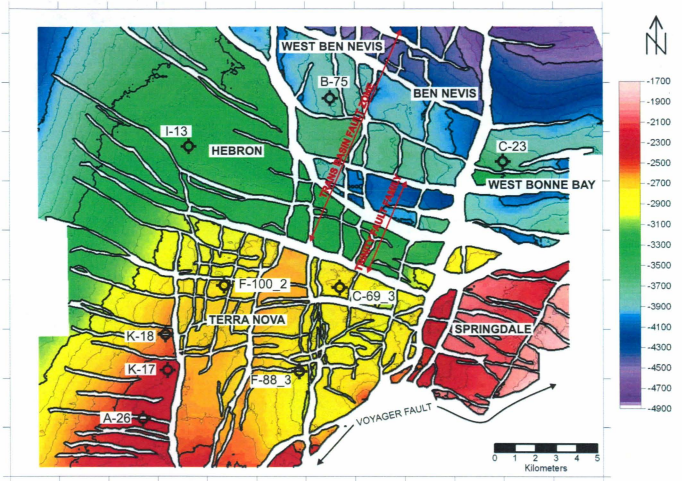


Figure 4.10: True vertical depth below sea-level map of the mid-Hibernia Formation. Contour interval is 100 meters with every 500 meters in bold lines. Note the easterly dip in the western and southern areas with the transition to a northerly dip within the Trans Basin Fault Zone.

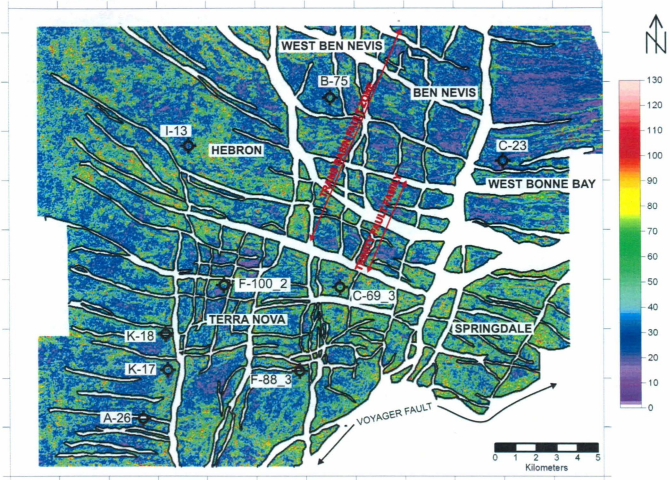


Figure 4.11: Seismic coherency map of the mid-Hibernia Formation. The scale bar is opposite to natural instinct, in which correlative events are displayed as lows and non-correlative events are displayed as highs. Overall, the mid-Hibernia Formation appears to be rather uniform and no distinct zoning is distinguishable, except for the very correlative region in the northeast. The thin zones of incoherency that mimic the overlain fault trends most likely represent the fault zone, where an abundance of seismically invisible faults exist.

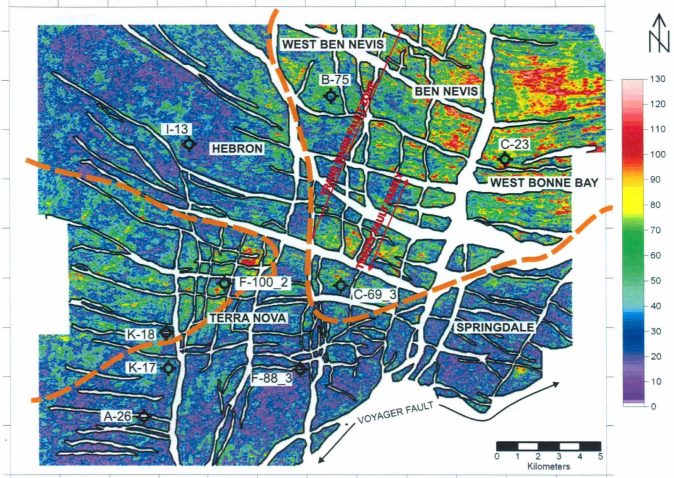


Figure 4.12: Reflection strength map of the mid-Hibernia Formation. Note the distinct increase in reflection strength in the northeast region, as well as the moderate reflection strength region in the west. Overall the mid-Hibernia Formation is of relatively weak reflection strength, except for several small, localized zones of high reflection strength. The dashed orange lines on the map highlight the two broader zones.

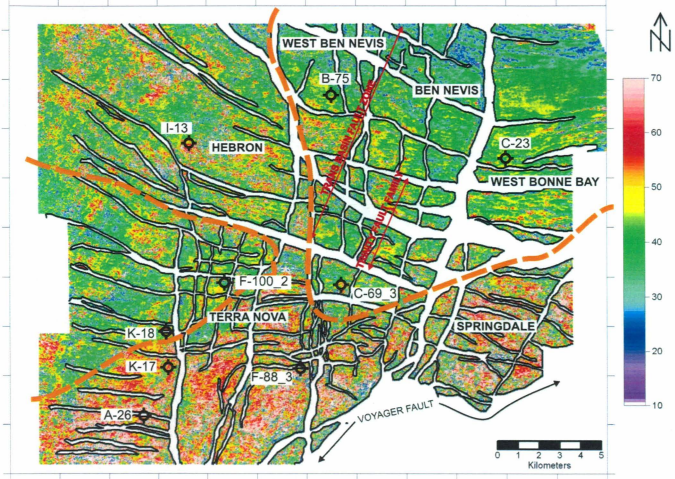


Figure 4.13: Instantaneous frequency map of the mid-Hibernia Formation. The southern region is dominated by the highest frequencies and the region in the northwest has moderately high frequencies as well. There is a zone of moderate frequencies in the central west region and a zone of low frequencies in the northeast region. The dashed orange lines on the map highlight these zones.

Anomalies seen in seismic attribute mapping can be seen in petrophysical signatures through Figures 4.14 – 4.16 and are discussed in greater detail in Chapter 6. Figures 4.14 – 4.16 display a fifty meter zone above and below the mid-Hibernia Formation boundary on nine selected wells; well locations are displayed on the maps of Figures 4.10 – 4.13. Beginning in the southwest with the King's Cove A-26, Terra Nova K-17, and Terra Nova K-18 wells the increase in reflection strength to the north can be seen (Figure 4.14). The King's Cove A-26 and Terra Nova K-17 wells both have abundant interbedded sandstone and shale above the mid-Hibernia Formation surface. Fluctuations in reflection strength may be sourced from the presence of multiple thin beds above the mid-Hibernia Formation boundary. Regions of low reflection strength may be indicative of abundant sandstone beds, such that the percentage of sandstone is greater than shale, thus reducing the reflection coefficient at the boundary if the thin beds are considered as a package. The opposite would be true for regions of high reflection strength if the interval below the boundary is considered to be relatively constant, which it is for approximately thirty meters below the boundary. At the Terra Nova K-18 well sandstone abundance is reduced above the boundary, providing greater contrast with the underlying thick sandstone interval, resulting in a stronger seismic response. Lesser sandstone content above the boundary is also seen at the King's Cove A-26, Terra Nova K-17, and Terra Nova K-18 wells along with the corresponding strengthening of the synthetic seismogram at the boundary. It is important to note that the peak seismic response does not correlate precisely with the stratigraphic marker since the maximum flooding surface is located within a shale package while the seismic data is primarily responding to the underlying thick sandstone interval. It is also

important to note that the thick sandstone interval below the boundary is highly correlative across the entire study area.

Further east, towards the Terra Nova oil field are the locations of the Terra Nova F-88_3, Terra Nova F-100_2, and Terra Nova C-69_3 wells (Figure 4.15). The Terra Nova F-88_3 well is located within the southern area of low reflection strength and high frequency as seen in the seismic attribute mapping. The low reflection strength is likely due to similar sandstone and shale content above and below the boundary providing minimal reflection coefficient definition. The Terra Nova F-100_2 and Terra Nova C-69_3 wells are located in the western and eastern regions, respectively, of higher reflection strength and lower frequency. At Terra Nova F-100_2, the presence of a thick sandstone bed above the mid-Hibernia Formation boundary creates a strong reflection coefficient at the boundary. Fairly homogenous lithology for more than ten meters above and below the boundary allows development of a strong seismic reflection at the boundary. Lithology at Terra Nova C-69_3 is primarily shale above and below the mid-Hibernia Formation boundary with no significant sources creating defined areas of similar reflection coefficients, which is emphasized by the rather long wavelength of the synthetic seismogram across the boundary.

North of the Trinity Fault System are the locations of the Hebron I-13, West Ben Nevis B-75, and West Bonne Bay C-23 wells (Figure 4.16). The Hebron I-13 well is located within the area of moderate frequency and low reflection strength in the northwest. Decreased frequencies to the north are primarily the result of increased depth. The low reflection strength at Hebron I-13 is caused by abundant thin sandstone beds above the mid-Hibernia Formation boundary providing lower contrast to the abundant thick sandstone beds below. Conversely, the West Ben Nevis B-75 and West

Bonne Bay C-23 wells indicate high reflection strength. Above the mid-Hibernia Formation boundary there is significantly less sandstone compared to Hebron I-13 providing good contrast with the underlying thick sandstone beds. It is also important to note that the sandstone interval directly below the mid-Hibernia Formation boundary is thicker in the northern region of the study area producing a near single-boundary response.

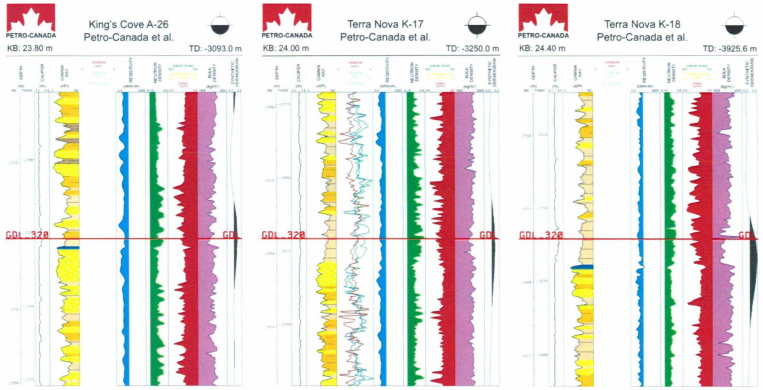


Figure 4.14: Petrophysical signature of the mid-Hibernia Formation boundary (represented as well pick GDL_320) at the King's Cove A-26, Terra Nova K-17 and Terra Nova K-18 wells. Locations of these wells can be seen in Figures 4.10 - 4.13. Abundance of sandstone and shale interbeds surrounding the mid-Hibernia Formation flooding surface is likely the source of low reflection strength at the King's Cove A-26 and Terra Nova K-17 wells. Reduced presence of sandstone beds above the flooding surface at Terra Nova K-18 provides greater contrast above and below the boundary to produce a higher reflection strength. Gamma ray log is filled with CanStrat® lithology interpretation where yellow=sandstone, orange=siltstone, brown=shale, and blue=carbonates or carbonate-cemented intervals.

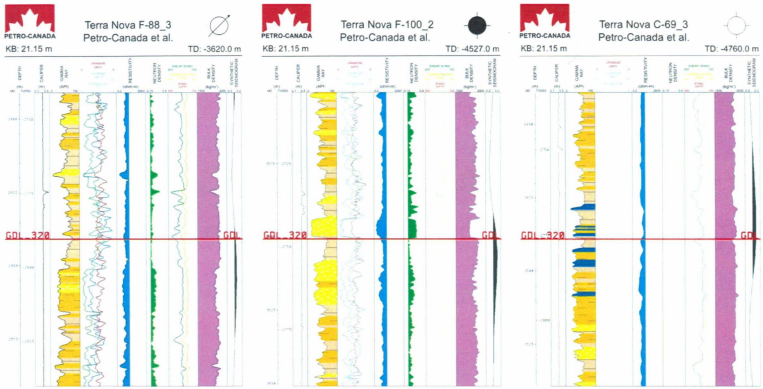


Figure 4.15: Petrophysical signature of the mid-Hibernia Formation boundary (represented as well pick GDL_320) at the Terra Nova F-88_3, Terra Nova F-100_2 and Terra Nova C-69_3 wells. Locations of these wells can be seen in Figures 4.10 - 4.13. All three wells have similar sandstone and shale content above and below the mid-Hibernia Formation boundary resulting in low to moderate reflection strength. Gamma ray log is filled with CanStrat® lithology interpretation where yellow=sandstone, orange=siltstone, brown=shale, and blue=carbonates or carbonate-cemented intervals.

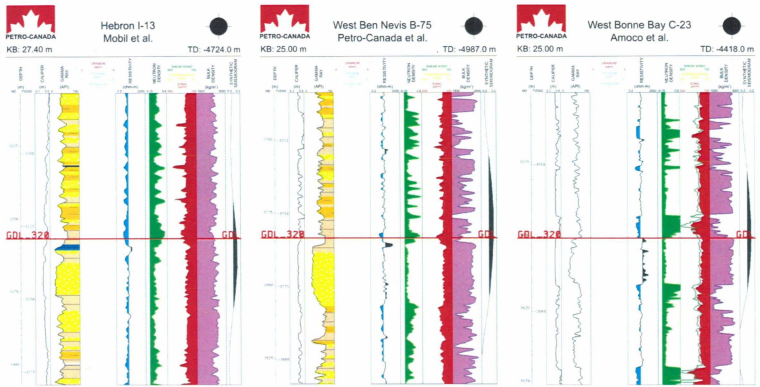


Figure 4.16: Petrophysical signature of the mid-Hibernia Formation boundary (represented as well pick GDL_320) at the Hebron I-13, West Ben Nevis B-75 and West Bonne Bay C-23 wells. Locations of these wells can be seen in Figures 4.10 - 4.13. Low reflection strength at Hebron I-13 is shown by the abundance sandstone above the boundary providing minimal contrast with the underlying sandstone. Conversely, the high shale content above the boundary provides good contrast with the underlying thick sandstone at West Ben Nevis B-75 and West Bonne Bay C-23 to produce a strong, near single boundary response. Gamma ray log is filled with CanStrat® lithology interpretation where yellow=sandstone, orange=siltstone, brown=shale, and blue=carbonates or carbonate-cemented intervals.

4.2.3 TOP OF HIBERNIA FORMATION

The top of the Hibernia Formation is a widespread seismic marker that is very easily correlated. It represents the end of the North Atlantic rifting episode and the onset of thermal subsidence (Enachescu, 1987; McAlpine, 1990; and Sinclair, 1993). Hibernia Formation sandstones are overlain by the 'B' Marker limestone, which provides excellent seismic contrast and a distinct seismic signature. 'B' marker limestone is notably denser and seismically faster than underlying Hibernia Formation sandstones creating a strong seismic trough signature. Figure 4.17 illustrates the character of the top Hibernia Formation boundary (represented as well pick GDL_330) in the Petro-Canada et al. Terra Nova G-90_5Z well (refer to Figure 2.1 for well location). Distinct changes in the sonic and bulk density logs mark the top of the Hibernia Formation. Changes in resistivity and neutron density also distinguish porous Hibernia Formation sandstones from the overlying low-porosity 'B' marker limestone.

The top of the Hibernia Formation ranges in depth from 1500 meters to 4500 meters below sea level and follows a similar structural trend as the previous two boundaries (Figure 4.18). As mentioned previously, this seismic marker is marked by a very strong seismic trough that is easily correlated throughout the study area. Figure 4.19 represents seismic coherency and illustrates the high correlativity of the top of the Hibernia Formation. The coherency map is nearly uniform except for fault zones and no distinct zoning is apparent. Figure 4.20 represents seismic reflection strength and illustrates the strong character that is seen in the seismic data. There is an area of lower reflection strength to the west of the Terra Nova oil field as well as along the Voyager Fault System. The lower reflection strength may be indicative of lower shale content below the top marker as can be seen in well logs in Figures 4.22 -4.24 but other

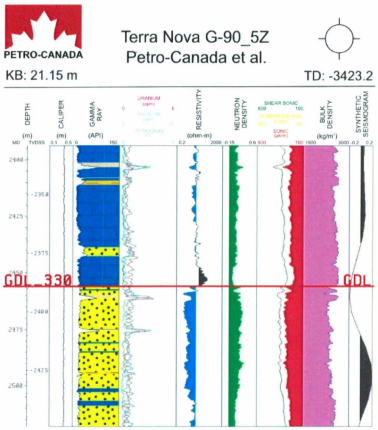


Figure 4.17: Petrophysical log at the Terra Nova G-90_5Z well over the depth interval: 2329-2449 meters TVDSS. Displayed well pick (GDL_330) marks the top of the Hibernia Formation. It is characterized by changes in the sonic and bulk density logs that create a strong seismic trough signature. It is also characterized by a distinct resistivity decrease from the 'B' Marker limestone (low porosity) to the Hibernia Formation sandstones (high porosity).

correlative trends are not observed. Figure 4.21 represents instantaneous seismic frequency. Variations in frequency appear to define distinct areas of the top Hibernia Formation boundary. Highest frequencies (more than fifty hertz) are contained in the southwest and southeast regions and gradually decrease to 40-50 Hz across the Terra Nova oil field, which is expected as the seismic marker dips gently to the north. There is an area of low frequency (approximately twenty hertz) in the northwest region as well as a larger area of low frequency over the Ben Nevis oil field. Comparing the well logs of

Ben Nevis I-45 (within low frequency area) with those of West Ben Nevis B-75 (outside low frequency area) it is feasible that the low frequency zone could represent an area with a low concentration of interbeds (Figure 4.24). Ben Nevis I-45 shows a sandstone bed bound by two shales, whereas West Ben Nevis B-75 shows multiple thinly interbedded sandstones and shales, which may produce a higher frequency reflectivity pattern.

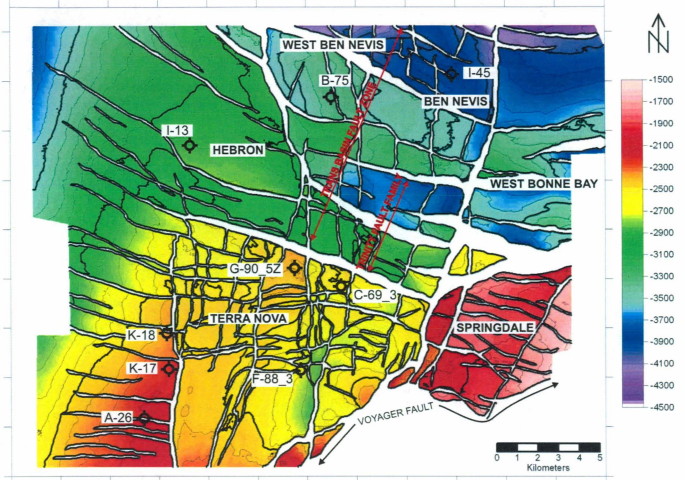


Figure 4.18: True vertical depth below sea-level map of the top of the Hibernia Formation. Contour interval is 100 meters with every 500 meters in bold lines. Note the easterly dip in the western and southern areas with the transition to a northerly dip within the Trans Basin Fault Zone.

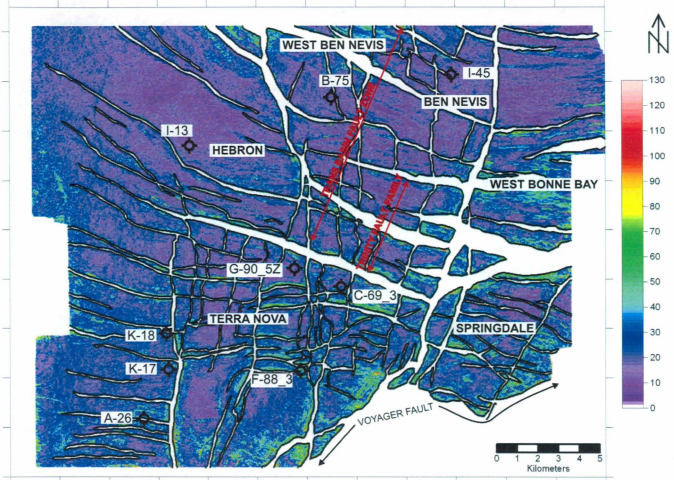


Figure 4.19: Seismic coherency map of the top of the Hibernia Formation. The scale bar is opposite to natural instinct, in which correlative events are displayed as lows and non-correlative events are displayed as highs. Overall, the top of the Hibernia Formation appears to be rather uniform and very coherent with no distinct zoning. The thin zones of incoherency that mimic the overlain fault trends most likely represent the fault zone, where an abundance of seismically invisible faults exist.

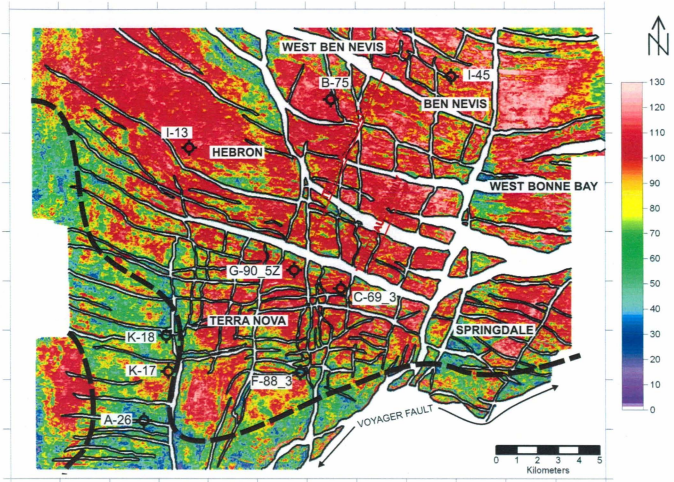


Figure 4.20: Reflection strength map of the top of the Hibernia Formation. Note the distinct increase in reflection strength to the north. Overall the top of the Hibernia Formation has a very high reflection strength in the north and has a moderate reflection strength along the southern region. The black lines on the map highlight the low reflection strength zone.

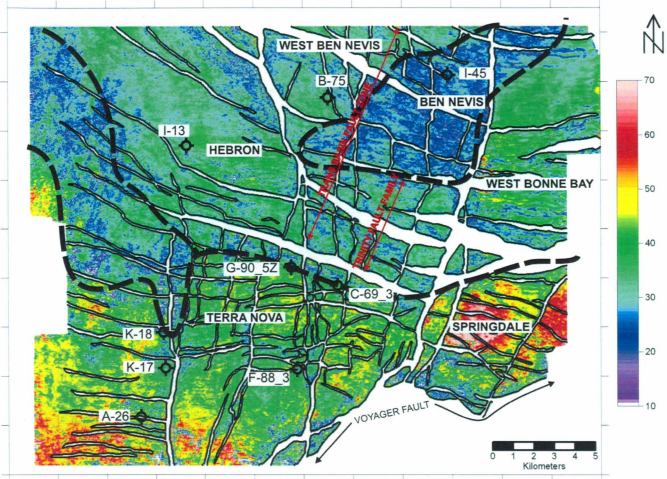


Figure 4.21: Instantaneous frequency map of the top of the Hibernia Formation. The southern region is dominated by the highest frequencies. Two regions of low frequencies are found in the northwest and northeast. The black lines on the map highlight these zones.

Anomalies observed in seismic attribute maps can be seen in the petrophysical character through Figures 4.22 – 4.24 and are discussed in greater detail in Chapter 6. Figures 4.22 – 4.24 display a fifty meter zone above and below the top Hibernia Formation boundary on nine selected wells; well locations are displayed on the maps of Figures 4.18 – 4.21. Beginning in the southwestern region of the study area are locations of the King's Cove A-26, Terra Nova K-17, and Terra Nova K-18 wells (Figure 4.22). These three wells highlight the lithologic consistency of the top Hibernia Formation boundary in the southern region. Thick sandstone overlain by a thick carbonate succession with a sharp boundary between the two produces a single boundary response at the top of the Hibernia Formation. This sharp contact provides an excellent seismic marker as there is a distinct change in density and seismic velocity across it, as can be seen from sonic and bulk density logs. The source of low reflection strength along a north-trending corridor in the western area (as seen in Figure 4.20) is not directly evident from the petrophysical log data.

Further east, towards the Terra Nova oil field are the locations of the Terra Nova F-88_3, Terra Nova G-90_5Z, and Terra Nova C-69_3 wells (Figure 4.23). These wells further illustrate the lithologic consistency of the top Hibernia Formation boundary. There are no noticeable differences aside from several thin shale beds deposited at the Terra Nova G-90_5Z well and a coarsening-upward trend at the top of the gamma ray log at the Terra Nova C-69_3 well. These differences alone do not fully explain the higher reflection strength noted in Figure 4.20 when compared to wells of Figure 4.22. Note that predominately calcareous intervals of limited thickness below the top Hibernia Formation are interpreted as carbonate cemented intervals and/or clastic carbonate

deposits and not necessarily fully established *in situ* carbonate deposits (*e.g.* bioherms) within the Hibernia Formation (see Chapter 5).

North of the Trinity Fault System, are the locations of the Hebron I-13, West Ben Nevis B-75, and Ben Nevis I-45 wells (Figure 4.24). These wells illustrate the distal end-member of the top of the Hibernia Formation within the study area, as can be seen through abundant shale deposition. All three wells confirm the sharp nature of the top Hibernia Formation boundary and this can be seen through the high reflection strength seen in Figure 4.20. The overall lower frequency character of the top Hibernia Formation in the northern area is likely due to burial depth since the boundary is very correlative and the character doesn't change across the majority of the study area. Localized areas of decreased instantaneous frequency may be indicative of the presence of thicker, homogeneous beds, as discussed earlier. The northern region of the study area records the increase in marine influence through shale deposition.

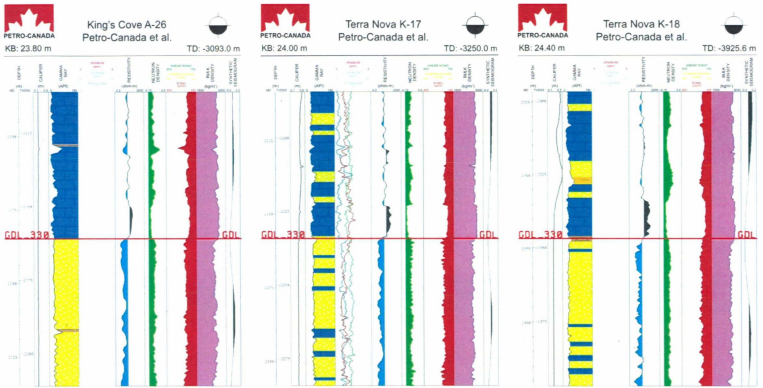


Figure 4.22: Petrophysical signature of the top Hibernia Formation boundary (represented as well pick GDL_330) at the King's Cove A-26, Terra Nova K-17 and Terra Nova K-18 wells. Locations of these wells can be seen in Figures 4.18 - 4.21. These three wells highlight consistency of the top of the Hibernia Formation. Thick carbonates of the 'B' Marker limestone overlying thick sandstones of the Upper Hibernia Formation provide excellent contrast and produce a strong seismic reflection. The north-trending corridor of low reflection strength in the west is not clearly evident from the petrophysical logs. Gamma ray log is filled with CanStrat® lithology interpretation where yellow=sandstone, orange=siltstone, brown=shale, and blue=carbonates or carbonate-cemented intervals.

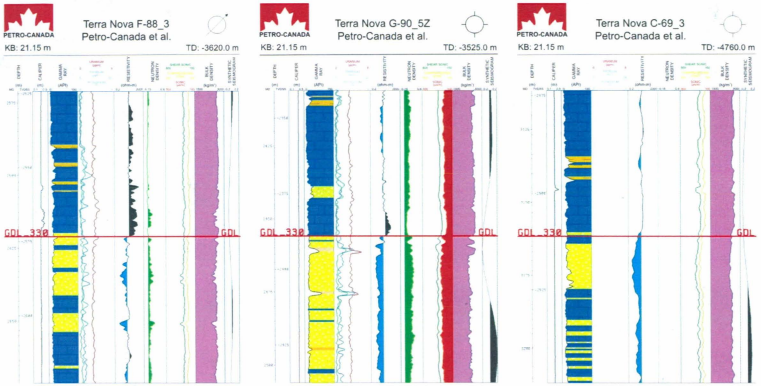


Figure 4.23: Petrophysical signature of the top Hibernia Formation boundary (represented as well pick GDL_330) at the Terra Nova F-88_3, Terra Nova G-90_5Z and Terra Nova C-69_3 wells. Locations of these wells can be seen in Figures 4.18 - 4.21. Consistency of the top of the Hibernia Formation is further illustrated through these wells. Deposition of fine-grained sediments is seen at the Terra Nova G-90_5Z and Terra Nova C-69_3 wells via the presence of thin shale beds and coarsening-upwards gamma ray signatures, respectively. The high reflection strength observed in seismic attribute mapping is explained through the sharp contact. Gamma ray log is filled with CanStrat® lithology interpretation where yellow=sandstone, orange=siltstone, brown=shale, and blue=carbonates or carbonate-cemented intervals.

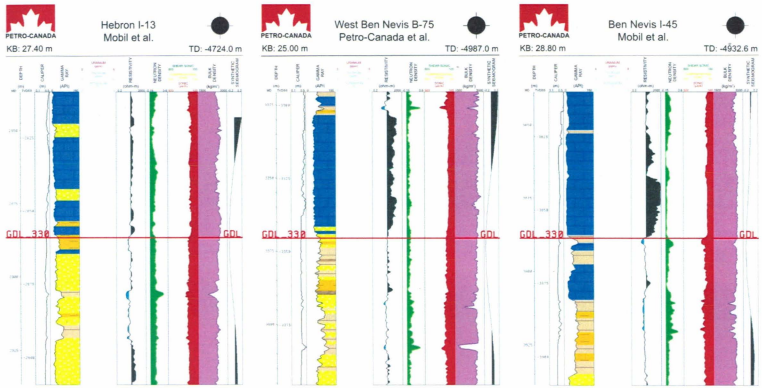


Figure 4.24: Petrophysical signature of the top Hibernia Formation boundary at the Hebron I-13, West Ben Nevis B-75 and Ben Nevis I-45 wells. Locations of these wells can be seen in Figures 4.18 - 4.21. All three wells have high reflection strength, which is evident through the distinct change from carbonates to siliciclastics. Gamma ray log is filled with CanStrat® lithology interpretation where yellow=sandstone, orange=siltstone, brown=shale, and blue=carbonates or carbonate-cemented intervals.

4.3 Unit Definition and Description

The following two sub-sections define the Upper and Lower Hibernia Members and describe the seismic character of each as units. Definition and description is based on several representative seismic sections and compares the seismic character and seismic attributes for the two major units. Seismic attributes chosen for analysis are coherency, reflection strength, and instantaneous frequency.

4.3.1 Unit Definition

The Lower Hibernia Member is bounded at the base by the base Hibernia Formation boundary and at the top by the mid-Hibernia Formation boundary (as defined in Section 4.2). Figure 4.25 illustrates the thickness of the Lower Hibernia Member across the study area. The unit generally thickens to the north and northwest with local variations due to faulting, highlighted by the bright purple contour fill, and is up to 550 meters thick within the study area. The Upper Hibernia Member is bounded at the base by the mid-Hibernia Formation boundary and at the top by the top Hibernia Formation boundary (as defined in Section 4.2). Figure 4.26 illustrates the relative uniformity of the upper unit compared to the lower unit. It generally displays a smoother increase in thickness to the north and northwest, ignoring signatures left by faults, and is up to 650 meters thick. Thickness variations across the north-south faults can easily be seen in the southern region. Some of the faults, i.e. the Trinity Fault, have large enough offsets (greater than one kilometer) to offset the entire Hibernia Formation across the fault, such that a well drilled through that fault may not encounter it. Growth across north-south trending faults is common as they were active during deposition of the Hibernia Formation and the North Atlantic Rifting episode, as discussed in Chapter 3.

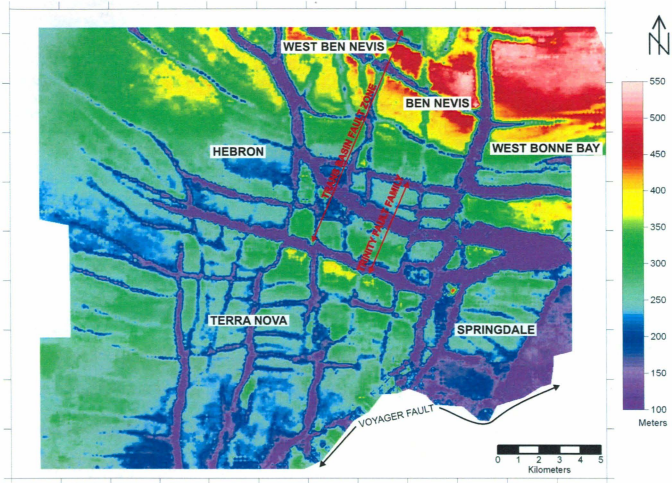


Figure 4.25: Thickness map of the Lower Hibernia Member. Overall the Lower Hibernia Member thickens to the north and northeast but has local variations that trend across multiple fault blocks, suggesting they are depositional in nature.

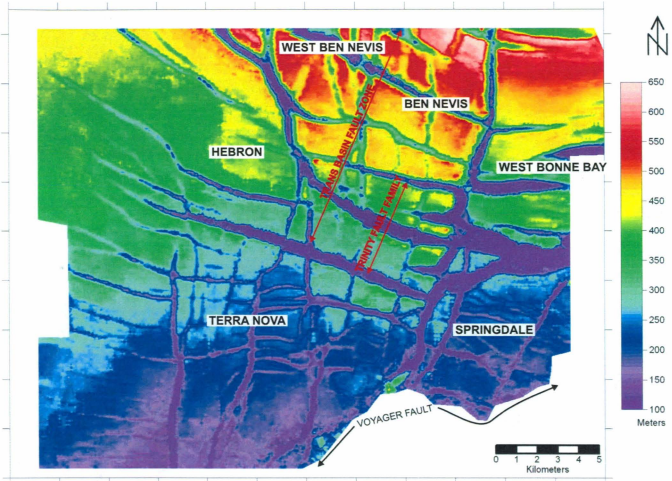


Figure 4.26: Thickness map of the Upper Hibernia Member. Overall the Upper Hibernia Member thickens rather uniformly to the north and northeast. Notice the southern step-back of thickening compared to the Lower Hibernia Member in the region south of Ben Nevis.

4.3.2 Unit Description

Having defined aspects regarding individual units within the Hibernia Formation, the formation as a whole can be discussed based on the seismic dataset in cross-section view. Figure 4.27 illustrates the excellent correlation between petrophysical logs and the seismic dataset, as well as the resulting interpretation of the position of the Hibernia Formation in the seismic section. High reflection strength and correlativity of the top Hibernia Formation boundary is one of the first observations made on seismic sections. Reflections surrounding the proximity of the mid-Hibernia Formation boundary appear to have lower reflection strength and don't have the same smooth character as the top Hibernia Formation seismic marker. This is likely due to the transition from the flooding-surface of the mid-Hibernia Formation boundary upwards into the rather uniform character of the Upper Hibernia Member and decreasing abundance of shale upwards (further discussed in Chapter 6). Immediately above and below the mid-Hibernia Formation boundary appears less coherent due to abundant interbedded sandstone and shale with limited lateral correlation lengths. The Lower Hibernia Member shows a noticeable increase in thickness in the north between the Hebron I-13 and Hebron M-04 wells. The growth of the Hibernia Formation as a whole to the north can also be seen from the seismic section of Fig. 4.27.

Seismic attribute characterization was also investigated along seismic sections (Figure 4.28). However, seismic attributes were not nearly as informative in cross-section as they were in map-view, and no additional interpretations were readily extracted from cross-sections. The most noticeable characteristic is the distinct decrease in instantaneous frequency with depth, as can be seen in Figure 4.28D.

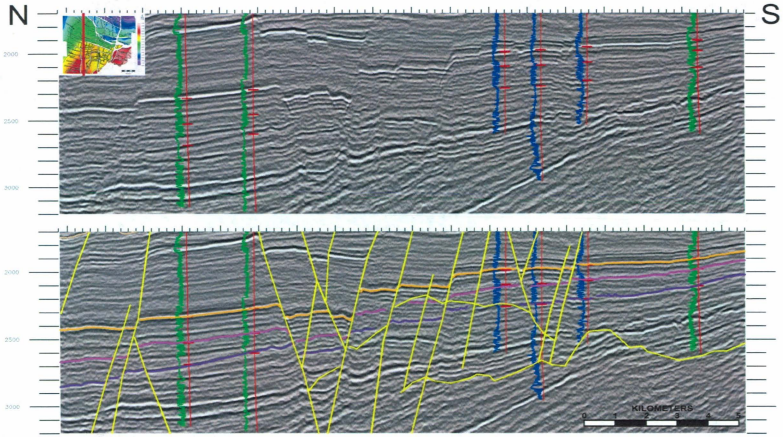


Figure 4.27: Seismic section illustrating the correlation of the well logs to the seismic dataset. Location of seismic section is shown in upper left corner. The upper panel is the uninterpreted section and the lower panel is the interpreted section. The yellow lines represent the interpreted faults. The three displayed horizons are the base Hibernia Formation (dark purple), the mid-Hibernia Formation (light purple), and the top Hibernia Formation (orange). The displayed wells are shown in red with their corresponding gamma ray logs (blue and green curves). Horizontal red lines across the wells represent the well picks for the Hibernia Formation boundaries. The displayed wells, from north to south, are Hebron M-04, Hebron I-13, Terra Nova C-09, Terra Nova K-08, Terra Nova K-07, and Beothuk M-05. This section highlights the significant growth seen in the Lower Hibernia Member between the Hebron M-04 and Hebron I-13 wells and overall thickening of the Hibernia Formation to the north.

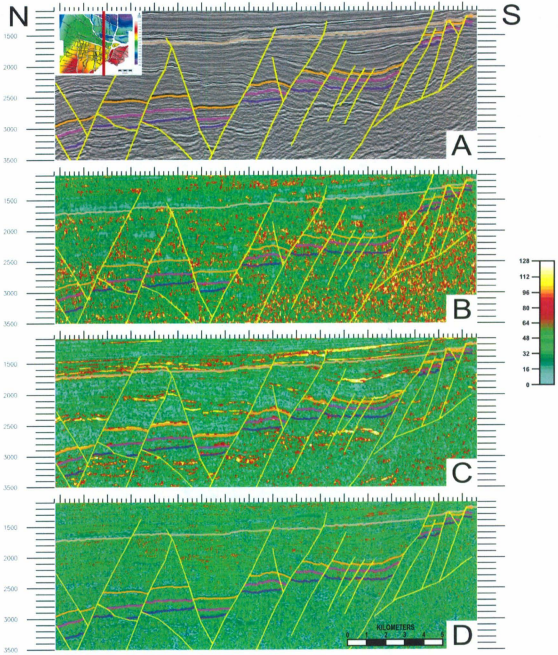


Figure 4.28: Seismic attribute extractions along the seismic section shown in Panel A. Panel B is the seismic coherency, Panel C is the reflection strength, and Panel D is the instantaneous frequency. For each section, the yellow lines represent faults. The four displayed horizons on each panel represent the base Hibernia Formation (dark purple), mid-Hibernia Formation (light purple), top Hibernia Formation (orange), and base Tertiary Unconformity (brown). The vertical scale for each panel is two-way travel time. The horizontal scale is traces with large divisions of 50 traces. Traces are at a 25 meter spacing.

4.4 CONCLUSIONS

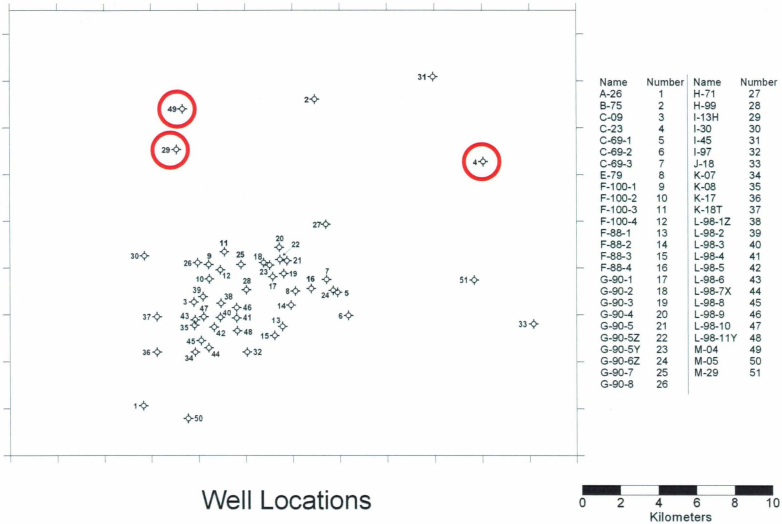
This chapter has illustrated the importance of seismic data in lateral correlation and coarse vertical sub-division of the Hibernia Formation. However, vertical resolution is limited due to the relatively low frequency of the seismic dataset, compared to the resolution obtained through petrophysical data. The Hibernia Formation is a reasonably well-defined stratigraphic unit in seismic data. Through mapping the three main bounding surfaces of the Hibernia Formation and extracting several seismic attributes (coherency, reflection strength, and instantaneous frequency) it was possible to laterally identify several seismically different zones. These seismic anomalies were further characterized using petrophysical logs by comparing lithology variations between identified anomalies and surrounding areas. Seismic attributes were also studied in cross-section across the study area and further analysis of seismically visible zones was attempted. However, due to the nature of the seismic attribute analysis and character of the Hibernia Formation no further subdivision was possible. It appears that seismic attribute analysis is optimized in map view along an interpreted seismic marker. It is clear, however, that the low frequency nature of the seismic dataset is limited to mapping general trends and not the extent of individual beds or bedsets. Using quarter-wavelength approximation of resolution, with a velocity of 4500 meters per second and peak frequency of 18-22 Hz, maximum resolution would be 50-65 meters. Sandstone and shale bedsets are generally much less than this resolution thickness and are therefore seismically unresolved as individual units. However, they are better interpreted when viewed as packages of sandstone-dominated versus shale-dominated interbeds, for example. Chapter 6 will illustrate the importance of petrophysical data in further sub-dividing the Hibernia Formation vertically.

CHAPTER 5 – CORE DESCRIPTIONS

5.1 SCOPE AND PURPOSE

Core is a valuable source of data that provides a stratigraphic record of the subsurface. Unlike seismic and petrophysical data, both of which are subject to the geoscientist's imagination, core provides physical evidence of the subsurface with respect to lithology. The only aspect that is left open to the geoscientist's interpretation is the depositional and/or diagenetic environment, which itself is constrained by sedimentological evidence displayed in core (*e.g.* lithology, physical and biogenic structures, cements). This chapter of the thesis will focus on the description of recovered core within the study area and presents an interpretation of depositional environments of the Hibernia Formation.

The following core descriptions provide fine-scale data needed to analyze the depositional environment of the Hibernia Formation. The depositional environment interpreted from core data is crucial to the interpretation of petrophysical well data such that correlations between wells are made to honour the interpreted depositional environment. However, only three of the fifty-one wells within the study have recovered core. These wells are all located in the northern-most part of the study area: i) Amoco et al. West Bonne Bay C-23 well, ii) Mobil et al. Hebron I-13 well, and iii) Chevron et al. Hebron M-04 well (see Figure 5.1).



Name	Number	Name	Number
A-26	1	H-71	27
B-75	2	H-99	28
C-09	3	I-13H	29
C-23	4	I-30	30
C-69-1	5	I-45	31
C-69-2	6	I-97	32
C-69-3	7	J-18	33
E-79	8	K-07	34
F-100-1	9	K-08	35
F-100-2	10	K-17	36
F-100-3	11	K-18T	37
F-100-4	12	L-98-1Z	38
F-88-1	13	L-98-2	39
F-88-2	14	L-98-3	40
F-88-3	15	L-98-4	41
F-88-4	16	L-98-5	42
G-90-1	17	L-98-6	43
G-90-2	18	L-98-7X	44
G-90-3	19	L-98-8	45
G-90-4	20	L-98-9	46
G-90-5	21	L-98-10	47
G-90-5Z	22	L-98-11Y	48
G-90-5Y	23	M-04	49
G-90-6Z	24	M-05	50
G-90-7	25	M-29	51
G-90-8	26		

Figure 5.1: Location of the fifty-one (51) exploration, delineation and development wells used in this study. The three wells used in the core evaluation are circled in red.

5.2 AMOCO ET AL. WEST BONNE BAY (C-23)

The Amoco et al. West Bonne Bay C-23 well was drilled in 1997 as an exploratory well and drilled to a true vertical depth (TVD) of 4411.65 meters. Its unique Well Identification number is 300 C23 46400 48150. The C-23 well encountered the Hibernia Formation between 3277 – 3929 meters measured depth (MD) and recovered two intervals of core from the Hibernia Formation. Recovered core was recorded as Core 1 (3788.0 – 3789.15 meters MD) and Core 2 (3798.0 – 3816.6 meters MD), both located within the Lower Hibernia Member (Figure 5.2). The detailed core description log and core photos are located in Appendix A.

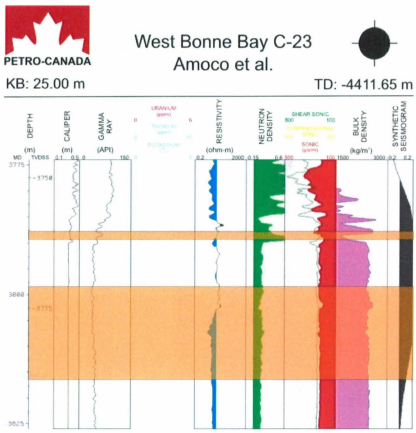


Figure 5.2: Petrophysical log for the West Bonne Bay C-23 well over the depth interval 3774 – 3826 meters MD. Orange highlighted regions represent cored intervals. Core 1 is the top thinner interval and Core 2 is the lower thicker interval. The displayed depth interval is located within the Lower Hibernia Member (sub-unit 308).

5.2.1 CORE DESCRIPTION

Starting at the base of the recovered core (Core 2), the C-23 well displays an interval of extensively bioturbated sandstone (**F1**), in which sedimentary structures have been completely reworked and are rarely distinguishable (Figure 5.3). **F1** is characterized by a low diversity of trace fossils consisting of very abundant, irregularly lined cylindrical burrows (*Ophiomorpha isp*) and commonly occurring, smoothly lined cylindrical burrows (*Paleophycus isp*), both of which are typically seen in cross-section as they trend horizontally. Other trace fossils include occasional, simple vertical burrows filled with sandstone (*Skolithos isp*) as well as occasional unlined, sandstone-filled, horizontal cylindrical burrows (*Planolites isp*). Intervals of **F1** are bounded by erosive, irregular surfaces and are often separated by thin beds of coarse-grained sandstone at the base of the overlying sequence of **F1** (Figure 5.4). Basal sandstone beds appear to contain diffuse, somewhat obscure laminations that have a predominant dip-direction with rare packages of thin laminations of opposing dip-directions. Irregular, discontinuous carbonaceous laminae and/or concentrations of thin shell fragments highlight foresets and bounding surfaces in these sandstones. The base of the C-23 well contains five identifiable intervals of medium-grained **F1** ranging in thickness from ~0.8 – >2 meters thick, with each interval becoming progressively thinner upwards. These intervals are located between ~3807.2 – 3816.6 meters MD, totaling 9.4 meters thickness.

F1 is erosively capped at ~3807.2 meters MD by a medium- to coarse-grained, horizontally to low-angle laminated sandstone with rare bioturbation (**F2**) that is 7.7 meters thick. However, several large trace fossils are present throughout the facies, such as *Ophiomorpha isp* and *Skolithos isp* (Figure 5.5). **F2** contains abundant

carbonaceous laminations ranging from planar, horizontal and low-angle orientations to arcuate, non-symmetric orientations (Figure 5.5). Thick-thin alternations of sandstone beds, separated by very thin carbonaceous laminae are common throughout **F2**. Two thinly laminated beds of carbonaceous matter are located at ~3801.5 meters MD approximately 1 – 2 centimeters thick and 0.75 meters apart. They have irregular boundaries and both layers appear to have been the foci for sideritization of adjacent sandstone (Figure 5.6). Overall, **F2** displays a coarsening-upwards trend. A 20 – 25 centimeter thick interval of **F1** is found at ~3799.5 meters MD within **F2** (Figure 5.7). This interval of **F1** gradationally overlies **F2** and is sharply capped by 1.2 meters of **F2**, marking the top of Core 2, at 3798.0 meters MD.

Core 1 is only 1.15 meters in length. The lower 0.55 meters is **F1** with two identifiable trace fossils. The most abundant trace fossil visible is *Ophiomorpha isp,* as well as commonly occurring, irregularly curving, smooth-walled burrows with a dark mud fill that contrasts the sandstone host rock. They commonly appear as tiny dark spots (transverse section) or dark lines (longitudinal section) 1-3 millimeters in diameter and are most likely *Helminthopsis isp* (Pemberton et al., 2001). The upper 0.6 meters of Core 1 is **F2** which sharply overlies the interval of **F1** below. Laminations are very faint due to a lack of contrasting sediment to highlight them.

5.2.2 Depositional Environment

Aside from lithology and the evidence for relatively low-angle current structures, trace fossils may provide the best indication of depositional environment. At the base of the recovered core, there exists the combination of *Ophiomorpha isp, Skolithos isp, Paleophycus isp,* and *Planolites isp* to form the *Skolithos* ichnofacies. Pemberton et al.



Figure 5.3: Extensively bioturbated sandstone (**F1**) found in the C-23 well (Core 2, Box 10). Examples of *Ophiomorpha isp* and *Skolithos isp* are shown with green and blue arrows, respectively. Black arrow shows a small patch of calcite cement at the top. Note absence of preserved sedimentary structures.



Figure 5.4: Example of coarse-grained sandstone (**F2**) separating intervals of **F1** in the C-23 well (Core 2, Box 11). Orange marker highlights erosive boundary that separates lag deposits of **F2** (above) from **F1** (below). Red arrow shows position of thin, wispy, left-dipping laminations of carbonaceous clay material within an interval of overall right-dipping laminations. Black arrows indicate the edge of a calcite cemented zone.

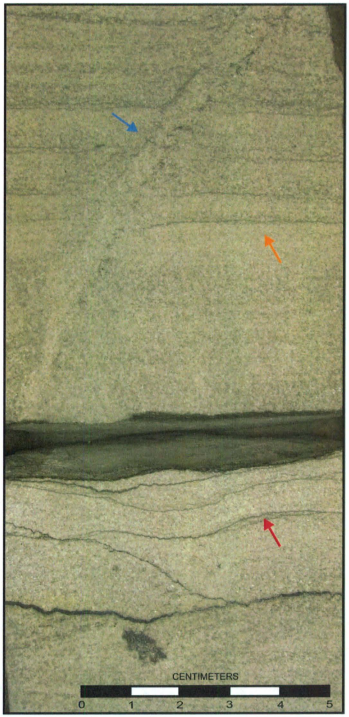


Figure 5.5: Laminated sandstone (**F2**) found in the C-23 well (Core 2, Box 9). A large *Skolithos isp* trace fossil is shown by blue arrow; however it is possibly the vertical shaft of an *Ophiomorpha isp* trace fossil. Orange and red arrows indicate locations of planar and arcuate carbonaceous laminations, respectively, that are present throughout the facies.

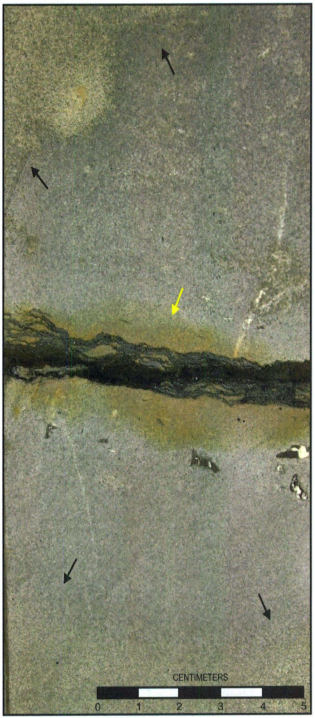


Figure 5.6: Organic matter layer from the C-23 well (Core 2, Box 4). Yellow arrow indicates location of ~1 centimeter thick organic matter-rich layer. Rusty red-brown discoloration surrounding organic matter highlights sideritization zone. Black arrows indicate edges of the calcite cement nodule that is present at this depth. Grey discoloration differentiates calcite cement from light brown uncemented sandstone.

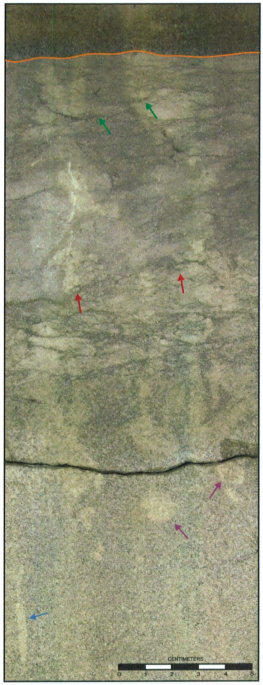


Figure 5.7: F1 located with the **F2** of the C-23 well (Core 2, Box 2). Trace fossils identifiable include: *Ophiomorpha isp* (green arrow), *Paleophycus isp* (red arrow), *Planolites isp* (purple arrow), and *Skolithos isp* (blue arrow). The upward-increase in cementation abundance is visible through the transition to the light grey coloration from the light brown sandstone. The sharp contact above the bioturbated interval is indicated by the orange coloured marker, where **F1** was overlain by **F2**.

(2001) provides a generalized description of possible environmental considerations for each of the common trace fossils, summarized below. *Ophiomorpha isp* are dwelling burrows of suspension-feeding shrimp. They can be found prolifically in marine shoreface environments, as well as brackish water, sandy substrates including estuaries and tidal shoals. *Skolithos isp* are thought to be dwelling burrows of suspension-feeding vermiform organisms or passive carnivores. They can be found in marine and brackish environments, where they are generally lined, however, they can be constructed by many different organisms and can be found in virtually any environment from marine to non-marine. *Paleophycus isp* are dwelling burrows of predaceous polychaete. They are associated with *Skolithos isp* in both high and low energy shoreface environments, and can be found in episodic deposition storm sands and brackish-water assemblages. *Planolites isp* are feeding burrows of deposit-feeders. They are essentially the unlined equivalent of *Paleophycus isp* and are often found together, however, *Planolites isp* are found in virtually all environments from freshwater to deep marine. Based on the above interpretations of associated depositional environments, the trace fossil assemblages indicate a suspension-feeding preference due to the high abundance of the *Ophiomorpha isp* and *Skolithos isp* trace fossils found in the cores. The lower abundance of *Planolites isp* and *Paleophycus isp* indicates the high ratio of suspension- to deposit-feeding organisms and suggests a possible middle to lower shoreface environment in a marine setting. However, Crimes *et al.* (1981) suggest that the *Skolithos isp* ichnofacies may be found in deeper water deposits where energy levels, food supplies, and hydrographic and substrate characteristics are suitable. Such environments include submarine canyons, deep-sea fans, and bathyal slopes with

strong contour currents. Clearly, trace fossils alone can not be the only evidence used for identification of depositional environments.

Abundant carbonaceous material and organic matter fragments and laminations may be indicative of close proximity to a terrestrial source. The typically parallel, horizontal to low-angle laminations in the sandstone may represent a wave-influenced upper shoreface-foreshore setting. Absence of high-angle cross-bedding or consistently bimodal dip directions suggest a dominance of wave reworking of sands. Rare preservation of opposing dip directions and presence of alternating thin-thick laminae could be indicative of local and temporary dominance by flood and ebb tidal currents with differing strengths. Coarse-grained beds found within the bioturbated facies indicate events of higher current energy, possibly storm-induced overwash or tidal or rip channels.

In Core 1, there are occurrences of *Helminthopsis isp* associated with *Ophiomorpha isp*. *Helminthopsis isp* are the grazing trails of worm-like organisms. They are a common element of distal *Cruziana* and proximal *Zoophycus* ichnofacies on a normal marine shallow shelf. They can also be associated with low energy, fine-grained bay environments (Pemberton et al., 2001). Due to the medium grain size of the host deposits and the low angle laminations found in the conformably overlying deposits, it is most likely due to a low energy, sheltered environment, such as a bay that was dominated by reduced sedimentation.

The relationship between Core 1 and Core 2 cannot be directly established due to missing section between the recovered intervals. Progressively upward-thinning packages of **F1** and progressively upward-thickening of **F2** are consistent with increasing current energy in a possibly regressive setting. Furthermore, it is worth

noting that Core 1 is located where the gamma ray log starts to increase-upwards, which indicates a fining-upwards succession (increased shale content). However, in Core 1 there are no significant shale beds and the upward-increasing gamma ray trends may be indicative of heavy mineral deposition, characteristic of upper shoreface sandstones (Saito, 2005). Overall, the West Bonne Bay C-23 core is interpreted as reflecting progradation of a wave-influenced succession with only occasional preservation of tidal influence, as reflected by the observed current structures. Deposition may have occurred within a partially protected embayment, based on the limited diversity of ichnospecies relative to that expected for an open, fully marine depositional setting. Maximum progradation was achieved through Core 2 with initiation of retrogradation occurring in Core 1.

5.3 MOBIL ET AL. HEBRON (I-13)

The Mobil et al. Hebron I-13 well was drilled in 1981 as an exploratory well and drilled to a TVD of 4695.7 meters. Its unique Well Identification number is 300 I13 46400 48300. The I-13 well encountered the Hibernia Formation between 2887 – 3537 meters MD and recovered one interval of core from the Hibernia Formation. The recovered core was recorded as Core 4 (2944 – 2962 meters MD) and located within the Upper Hibernia Member (Figure 5.8). It is important to note that the physical condition of the I-13 core is very poor. The core has been extensively sampled and is intensely broken-up making it difficult to view and interpret the true nature of lithofacies boundaries. The detailed core description log and core photos are located in Appendix B.

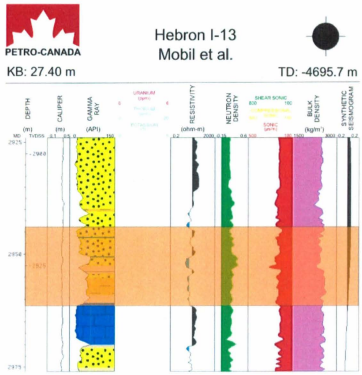


Figure 5.8: Petrophysical log for the Hebron I-13 well over the depth interval 2924 – 2976 meters MD. Orange highlighted region represents cored interval (Core 4). Displayed depth interval is located within the Upper Hibernia Member (sub-unit 328).

5.3.1 CORE DESCRIPTION

Starting at the base of the recovered core, the I-13 well displays an interval of extensively bioturbated, very fine-grained sandstone (**F1**) from 2962 – 2958.6 meters MD, in which sedimentary structures have been completely reworked and are unidentifiable (Figure 5.9). Trace fossils include occasional sandstone-filled groups of elliptical burrows (*Chondrites isp*), as well as commonly occurring concentric laminations of sandstone and clay with a generally smooth surface (*Asterosoma isp*). The most abundant trace fossil occurring appears to be a vertical series of tightly packed concave-up laminae (*Teichichnus isp*). Other commonly occurring trace fossils are smoothly-lined, cylindrical burrows (*Thalassinoides isp*). Throughout this facies, shell fragments are common, as well as occasional fragments of calcareous serpulid tubes, often preserving a typical, colonial growth habit (Figure 5.10). Thin organic matter laminations and fragments are occasionally preserved and are easily identifiable by their rusty-red sideritization appearance along their outer edges. Within this succession of **F1** exists a 10 – 12 centimeters thick fossiliferous grainstone bed with a sharp basal contact (**F3**) at ~2960.6 meters MD (Figure 5.11).

The upper interval of **F1** is sharply truncated at 2958.6 meters MD by a medium-grained, low-angle to horizontally laminated sandstone (**F2**) ~1 meter thick with abundant shell fragments that occasionally appear to be aligned along bedding planes (Figure 5.12). The laminae are difficult to see due to a lack of carbonaceous material or other contrasting material to highlight them. The sandstone is fining-upwards above ~2957.5 meters MD and bioturbation increases, representing deposition of **F1** (Figure 5.13). However, the degree of bioturbation is slightly less than that of **F1** below, and thin horizontal laminations are sometimes preserved, more commonly up-section.



Figure 5.9: Extensively bioturbated sandstone (**F1**) found in the I-13 well (Core 4, Box 13). Identified trace fossils include *Asterosoma isp* (light blue arrows), *Chondrites isp* (orange arrows), and *Chondrites isp* in longitudinal section (dark blue arrow). Shell fragments are common (purple arrow).

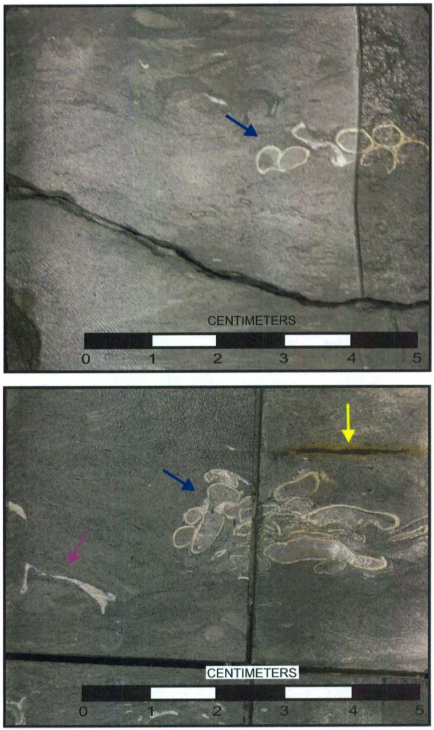


Figure 5.10: Calcareous serpulid tube fossils (blue arrows) commonly found in **F1** of the I-13 well (Top image: Core 4, Box 13; Bottom image: Core 4, Box 12. Shell fragment is shown by purple arrow. Organic matter lamination/fragment is shown by yellow arrow.



Figure 5.11: Grainstone (**F3**) found in the I-13 well (Core 4, Box 12). The orange line highlights irregular base of **F3** overlying **F1**. Note abundant carbonate material and shell fragments of **F3**.

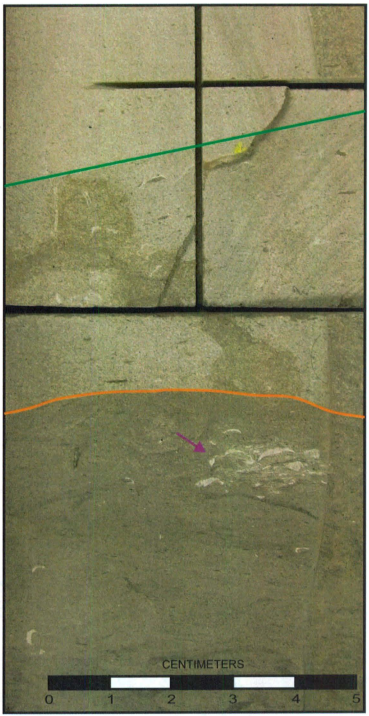


Figure 5.12: F2 sharply truncating underlying **F1** in the I-13 well (Core 4, Box 11). Erosive base of **F2** is shown by orange line. Green line highlights one of the low-angle laminations. A cluster of shell fragments is indicated by purple arrow.

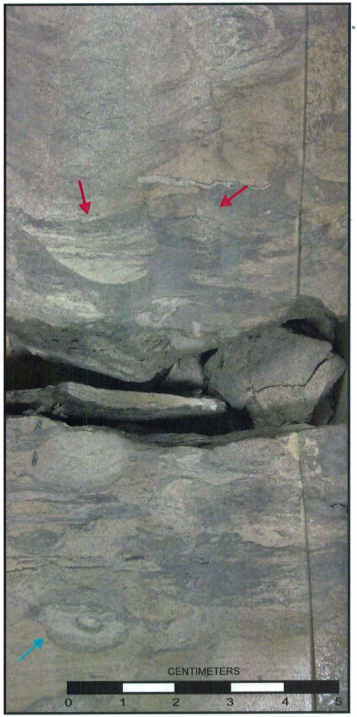


Figure 5.13: Transition to **F1** deposition from **F2** below in the I-13 well (Core 4, Box 10). Areas that are light brown highlight original laminated sandstone while light and dark grey areas highlight bioturbated portions of the sandstone. Light blue arrow identifies an *Asterosoma isp.* Red arrows identify *Teichichnus isp.*

The interval of **F2** occasionally contains irregularly-lined, cylindrical burrows (*Ophiomorpha isp*) until bioturbation is fully established upwards, in which trace fossils of the *Cruziana* ichnofacies become predominant (i.e. *Asterosoma isp and Teichichnus isp*).

A shell-rich bed sharply truncates **F1** at ~2955.1 meters MD and grades upwards into **F2**. From 2955.1 – 2948.9 meters MD is a number of successions of basal **F3** that fine-upwards into either **F1** or **F2**. **F3** is typically a mixture of carbonate clasts and shell fragments, with poor sorting and no apparent internal laminations or structure (Figure 5.14). The uppermost succession of **F3** grades upwards into **F2**, which displays a cross-laminated character (Figure 5.15). Within the entire interval, the basal carbonate portion of each given fining-upward successions generally becomes progressively thicker upwards. Trace fossils in **F1** are dominantly *Ophiomorpha isp*; however there are rare occurrences of *Teichichnus isp* and *Asterosoma isp.* Beds of **F2** occasionally contain *Ophiomorpha isp* and *Skolithos isp* trace fossils. Overall, series of fining-upwards successions becomes coarser-grained upwards. The uppermost grainstone contains a ~3-4 cm thick zone of carbonaceous laminations, which are the locus of heavy sideritization (Figure 5.16).

Overlying the series of **F3** grading into **F1** or **F2** is a bed of **F1** extending from 2948.6 – 2944 meters MD. Trace fossils are predominantly *Ophiomorpha isp* and occasional *Skolithos isp*. Organic matter fragments and laminations are common, up to 3 centimeters thick, and are often sideritized. A carbonate-rich bed similar to **F3** is present at ~2946.7 meters MD and is ~25 centimeters thick. An organic matter rich layer is also present at ~2945 meters MD and is ~20 centimeters thick. It is impossible to determine depositional nature of the organic matter as the core condition is very poor

for this specific interval. The recovered portion consists of a mass of broken pieces of organic matter 1-2 centimeter in diameter.

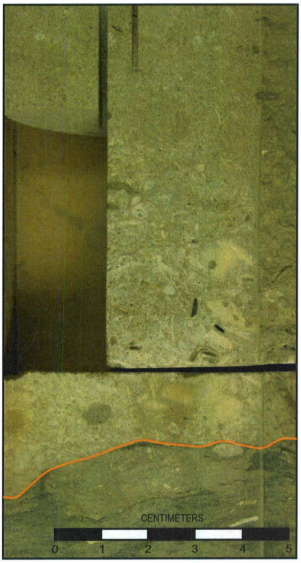


Figure 5.14: Fining-upwards, irregularly based **F3** overlying **F1** in the I-13 well (Core 4, Box 7). Erosive to irregular base of **F3** is highlighted by orange line.

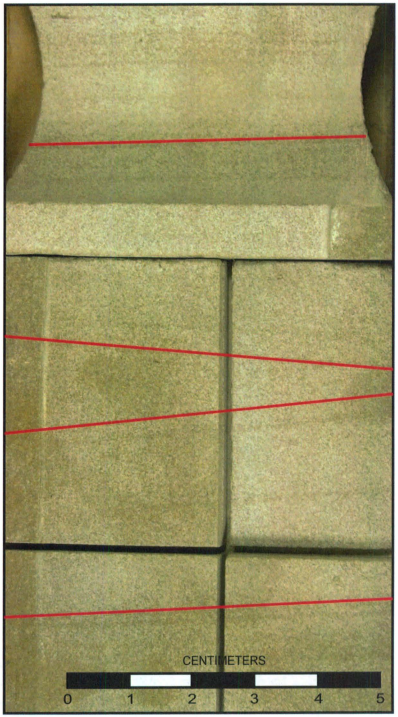


Figure 5.15: Low-angle cross-laminated sandstone (**F2**) found in the I-13 well (Core 4, Box 7). Red lines highlight four visible laminations with different dip directions.



Figure 5.16: Heavily sideritized organic matter laminations contained within a grainstone bed (**F3**) in the I-13 well (Core 4, Box 4). Yellow arrow marks location of organic matter laminations.

5.3.2 DEPOSITIONAL ENVIRONMENT

Trace fossil assemblages observed in the Hebron I-13 core are indicative of an overall low current energy, fully marine depositional environment (based on the diversity of trace fossils) developing upward into a setting of higher current energy. Pemberton et al. (2001) provides possible depositional environments for the visible trace fossils. *Chondrites isp* represents a complex deposit-feeding strategy. They are a common element of the *Cruziana* ichnofacies; however, the complexity of the burrows is often associated with fully marine conditions. *Asterosoma isp* is the selective deposit-feeding burrow of a vermiform organism. Their specialized feeding structure is often associated with fully marine conditions and is a common element of the *Cruziana* ichnofacies. *Teichichnus isp* are the dwelling/feeding burrows of a deposit-feeding organism. They are commonly associated with lower shoreface to offshore environments with the *Cruziana* ichnofacies. They are also prevalent in lagoon and bay facies characterized by brackish-water and are never associated with freshwater. *Thalassinoides isp* are dwelling/feeding burrows of a deposit-feeding crustacean. They are associated with the *Cruziana* ichnofacies in lower shoreface to offshore environments and are also found in low diversity, brackish-water suites. Based on an assemblage of traces including *Chondrites isp, Asterosoma isp, Teichichnus isp, Thalassinoides isp, and Ophiomorpha isp* the depositional environment at the base of the core is likely a lower shoreface to offshore setting. The overall coarsening-upwards pattern of the core, in conjunction with increasing abundance of *Ophiomorpha isp* trace fossils and current laminations, is taken to suggest that the depositional environment is shallowing-upwards into upper to middle shoreface environments.

Abundant carbonate debris and rudstone deposits are indicative of nearby associated carbonate deposition, possibly the development of localized carbonate banks. The carbonate deposits are clastic intervals, made-up of serpulid and mollusc shell fragments, evidently the result of erosion and are not representative of *in situ* deposition (*e.g.* between 2955.1 – 2948.9 meters MD). Perhaps the clasts are sourced from shell-serpulid banks along the margins of a quasi-open embayment, tidal channels or tidal inlets, areas affected by oxygenated as well as nutrient-rich currents in which such organisms thrived. The occasionally delicate texture of serpulid tube fragments indicate that this source could not have been very far away. Upward-thickening of grainstones is consistent with lateral migration of tidal inlet or tidal channels to a position closer to the depositional site. Common occurrence of sharp-based, erosional, and conglomeratic **F3** is also consistent with deposition as basal lag of tidal channel deposits. The shallowing-upwards character seen in the core from trace fossil assemblages as well as the overall coarsening-upwards pattern suggests that siliciclastic sedimentation is increasing through time and interacted with the depositional environment needed for the development of carbonate deposits. This increase in siliciclastic sedimentation may be due to renewed nearby fault activity before it ceased altogether at the top of the Hibernia Formation for the deposition of the widespread Catalina Formation and 'B' Marker limestone. The well-sorted nature of non-bioturbated sediments (Figure 5.15) and low-angle cross-laminations suggest a strong influence from wave currents, perhaps punctuated by storm events. Storm events are evidenced by sharp-based rudstone beds, possibly found along the base of channel forms, which would have acted as the major sites of erosion/deposition during storm events.

5.4 CHEVRON ET AL. HEBRON (M-04)

The Chevron et al. Hebron M-04 well was drilled in 2000 as a delineation well and drilled to a TVD of 4584.2 meters. Its unique Well Identification number is 300 M04 46400 48300. The M-04 well encountered the Hibernia Formation between 2991 – 3646 meters MD and recovered one interval of 111 meter long core from the Hibernia Formation. Recovered core was recorded as Core 3 (2983 – 3094 meters MD) and located at the upper boundary of the Hibernia Formation (Figure 5.17). The detailed core description log and core photos are located in Appendix C.

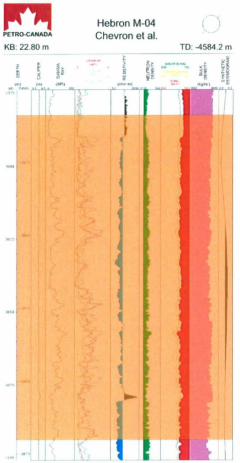


Figure 5.17: Petrophysical log for the Hebron M-04 well over the depth interval 2974 – 3101 meters MD. Orange highlighted region represents cored interval (Core 3). The displayed depth interval is located within the Upper Hibernia Member (sub-units 328 and 330) and the "B"-Marker limestone.

5.4.1 CORE DESCRIPTION

Starting at the base of the recovered core, the M-04 well contains five distinguishable successions (3 – 5 meters thick) consisting of low-angle laminated sandstone (**F2**) that gradationally fine-upwards into extensively bioturbated sandstone (**F1**) from 3094 – 3074.2 meters MD. **F2** has a sharp, erosive base that is commonly accompanied by a thin bed of shell fragments and mud rip-up clasts at the base. Assumed to be a basal lag, it is very carbonate-rich and contains large shell fragments (up to 4 centimeters). The basal lag located at ~3086.7 meters MD, is approximately 15 centimeters thick and has a high abundance of carbonate material (Figure 5.18). It is overlain by a mudstone rip-up clasts deposit and grades upwards into horizontally laminated sandstone. Basal sandstones are predominantly medium-grained with horizontal to low angle laminations (up to 10°) that are commonly highlighted by carbonaceous material or occasionally lithic fragments (<1 millimeter in diameter) (Figure 5.19). The basal sandstone located at ~3090 meters MD displays a cross-lamination pattern, whose laminations exhibit the highest dip angle (~10-15°) of the five intervals. **F1** is characterized by extensively burrowed and bioturbated sandstone (Figure 5.20). Abundant trace fossils include irregularly-lined, cylindrical burrows (*Ophiomorpha isp*), smoothly-lined cylindrical burrows (*Paleophycus isp*). Commonly occurring trace fossils include unlined, sandstone-filled groups of elliptical burrows (*Planolites isp*), and simple, sandstone-filled vertical burrows (*Skolithos isp*). Shell fragments occur occasionally throughout **F1** as well as calcareous tubes. The shell fragments appear to be slightly increasing in abundance upwards in some successions. Organic matter laminations and fragments are occasionally found **F1** and are generally 1-5 millimeters thick, displaying various degrees of sideritization.

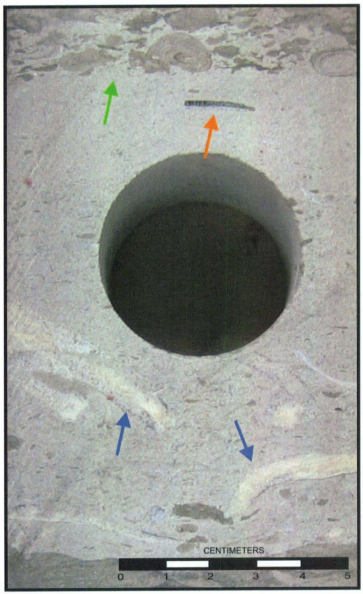


Figure 5.18: Basal carbonate-rich lag deposit found in the M-04 well (Core 3, Box 82). Purple arrows show locations of large shell fragments. Orange arrow shows location of a thin organic matter fragment. Green arrow shows location of overlying mud-clasts.

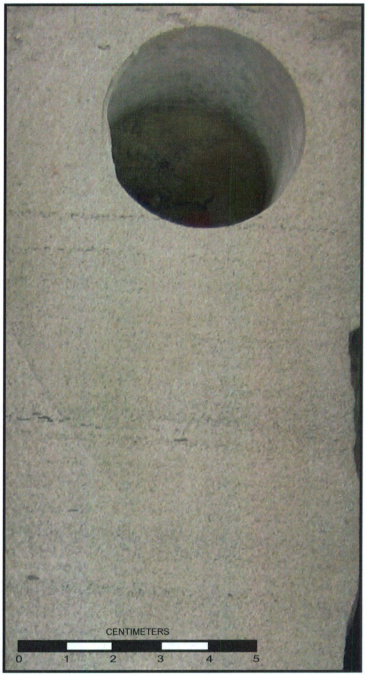


Figure 5.19: Low-angle laminated sandstone (**F2**) found in the M-04 well (Core 3, Box 84). Note abundant carbonaceous material and small lithic fragments that highlight laminations.

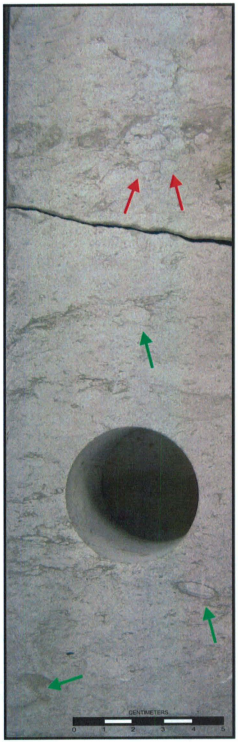


Figure 5.20: Burrowed sandstone (**F1**) found in the M-04 well (Core 3, Box 87). Green and red arrows show locations of *Ophiomorpha isp* and *Paleophycus isp* trace fossils, respectively.

The top of the five successions is marked at ~3074.2 meters MD by the change from **F1** to a very-coarse-grained grainstone (**F3**) (Figure 5.21). The base of **F3** consists of ~15 centimeters of predominantly large shell fragments (>3-4 centimeters), and carbonate clasts with a muddy matrix and appears to be predominantly matrix-supported. It is clast-supported in the overlying 10 – 15 centimeters and the muddy matrix is minimal. Carbonate clasts range from 2 – 6 millimeters to 2 – 15 centimeters in diameter. **F3** can be classified as a grainstone to rudstone that is poorly sorted with angular to sub-angular clasts. There is a ~6 centimeters thick lens of low-angle thinly laminated sandstone (**F2**) located at ~3073 meters MD. Above ~3072.4 meters MD the muddy matrix increases in abundance but **F3** is still predominantly clast-supported. **F3** is overlain by **F1** at ~3071.7 meters MD. Two more intervals of **F3**, 15 – 20 centimeters thick, were deposited at ~3071.4 meters MD and ~3070.9 meters MD before being overlain by ~ one meter of **F1**.

From ~3069.3 - 3054 meters MD four distinguishable successions of **F2** gradationally overlain by **F1** were deposited, similar to the successions deposited from 3094 – 3074.2 meters MD. Above ~3054 meters MD **F1** gradually fines-upwards into a massive grey-shale deposit (**F4**) and trace fossils become difficult to distinguish. In the lowermost part of **F4**, trace fossils of **F1** disappear and become predominantly tightly packed concave-up laminae (*Teichichnus isp*), concentric laminations of sandstone and clay (*Asterosoma isp*), and unlined, cylindrical burrows in shale (*Thalassinoides isp*). **F4** includes a 15 centimeter thick bed of red-coloured shale at ~3051.7 meters MD (Figure 5.22). At ~3051 meters MD **F4** gradually coarsens-upwards into **F1** and the identifiable trace fossils are *Ophiomorpha isp, Thalassinoides isp,* and *Paleophycus isp.*

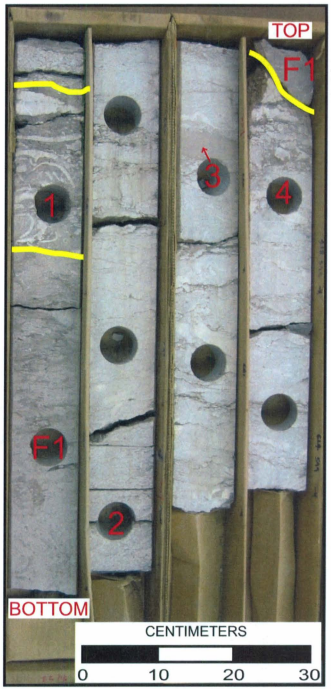


Figure 5.21: Thick grainstone deposit (**F3**) found in the M-04 well (Core 3, Boxes 71 & 72). Base of cored section is in lower left corner and top is in upper right corner. 1: Matrix-supported shell fragments and carbonate clasts overly **F1**. 2: Fully clast-supported grainstone with minimal muddy matrix. 3: Approximately 4-5 centimeter thick laminated fine-grained sandstone lens (**F2**). 4: Top of fully clast-supported grainstone, above which carbonate fragments become matrix-supported and increasingly absent in overlying two meters. **F1** overlies uppermost carbonate-rich interval.

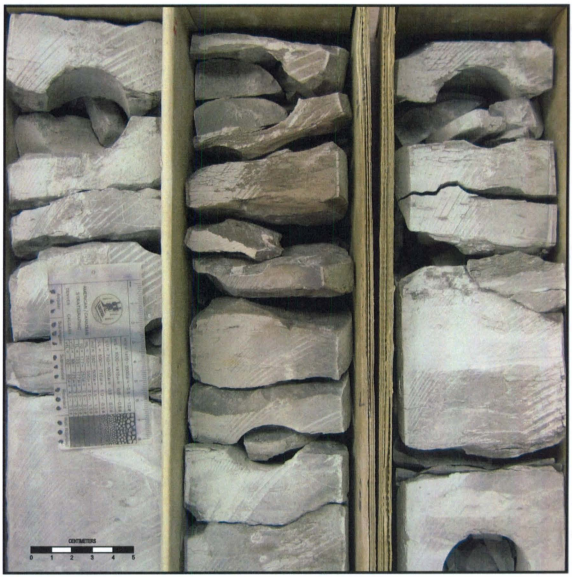


Figure 5.22: Massive shale deposit (**F4**) containing an interval of red shale found in the M-04 well (Core 3, Boxes 53 & 54). Full length of core boxes is not shown so displayed intervals do not stack directly together to form a continuous zone. Left grey shale contains minimal identifiable trace fossils and grades upwards into ~15 centimeter thick red shale. Gradationally above the red shale, the grey shale was re-established and contains minimal trace fossils. *Note: As shown, the core quality is the lowest of the recovered core and the shale is fairly broken up. The shale also swells when wet, so identifying trace fossils and cleaning the core samples are difficult tasks.*

F1 is erosively truncated at ~3049.4 meters MD by rudstone with clasts up to 25 centimeters in diameter (**F5**) (Figure 5.23). The clasts in **F5** are sub-angular in shape and appear to be matrix-supported but may also be considered clast-supported in some areas. **F5** is ~40 centimeters thick conglomeratic rudstone capped by grainstone fining-upwards into mudstone. **F1** overlies **F5** and contains abundant carbonate and shell fragments.

Another set of five distinguishable successions of **F2** fining-upwards into **F1** occurs from ~3047.7 – 3042.1 meters MD that is primarily fine- to medium-grained sandstone with a higher preservation of **F2** versus **F1**. There is a high occurrence of carbonaceous material highlighting laminations in **F2**. Uppermost **F1** fines-upwards into ~1.1 meters of **F4** where no sedimentary structures or trace fossils are identifiable and occasional shell fragments are present. **F4** is sharply truncated at ~3041.0 meters MD by **F1** extending to ~3035.9 meters MD. This interval of **F1** is a series of fining-upwards sandstone; however occurrence of **F2** is very rare. Shell fragments are common and increase in abundance upwards. At ~3039.6 meters MD is a 10 – 12 centimeter thick deposit of **F3**. It is very carbonate rich and contains abundant shell fragments.

F2 erosively overlies **F1** at ~3035.9 meters MD. Several successions of fining-upwards sandstone are identifiable and intervals of **F2** overlain by **F1** are very rare in the lower successions and increasingly preserved up-section. This pattern exists from ~3035.9 – 3018 meters MD. Overall, the sandstone discontinuously (step-wise) fines-upwards from very coarse- to coarse-grained in the lower successions to fine-grained in the upper successions through multiple fining-upward intervals (Figure 5.24). Individual continuous successions range from <1 meter to over 3 meters thick. At ~3018 meters MD **F1** fines-upwards into a ~2.2 meter thick interval of **F4**.



Figure 5.23: Rudstone (**F5**) found in the M-04 well (Core 3, Box 52). Note large size and sub-angular nature of clasts, as well as abundance of muddy matrix that supports some clasts.

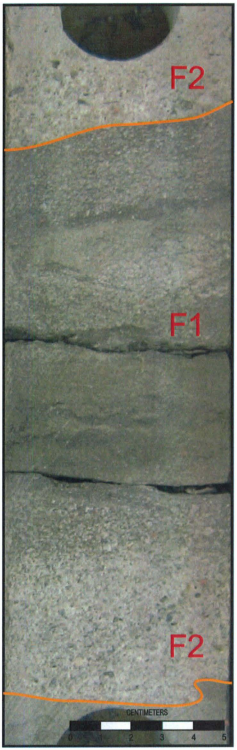


Figure 5.24: Fining-upwards succession of sandstone found in the M-04 well (Core 3, Box 38). The base is coarse-grained sandstone with no distinguishable internal character (**F2**) that fines-upwards into **F1**.

Overlying **F4** are three fining-upwards beds (~0.5 – 1.3 meters thick) of **F1** from ~3015.8 – 3013.4 meters MD. **F1** is not completely bioturbated and occasional horizontal laminations are preserved. The lowermost **F1** contains a thin shell fragment bed deposited at the base. **F1** is erosively overlain by a moderately bioturbated shale at ~3013.4 meters MD. Bioturbation of the shale appears to be sporadic and is dominated by *Chondrites isp, Planolites isp,* and *Paleophycus isp.* The shale coarsens-upwards over 1 – 2 meters back into typical **F1**. **F1** contains common shell fragments and is dominantly bioturbated by *Ophiomorpha isp* trace fossils.

At ~3010.7 meters MD, **F1** is sharply capped by a ~2 centimeter thick **F4**, overlain by a ~25 centimeter thick **F3** (Figure 5.25). **F3** is predominantly shell fragments and carbonate grains. There are occasional faint observable low-angle laminations, but overall seems to lack an internal structure. There are rare occurrences of *Ophiomorpha isp.* **F3** is also capped by a ~2-3 centimeter thick **F4**. From ~3010.4 – 3007.1 meters MD exists coarsening-upwards **F1**. Bioturbation is extensive at the base and decreases upwards to preserve occasional sections of low-angle laminations and essentially absent near the top to preserve ~0.8 meters of **F2** with occasional traces of *Ophiomorpha isp.* Multiple fining-upwards successions of **F3** to **F2** are found between ~3007.1 – 3004.0 meters MD. Each individual succession is from ~0.4 – 1.2 meters thick. **F3** is typically very shell fragment rich and deposited at the base of the successions, possibly as lag deposits. **F2** is very fine- to coarse-grained, parallel to divergent, horizontal to low-angle laminations, and with rare bioturbation. Erosively overlying the multiple **F3** to **F2** successions at ~3004.0 meters MD is an interval of **F3** over 2 meters thick with minimal sandstone content and contains faint low-angle laminations.



Figure 5.25: Grainstone (**F3**) found in the M-04 well (Core 3, Box 22). **F3** is rich in shell fragments and has no distinguishable internal structure. There are faint low-angle laminations in the upper section. Green arrows indicate two trace fossils that resemble *Ophiomorpha isp* in cross-section of a horizontal burrow (left arrow) and a vertical shaft (right arrow).

At ~3001.7 meters MD **F3** is capped by **F2** fining-upwards into **F1**. Primary trace fossils include *Ophiomorpha, Paleophycus,* and *Skolithos.* There are two intervals of **F3** ~10 – 12 centimeters thick composed primarily of shell fragments located at ~2999.6 meters MD and ~2999.0 meters MD. Both have sharp base contacts and gradational top contacts into **F1**. Below ~2993.8 meters MD **F2** is rarely preserved. From ~2993.8 – 2987.1 meters MD successions of **F2** fine-upwards into **F1**. Several thin intervals of **F3** (4-6 centimeters) are present below some occurrences of **F2**. Overall, the entire interval from ~3001.7 – 2987.1 meters is coarsening upwards, while individual successions are fining-upwards.

From ~2987.1 – 2984.0 meters MD is **F1** with ~5 centimeter thick **F3** located at ~2986.2 meters MD with irregular upper and lower boundaries. Above ~2984.0 meters MD to the top of Core 3 at 2983.0 meters MD **F5** was deposited with interbedded laminations of muddy matrix. Several large shell fragments are commonly found. Overall there appears to be no distinguishable internal structure to the deposit.

5.4.2 Depositional Environment

Trace fossil assemblages of the Hebron M-04 core record multiple transitions between upper and lower shoreface environments. Upper shoreface environments are indicated by the presence of *Ophiomorpha isp, Paleophycus isp,* and *Skolithos isp* trace fossils. Lower shoreface environments are indicated by the presence of *Asterosoma isp, Teichichnus isp,* and *Thalassinoides isp* trace fossils. The different assemblages highlight the change from the higher current energy depositional environments of *Ophiomorpha isp, Skolithos isp, Paleophycus isp,* and *Planolites isp* to somewhat lower energy depositional environments where *Asterosoma isp, Teichichnus isp,* and

Thalassinoides isp are found. Associations of these trace fossils with sedimentary structures and features further support the type of depositional environment suggested through the trace fossil assemblages.

From the base of the core (~3093.6 meters MD) through to ~3074.2 meters MD siliciclastic sediments form fining-upwards successions suggesting a landward shift in the shoreline. Trace fossil assemblages present indicate an upper shoreface depositional environment. Erosively-based coarser-grained beds at the base of the fining-upwards successions may represent storm deposits. They are characterized by low-angle laminated sandstone with abundant lag deposits that may correspond to preserved storm beds or episodic, rapid influxes of sediment, each subject to subsequent flooding and deposition of finer-grained, burrowed sandstones. Preservation of a thin carbonate bed suggests that the environment occasionally experienced periods of low siliciclastic sedimentation. During these periods of low siliciclastic sediment input it is possible that localized carbonate banks may have developed and were re-deposited as grainstone beds during storm events.

The thick limestone deposit overlying the upper shoreface sandstones represents a period of time where siliciclastic sediment deposition is at a minimum for the Hibernia Formation. Large, intact shells that are abundant at the base suggest deposits are nearly *in situ*. A carbonate bank subsequently developed and formed a ~4 – 5 meter thick deposit. The top of the carbonates record the gradual increase in siliciclastic sediments as alternating sandstone and carbonate deposits suggest an episodic nature to the return to siliciclastic deposition by ~3069.3 meters MD. Renewed siliciclastic upper shoreface deposition was established through to ~3054 meters MD, where sandstones are very similar to previous deposits from ~3093.6 – 3074.2 meters MD.

Sandstones gradually coarsen-upwards until ~3062 meters MD, above which they show a fining-upwards pattern where no primary sedimentary structures are preserved. This represents progradation of the shoreface environment through to ~3062 meters MD followed by a rapid retrogradation into predominantly shale deposition by ~3054 meters MD. Preceding the shale deposition is an interval where large, intact shell fragments are common, representing the onset of a period of minimal coarse-grained siliciclastic sedimentation. Above this interval visible trace fossils begin to decrease in abundance and shale deposition is established. The shale coarsens-upward above ~3051 meters MD and bioturbation is re-established as well. However, bioturbated deposits are sharply truncated by a large clast rudstone at ~3049.4 meters MD. Rudstone carbonate clasts are not *in situ* and may have been transported a relatively short distance due to the large clast size. Perhaps the rudstone represents the remains of a carbonate bank that developed during the period of low siliciclastic sedimentation coeval with shale deposition around it. The carbonate bank may have been destroyed during a large storm event or an episodic event due to renewed fault activity that is likely associated with short duration increases in coarse-grained siliciclastic sedimentation. This increase in siliciclastic sedimentation is recorded through the coarsening-upwards package of sandstone above the rudstone.

Continuing up-section, siliciclastic sediments coarsen-upwards in a step-wise appearance and reach maximum progradation near ~3031 meters MD through a series of fining-upwards successions (~0.4 - >3 meters thick). The low-angle laminated sandstone base is progressively thicker up-section and has abundant carbonaceous material and occasional cross-bedding signifying the increasing proximity to the source and shoreline. Similar dip-directions of preserved laminations suggest a predominantly

uni-directional flow deposition. Absence of trace fossils through the uppermost laminated sandstone suggests currents were intense and sedimentation rapid. Sedimentation appears to be retrogradational above ~3031 meters MD through to ~3016 meters MD and grain size ultimately fines upwards into a thick massive shale deposit. The change from progradation may be due to a decrease in fault activity, and subsequent reduction of depositional slope, causing the energy of the depositional system to decrease, and suppression of coarse-grained sediment sources. The change may also be related to a relative sea level rise. Gradual, but punctuated decrease in energy is not typical of a waning depositional system due to flow diversion or system abandonment. The predominantly medium-grained sandstone that is deposited through to the shale deposit suggests that the fault activity is decreasing causing discrete influxes of coarse-grained sediments into the depositional system to be spaced further apart in time. The massive shale is likely due to decreased sediment influx rather than a rapid transition from upper shoreface to lower shoreface since the supporting trace fossil evidence is absent.

Above the massive shale, there appears to be one final prograding sedimentary succession before the overlying thick limestone at ~2984 meters MD. However, there is an abundance of thin grainstone beds mixed throughout the succession. Most seem to have been transported some distance and are typically found at the base of a siliciclastic fining-upwards interval. Peak progradation is near ~3004 meters MD where the coarsest sediment is found, above which the succession is gradually fining-upwards. This succession marks the top of the Hibernia Formation stratigraphically. The vertically discontinuous (step-wise) nature of the succession is likely due to intermittent fault activity before faulting ceased at the end of the Hibernia Formation deposition. It is

possible that sedimentation rates were low between individual faulting episodes, and that temporarily stable conditions were ideal to establish carbonate banks. At the onset of the next faulting episode, these carbonate banks would be destroyed by renewed influx of siliciclastic sediments and likely re-distributed at the base of the sandstone successions.

The limestone at the top of the core is different in composition and visual character when compared to the other carbonates found throughout the cored interval. The top unit has abundant shell fragments and a brown coloration compared to the other carbonates which have a light grey coloration. The uppermost carbonate interval represents the onset of the Catalina Formation and 'B' Marker limestone deposition, and marks the top of the Hibernia Formation. Deposition of this limestone may be taken as the end of the North Atlantic Rifting episode that formed the Hibernia Formation (Enachescu, 1987; McAlpine, 1990; and Sinclair, 1993).

5.5 CONCLUSION

Fine-scale interpretations that were extracted from the core data are very valuable in assessment of the Hibernia Formation depositional environment. They provide missing details that are not visible in seismic and petrophysical data. Sedimentary structures, grain size, and trace fossils all provide valuable information towards understanding the depositional environment of the Hibernia Formation. Together with depositional patterns derived from petrophysical well correlations (see Chapter 6), core interpretations add small-scale details to the depositional model to improve validity of the proposed model (see Chapter 7 for further discussion of the overall model of the paleo-depositional environment). On the other hand, available cores

are widely spaced, both stratigraphically and laterally, providing no more than a glimpse into possible depositional settings.

The Amoco et al. West Bonne Bay C-23 well represents the relatively uniform character of one of the coarsening-upwards successions seen in the Lower Hibernia Member. Characteristics noted in the core suggest occasional bi-modal current influence. It suggests a close proximity to the siliciclastic sediment source and/or shoreline through the low diversity of trace fossils, abundant carbonaceous material and overall coarse sediment accumulation.

The Mobil et al Hebron I-13 well represents the base of a coarsening-upwards succession in the Upper Hibernia Member. Abundant fine-grained sediments and carbonate material are indicative of periods of low siliciclastic sedimentation and/or low energy. However, the transported nature of some carbonate beds suggests lateral shifting of a high-energy depositional system. Evidence presented in the cored interval suggests a primarily wave-influenced depositional environment.

The Chevron et al Hebron M-04 well records multiple fining-upwards successions in the Upper Hibernia Member, sometimes combining to form step-like coarsening-upwards sequences. Abundance of carbonate beds, some of which appear to be *in situ* (or nearly so), mark decreasing siliciclastic sediment supply into the depositional site with time and overall transition into the overlying 'B' Marker limestone of the Catalina Formation. The shift in environments seems to be gradual through the multiple successions that are identifiable; however, stratigraphically the base of the 'B' Marker limestone is clearly identifiable in both the core and petrophysical well logs (see Chapter 6). Overall, based on interbedding of laminated-to-bioturbated sandstones with carbonate beds, the top of the Hibernia Formation appears to be a mixed depositional

environment of increasingly marine influence, likely reflecting the waning stages of the regional siliciclastic source. Predominance of the *Skolithos* ichnofacies suggests an established upper shoreface regime with varying influx of siliciclastic sedimentation.

CHAPTER 6 – PETROPHYSICAL LOG DATA

6.1 SCOPE AND PURPOSE

Seismic data, presented in Chapter 4, provide large-scale structural and stratigraphic information about the subsurface while core data, presented in Chapter 5, provide fine-scale sedimentary and lithological information about depositional settings. However, petrophysical log data are needed to further refine the stratigraphy and lithology. Fifty-one (51) existing exploration, delineation, and development wells that span the study area allowed a detailed interpretation of the Hibernia Formation stratigraphy. They show thickness variations, lateral lithology variations, vertical stacking patterns and petrophysical characteristics of correlated stratigraphic units. For example, based on percent-sandstone maps derived from petrophysical data, the relative location of siliciclastic sediment sources and general sediment dispersal directions can be inferred.

This chapter focuses on petrophysical log data and begins by describing the methodology used to subdivide the Hibernia Formation into two major lithostratigraphic units (Upper and Lower Members) and then describe the hierarchy of sub-units that compose each of the two major Members. The methodology also describes the loop-tying procedure used to correlate the units between wells. Description of individual sub-units consists of parameters for the top and bottom boundaries as well as lateral variations of petrophysical signature, sandstone distribution and thickness changes. Consideration of informal Members and sub-units as a linked series of geological successions leads to the interpretation of possible depositional environments.

6.2 UNIT DEFINITION

Note: Plates are located at the end of the thesis, following the Appendices, and are meant to compliment sub-unit descriptions.

6.2.1 LOWER HIBERNIA MEMBER

The Lower Hibernia Member is typically characterized by four coarsening-upward successions overlain by a thick (>100 meters) interval of interbedded sandstone and shale. To the north, log-facies of coarsening-upward successions change laterally into fully marine shales of the Fortune Bay Formation. The uppermost interval of the Lower Hibernia Member consists of interbedded sandstone and shale with no discernible characteristics or lateral correlativity. Moving north towards the basin depocentre, sandstone content of some cycles decreases while other cycles increase illustrating possible progradation and retrogradation fluctuations. Gross thickness trends of the Lower Hibernia Member are illustrated in Figure 6.1. Thickening is present in the central, south-north trending part of the study area, localized primarily in the Far East block. Thickness variations occur across the four major north-south faults with increased thickening in the Far East block. Percent-sandstone trends are illustrated in Figure 6.2. Sandstone content is greatest in the southeast, along the Voyager Fault System and generally decreases to the north and northwest. Sandstone content also increases in the northeast, at the Ben Nevis I-45 well. A loose correlation of increased thickness to increased sandstone content is present across the study area, with the exception of the Terrace region which has an opposite relationship perhaps indicative of its role as a region of sediment bypass.

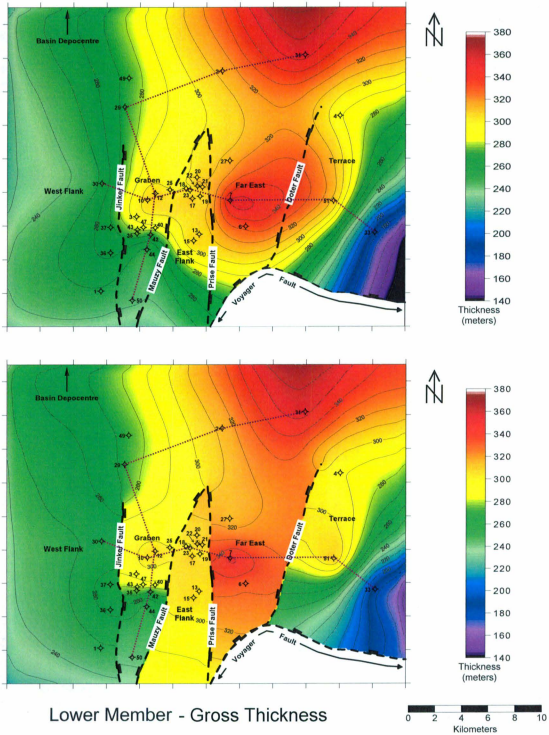


Figure 6.1: Gross thickness maps of the Lower Hibernia Member. Top map shows contouring without the influence of faulting. Bottom map shows contouring with the influence of faulting. Purple dotted lines show locations of Plate 1 (S-N/NE) and Plate 2 (W-E).

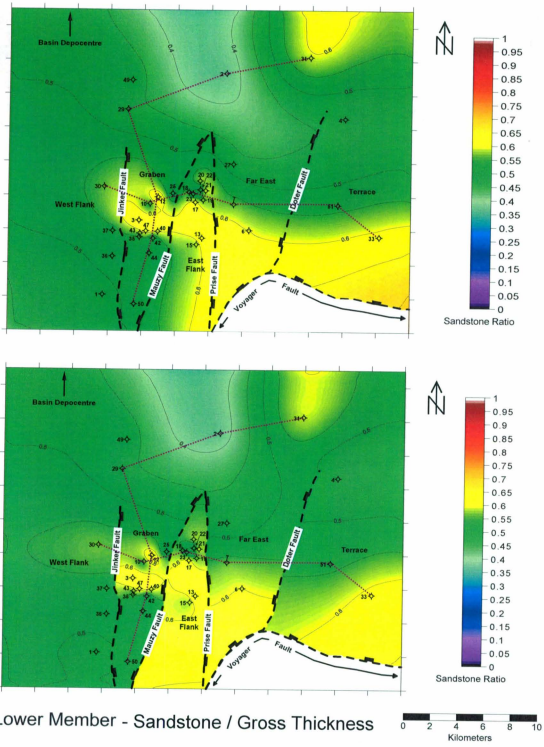


Figure 6.2: Percent-sandstone maps of the Lower Hibernia Member. Top map shows contouring without the influence of faulting. Bottom map shows contouring with the influence of faulting. Purple dotted lines show locations of Plate 1 (S-N/NE) and Plate 2 (W-E).

Plate 1 is a south to north-northeast cross-section of the Lower Hibernia Member cutting northward through the Graben and intersecting wells through the northern region of the study area, as shown in the inset location map (note that Plate locations are highlighted on maps that accompany unit descriptions). Overall, thickening to the north is evident except at the Hebron I-13 well, which exhibits thinning in Lower Member sub-units 306 and 320. Decreasing sandstone content northward is also apparent as several coarsening-upwards successions (Lower Member sub-units 306, 310 and 312) are composed entirely of shale in the north. However increased sandstone content to the north exists in Lower Member sub-unit 320, which is displayed as a thickening sandstone package overlying a shale bed of varying thickness.

Plate 2 is a west to east cross-section of the Lower Hibernia Member as shown in the inset location map. Thickness variations are relatively minor along this section which is deemed to be parallel to depositional strike. The thickness variations that exist are mainly due to the horst and graben structures found across the study area, which likely controlled the deposition of sediment and accommodation space. The southern half of the study area is primarily composed of two main horsts, West Flank and East Flank, and two main grabens, Graben and Far East. The Terrace, east of the Doter Fault, is a horst structure that is significantly structurally higher than the main horst and graben development to the west of the Doter Fault. This structure results in typical stratigraphic thinning over the horst blocks due to decreased accommodation space. Sandstone content also remains relatively constant along the strike section, with the exception of increased sandstone at the Springdale M-29 and Voyager J-18 wells.

6.2.1.1 Lower Hibernia Member sub-unit 306

Lower Hibernia Member sub-unit 306 consists of a coarsening-upwards sequence of interbedded sandstone and shale immediately overlying the thick shale deposit of the Fortune Bay Formation. Well sections considered to be typical of sub-unit 306 are shown in the Terra Nova K-08 and G-90_5 wells (Figure 6.3). The base of sub-unit 306 is defined as the gradational onset of sandstone deposition above Fortune Bay Formation shales. Along the southern and eastern basin margins several thin sandstone beds are visible in the upper Fortune Bay Formation (see Beothuk M-05 well in Plate 1). Sub-unit 306 is primarily a coarsening-upwards sandstone sequence with common occurrences of shale and siltstone beds ranging from one to four meters thick. To the north, sub-unit 306 changes to shale and becomes indistinguishable from shale of the Fortune Bay Formation below and boundaries are arbitrarily chosen within the shale as the coarsening-upwards trend is no longer present. The top of sub-unit 306 is sharply marked by deposition of a shale to siltstone bed greater than five meters thick, marking the top of the coarsening-upwards trend.

Gross thickness trends of sub-unit 306 are illustrated in Figure 6.4. Increased thickness is present within the Far East block and likely suggests greater displacement along the southern portion of the Doter and Prise faults, in conjunction with the basin-bounding Voyager Fault System displacement, creating greater accommodation space. Thinning to the north is likely due to increased distance from primary siliciclastic sediment sources along the southeastern basin margin. However, thinning in the north was also caused through erosion by the overlying sub-unit 308, which is discussed further in section 6.2.1.2. Thickness across the Jinker and Mauzy faults are relatively consistent and any gross thickness trends west of the Prise Fault are considered to be

primarily depositional with minimal active faulting. Percent-sandstone trends of sub-unit 306 are illustrated in Figure 6.5. Shale deposition generally increases northward from the Voyager Fault System. However, across the northern portion of the West Flank and Graben there exists a localized area of high sandstone content. This is likely due to development of a blocky sandstone bedset (~fifteen to twenty meters thick) within the middle of sub-unit 306, which is bounded by siltstone to shale beds one to three meters thick. This character is only present west of the Prise Fault and located within the overall coarsening upwards trend of sub-unit 306, which can be observed in Plate 1 when comparing Terra Nova L-98_5 with surrounding wells Beothuk M-05 and Terra Nova F-100_4.

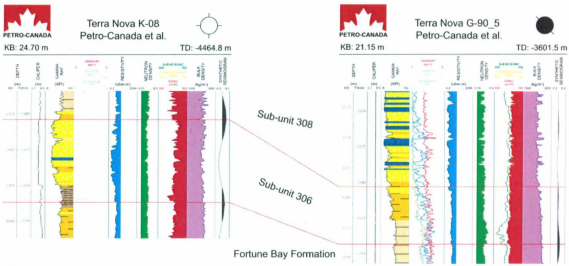


Figure 6.3: Type-sections of Lower Hibernia Member sub-unit 306.

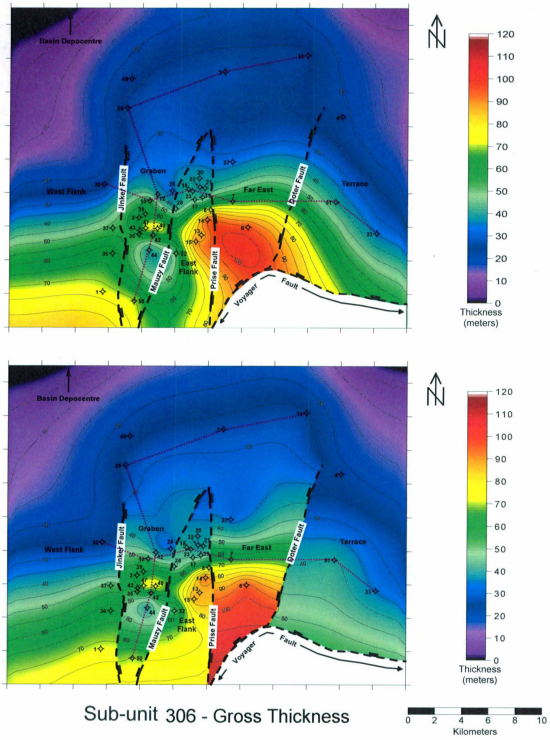


Figure 6.4: Gross thickness maps of Lower Hibernia Member sub-unit 306. Top map shows contouring without the influence of faulting. Bottom map shows contouring with the influence of faulting. Purple dotted lines show locations of Plate 1 (S-N/NE) and Plate 2 (W-E).

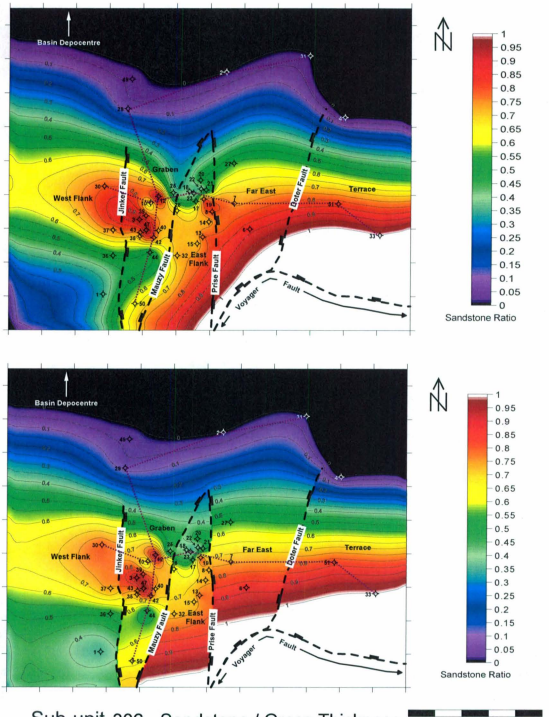


Figure 6.5: Percent-sandstone maps of Lower Hibernia Member sub-unit 306. Top map shows contouring without the influence of faulting. Bottom map shows contouring with the influence of faulting. Purple dotted lines show locations of Plate 1 (S-N/NE) and Plate 2 (W-E).

6.2.1.2 Lower Hibernia Member sub-unit 308

Lower Hibernia Member sub-unit 308 is defined as a coarsening-upwards deposit of thick basal shale, with minor thin sandstone beds, overlain by thick sandstone with sharp base and top contacts. From the southern edge through the center of the study area and further north, however, sub-unit 308 rapidly thickens becoming predominantly sandstone with a thinner basal shale bed. Well sections considered to be typical of sub-unit 308 are shown in the Terra Nova K-08 and F-100_2 wells (Figure 6.6). The southern area is characterized by thick basal shale with occasional sandstone beds, one to two meters thick, overlain by a sandstone bedset, six to fifteen meters thick. The northern area is characterized by basal shale overlain by a much thicker sandstone interval with minimal shale. The top of sub-unit 308 is marked by the deposit of a five to ten meter thick shale interval that is traceable across the study area.

Gross thickness trends of sub-unit 308 are illustrated in Figure 6.7. The forty-five meter contour (bolded) approximately represents the division of the southern and northern depositional patterns of sub-unit 308. Sandstone deposition in sub-unit 308 thickens dramatically to the north and possibly represents some erosion into the underlying sub-unit 306, since that depositional trend thins to the north. Percent-sandstone trends of sub-unit 308 are illustrated in Figure 6.8. Presence of thick basal shale are indicated across the north-east and southern margins of the study area where percent-sandstone decreases. Across the centre of the study area, the east-west trend of sandstone deposition is clearly visible with minimal shale content. Lower percent-sandstone in the northern portions of the Graben and Far East, compared to the East Flank, is due to increased abundance of interbedded shale deposits. This character is illustrated in Plate 2 where the Terra Nova F-100_2 and C-69_3 wells (located in graben

structures) have occurrences of thin shale beds separating thicker sandstone bedsets, which are not present in the Terra Nova G-90-5Y well (located in a horst structure).

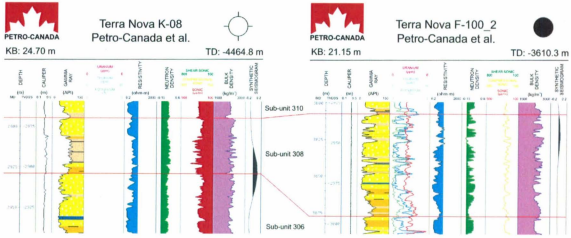


Figure 6.6: Type-sections of Lower Hibernia Member sub-unit 308.

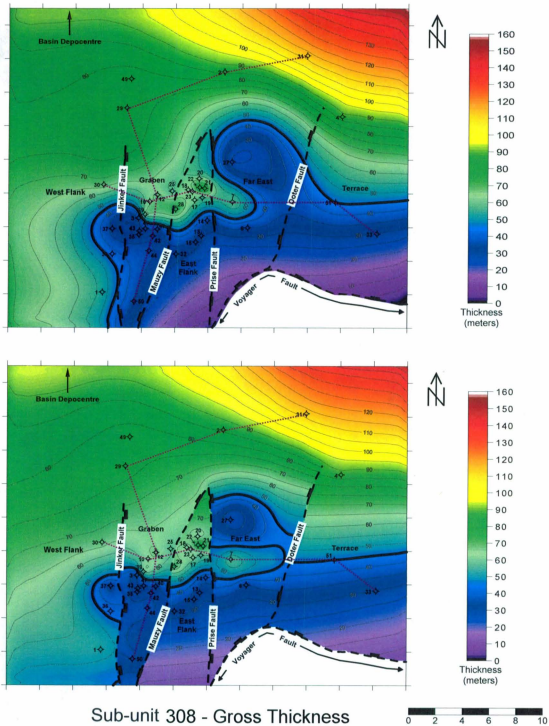


Figure 6.7: Gross thickness maps of Lower Hibernia Member sub-unit 308. Top map shows contouring without the influence of faulting. Bottom map shows contouring with the influence of faulting. Black line represents the division between northern and southern depositional character. Purple dotted lines show locations of Plate 1 (S-N/NE) and Plate 2 (W-E).

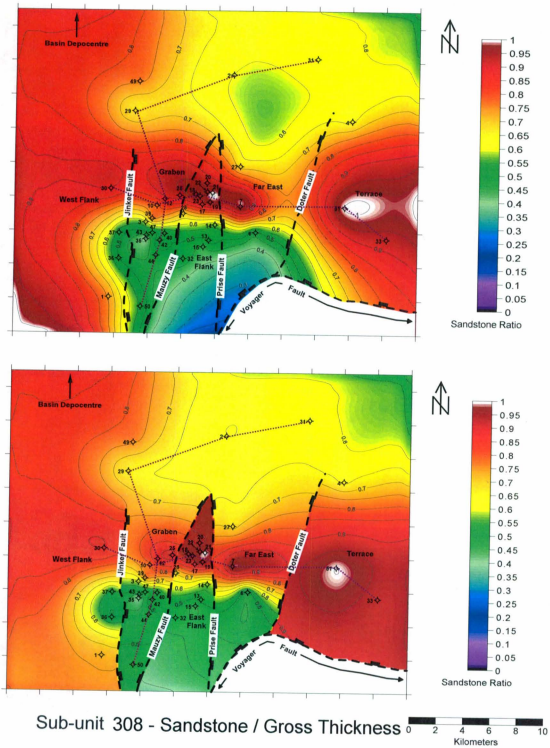


Figure 6.8: Percent-sandstone maps of Lower Hibernia Member sub-unit 308. Top map shows contouring without the influence of faulting. Bottom map shows contouring with the influence of faulting. Purple dotted lines show locations of Plate 1 (S-N/NE) and Plate 2 (W-E).

6.2.1.3 Lower Hibernia Member sub-unit 310

Lower Hibernia Member sub-unit 310 is defined as basal shale, five to ten meters thick, overlain by coarsening-upwards, then fining-upwards sandstone. Well sections considered to be typical of sub-unit 310 are shown in the Terra Nova K-08 and F-100_2 wells (Figure 6.9). The base of sub-unit 310 is defined by five to ten meter thick shale bed overlying the thick sandstones of sub-unit 308. Across the study area, sub-unit 310 is predominantly coarsening-upwards sandstone and varies in thickness from less than five meters to twenty meters thick. Towards the northern margin of the study area sub-unit 310 is entirely shale. The upper section of sub-unit 310 can appear fining-upwards (increasing gamma ray character), however, the coarsening-upwards pattern occasionally continues to the top of the interval, where it has a sharp upper contact. The top of sub-unit 310 is marked by a five to ten meter thick shale bed that is correlative across the study area.

Gross thickness trends of sub-unit 310 are illustrated in Figure 6.10. Maxima in thickness appear more discrete, with lobe-like features, which thin to the north and south from the central region of the study area. Thickness variations across major faults appear to be minimal, suggesting depositional patterns are dependant on depositional environment and fault activity was relatively minor during this time. However, increased fault displacement along the Prise and Doter faults is possibly suggested by the overall increased thickness across the Far East block. Percent-sandstone trends of sub-unit 310 are illustrated in Figure 6.11. Across the southern region of the study area the zone is predominantly sandstone and rapidly decreases in sandstone content to the north. However, the percent-sandstone trend is fairly uniform in the east-west direction, indicating a low influence of major fault activity during deposition of sub-unit 310.

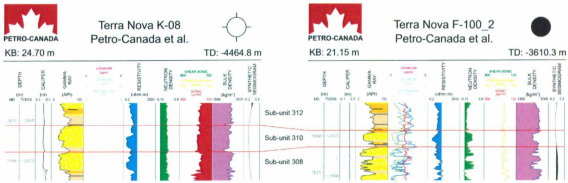


Figure 6.9: Type-sections of Lower Hibernia Member sub-unit 310.

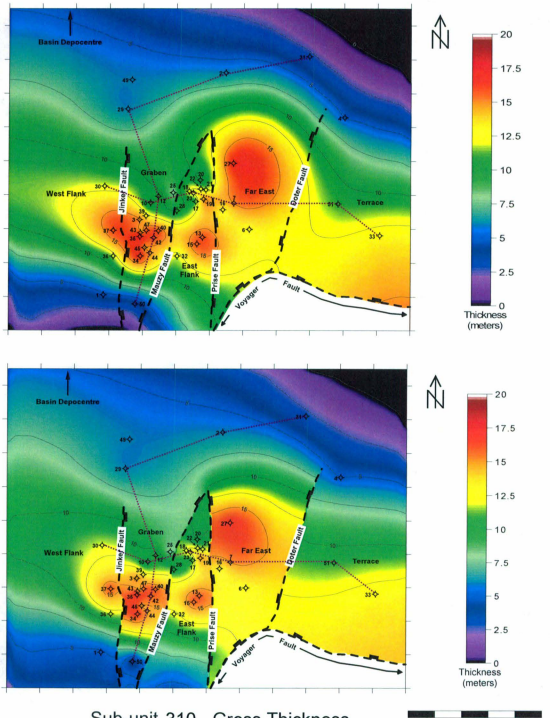


Figure 6.10: Gross thickness maps of Lower Hibernia Member sub-unit 310. Top map shows contouring without the influence of faulting. Bottom map shows contouring with the influence of faulting. Purple dotted lines show locations of Plate 1 (S-N/NE) and Plate 2 (W-E).

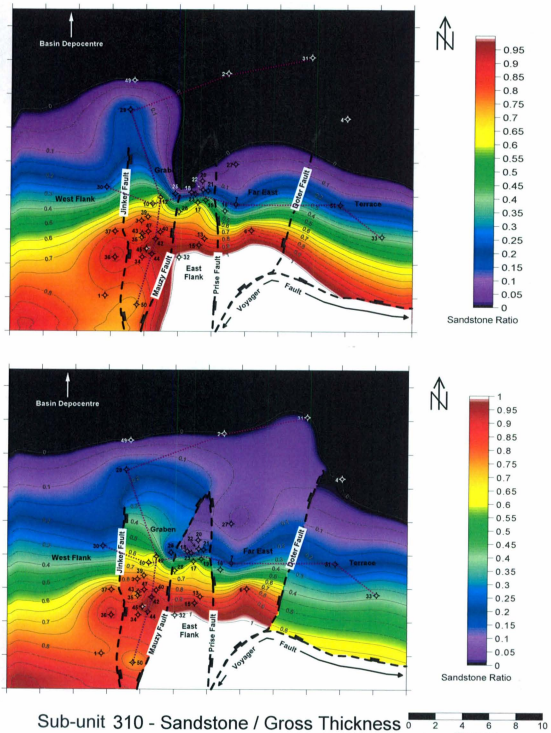


Figure 6.11: Percent-sandstone maps of Lower Hibernia Member sub-unit 310. Top map shows contouring without the influence of faulting. Bottom map shows contouring with the influence of faulting. Purple dotted lines show locations of Plate 1 (S-N/NE) and Plate 2 (W-E).

6.2.1.4 Lower Hibernia Member sub-unit 312

Lower Hibernia Member sub-unit 312 is characterized by shale gradually coarsening-upwards into a thick sandstone interval, generally greater than twenty meters thick. Well sections considered to be typical for sub-unit 312 are shown in the Terra Nova K-08 and F-100_2 wells (Figure 6.12). The base is marked by a five to twenty meter thick shale interval that is laterally continuous across the entire study area. The thick shale coarsens-upwards into a sandstone interval, generally greater than twenty meters thick. This character differs only at the northern wells, such as Hebron I-13 and West Ben Nevis B-75, where the thick sandstone interval is represented by multiple sandstone bedsets with interbedded shales. Coarser (lowest gamma ray character) and thicker sandstone beds are generally located in the upper portion of sub-unit 312, indicating the overall coarsening-upwards nature of the zone is still present in the northern section of the study area, but is punctuated by thin shale beds. The top of sub-unit 312 is marked by the sharp truncation of the thick sandstone interval by overlying shale that is often greater than ten to fifteen meters thick.

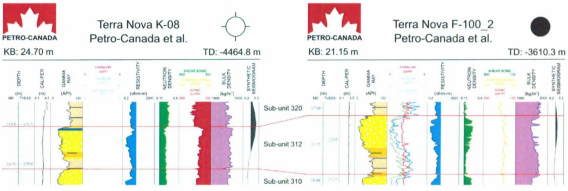


Figure 6.12: Type-sections of Lower Hibernia Member sub-unit 312.

Gross thickness trends of sub-unit 312 are illustrated in Figure 6.13. Gradual thickening to the north and northeast is clearly evident with minimal fault-influenced thickening across the major faults. However, there are several areas where thickness variations across faults are contrary to expectations; for example the thinning in the southern half of the Far East graben-structure across the Prise and Doter faults. This can be interpreted to indicate that these faults, aside from controlling depositional thickness variations, may also influence points of sediment input and dispersal from nearby sediment source regions. Therefore indicating thickness variations are dominantly depositional and less structural for sub-unit 312. Percent-sandstone trends of sub-unit 312 are illustrated in Figure 6.14. The gradual increase in shale content to the north is clearly shown across the study area; however, the rate of change is much more gradational compared to the underlying sub-unit 310. There is also a strong east-west trend to sandstone deposition with minor variations across major faults. Lower percent-sandstone values exist across the southern portion of the Far East, compared to the neighbouring Terrace and East Flank, which is due to a thickening of the basal shale interval in this region while the sandstone interval is relatively unchanged, as is shown in Plate 2 (Terra Nova G-90_5Y and C-69_3 wells).

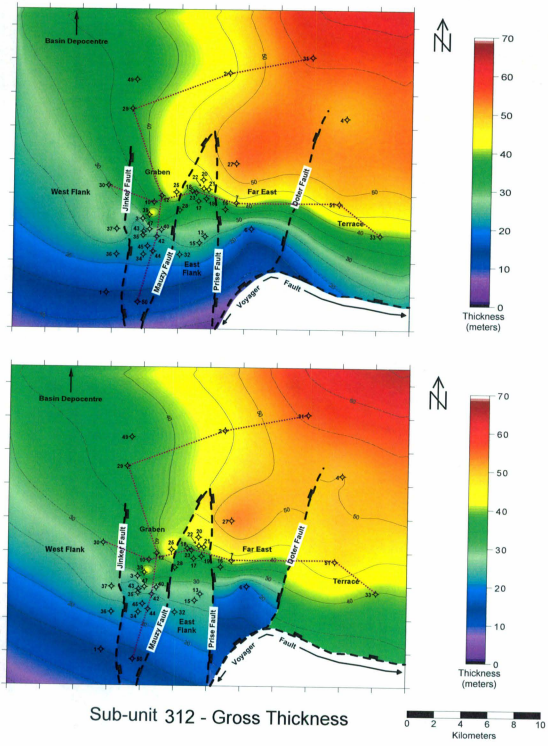


Figure 6.13: Gross thickness maps of Lower Hibernia Member sub-unit 312. Top map shows contouring without the influence of faulting. Bottom map shows contouring with the influence of faulting. Purple dotted lines show locations of Plate 1 (S-N/NE) and Plate 2 (W-E).

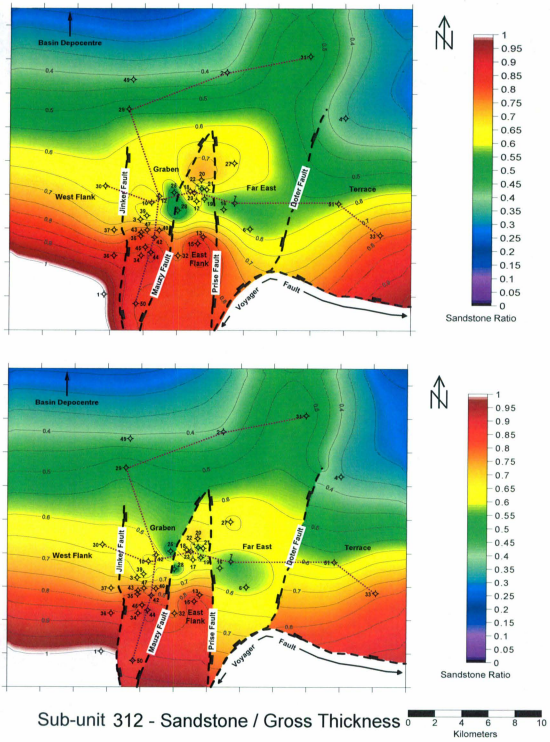


Figure 6.14: Percent-sandstone maps of Lower Hibernia Member sub-unit 312. Top map shows contouring without the influence of faulting. Bottom map shows contouring with the influence of faulting. Purple dotted lines show locations of Plate 1 (S-N/NE) and Plate 2 (W-E).

6.2.1.5 Lower Hibernia Member sub-unit 320

Lower Hibernia Member sub-unit 320 is characterized by laterally discontinuous, interbedded sandstones, siltstones, and shales. Well sections considered to be typical of sub-unit 320 are shown in the Terra Nova K-08 and F-100_2 wells (Figure 6.15). The base of sub-unit 320 is marked by laterally continuous shale that sharply overlies the thick sandstone interval of sub-unit 312. Above this shale deposit, sub-unit 320 is characterized by interbedded sandstone, siltstone, and shale with no obvious correlations between adjacent wells. For this reason, sub-unit 320 is significantly thicker than previous zones and likely includes multiple genetic units. Sandstone bedsets are typically two to five meters thick and are rarely above ten meters thick. The uppermost sandstone interval is fifteen to twenty meters thick and abruptly overlain by shale. This sandstone bed is laterally continuous and is present in almost every well, except where faulted out, and marks the top of sub-unit 320 and top of the Lower Hibernia Member.

Gross thickness trends are illustrated in Figure 6.16. Thickness increases over the Graben, East Flank, and Far East suggest the Jinker and Doter Faults are significantly active creating a depositional low (possibly a broad valley) oriented north-south through the centre of the study area. Increased thickness over the Far East suggests greater displacement along the Prise and Doter faults. It appears the Mauzy Fault was relatively inactive during this time based on gross thickness variations. Percent-sandstone trends are illustrated in Figure 6.17. Sub-unit 320 is predominantly an even mixture of sandstone and shale with sandstone content between forty to sixty percent with minimal variations across the major faults. Sub-unit 320 represents a clear shift in sediment source regions as derived from percent sandstone trends. Primary siliciclastic sedimentation may have shifted to the south of the study area as basin lows

were filled and depositional slope was reduced. Increased sandstone deposition in the northeast possibly suggests a new siliciclastic source, located further northeast along the basin-bounding Voyager Fault System, which may have been connected to the study area due to the reduced depositional slope. Recall from Chapter 1 (Figure 1.2) that the Voyager Fault System trends roughly northeast, east of the study area, and gradually rotates counterclockwise to trend north-northwest approximately twenty-five kilometers east of the study area.

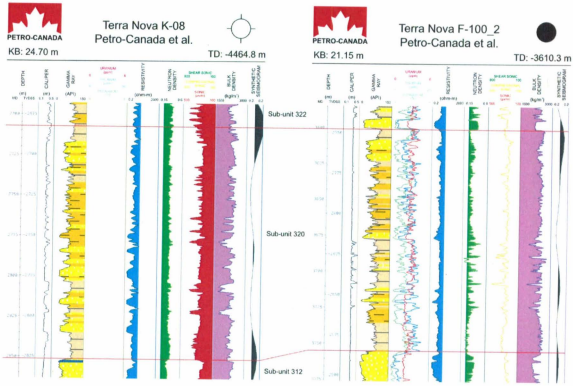


Figure 6.15: Type-sections of Lower Hibernia Member sub-unit 320.

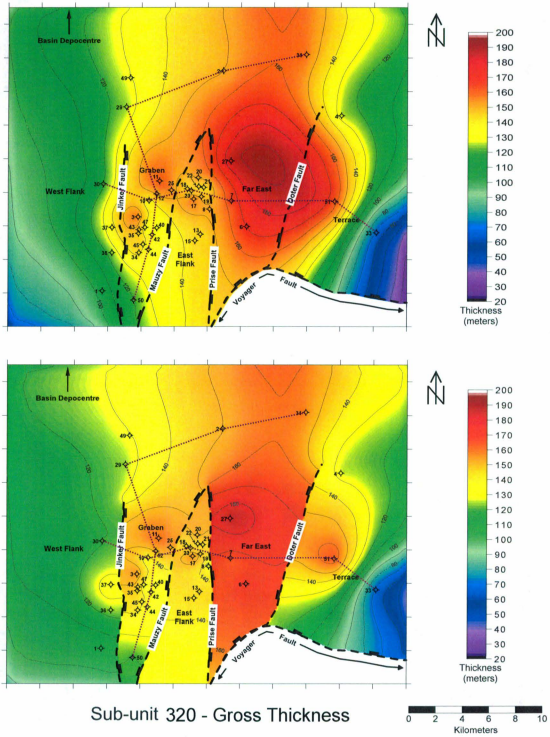


Figure 6.16: Gross thickness maps of Lower Hibernia Member sub-unit 320. Top map shows contouring without the influence of faulting. Bottom map shows contouring with the influence of faulting. Purple dotted lines show locations of Plate 1 (S-N/NE) and Plate 2 (W-E).

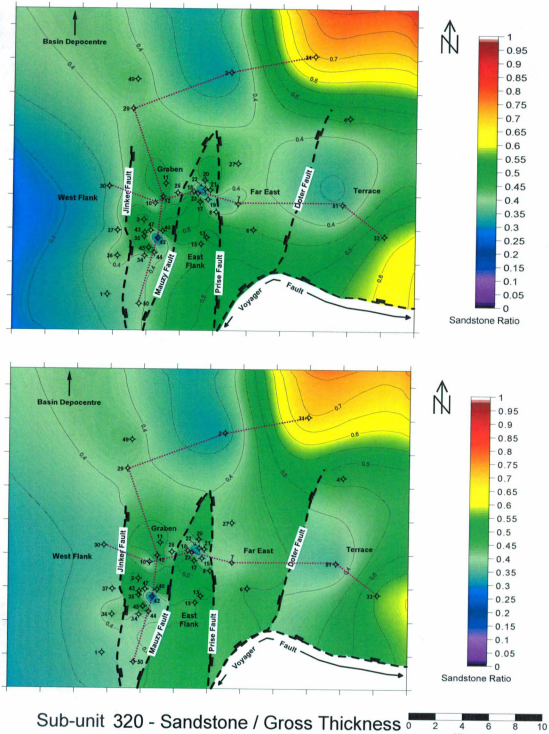


Figure 6.17: Percent-sandstone maps of Lower Hibernia Member sub-unit 320. Top map shows contouring without the influence of faulting. Bottom map shows contouring with the influence of faulting. Purple dotted lines show locations of Plate 1 (S-N/NE) and Plate 2 (W-E).

6.2.2 Upper Hibernia Member

The Upper Hibernia Member is characterized by five distinct sub-units of mixed siliciclastics and carbonates. Carbonates were described in detail in Chapter 5 through core descriptions and are generally conglomeratic carbonate grainstone to rudstone deposits, likely the result of storm events (high energy). For the purpose of correlating well logs, it is assumed carbonates highlighted by drill cuttings (shown via the gamma ray log fill) are clastic in nature and do not represent *in situ* deposits. In some cases they also represent calcite-cemented zones, which have been identified in core descriptions. In the south, where the Upper Hibernia Member is thinnest, the five sub-units are essentially amalgamated forming an overall coarsening-upwards sequence of interbedded sandstone, siltstone and shale near the base with predominantly thick sandstone at the top. As the Upper Hibernia Member thickens to the north, the five sub-units are more clearly defined due to increased shale deposition. Maximum progradation of the Upper Hibernia Member occurs in sub-unit 326 where thick sandstone is deposited across the entire study area. Following the deposition of sub-unit 326 the Upper Hibernia Member enters a period of retrogradation that marks the transition from deposition of Hibernia Formation siliciclastics to widespread deposition of the 'B' Marker limestone above sub-unit 330. Figures 6.18 and 6.19 illustrate gross thickness and percent-sandstone variations of the Upper Hibernia Member, respectively. Notice the character of the maps over the grabens and horsts of the Terra Nova field, with increased thickness and decreased sandstone ratios over graben areas, which were areas of increased accommodation space during deposition.

Plate 3 is a south to north-northeast cross-section of the Upper Hibernia Member starting in the southwest moving northward through the Graben and intersecting wells in

the northern region of the study area, as shown in the inset map. Deposition of the Upper Hibernia Member appears to be much more regular and systematic, compared to the Lower Hibernia Member, as thickness steadily increases to the north, towards the basin depocentre. Similarly, percent-sandstone decreases to the north as shale deposition increased due to increased accommodation space and increased distance from coarse-grained sediment sources.

Plate 4 is a west to east cross-section of the Upper Hibernia Member across the study area, as shown in the inset map. Increased thickness over graben structures are shown in the Terra Nova F-100_2 and C-69_3 wells. Lithological changes along the cross-section are relatively minor illustrating the high lateral correlativity of the Upper Hibernia Member along depositional strike.

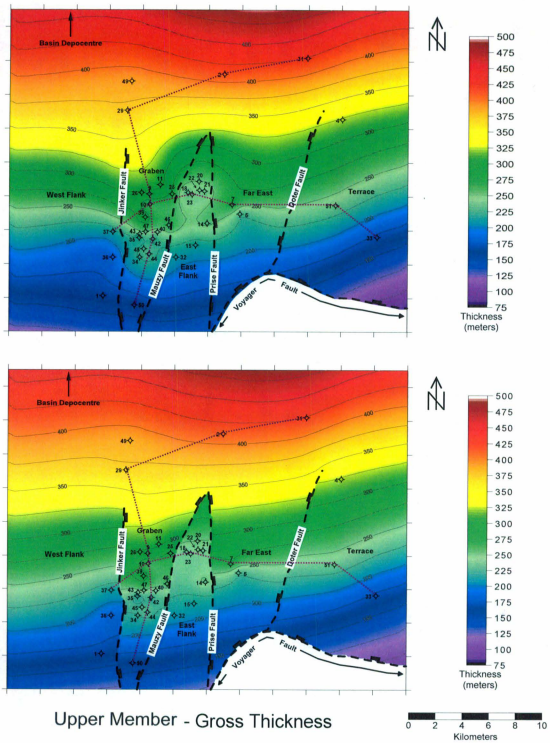


Figure 6.18: Gross thickness maps of the Upper Hibernia Member. Top map shows contouring without the influence of faulting. Bottom map shows contouring with the influence of faulting. Purple dotted lines show locations of Plate 3 (S-N/NE) and Plate 4 (W-E).

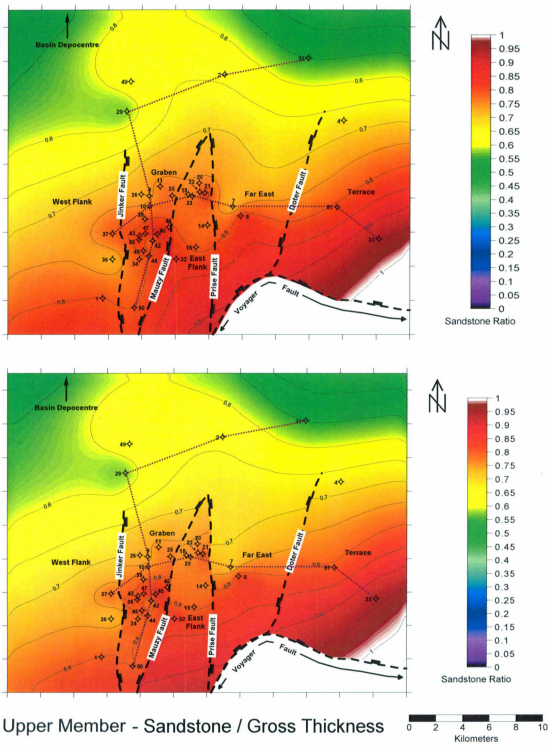


Figure 6.19: Percent-sandstone maps of the Upper Hibernia Member. Top map shows contouring without the influence of faulting. Bottom map shows contouring with the influence of faulting. Purple dotted lines show locations of Plate 3 (S-N/NE) and Plate 4 (W-E).

6.2.2.1 Upper Hibernia Member sub-unit 322

Upper Hibernia Member sub-unit 322 is composed of interbedded sandstone and shale that increases in sandstone abundance upwards forming an overall coarsening-upwards package. Well section considered to be typical of sub-unit 322 is shown in the Terra Nova G-90_5Y well (Figure 6.20). The base of sub-unit 322 is marked by a shale package that is typically eight to twelve meters thick and overlies the laterally continuous sandstone bed at the top of Lower Hibernia Member sub-unit 320. Above the shale, the sub-unit gradually coarsens-upwards (overall trend of decreasing gamma ray) through decreasing shale presence in the alternating sandstone, siltstone, and shale interbeds. Individual sandstone beds appear to be laterally discontinuous between adjacent wells and sandstone beds are rarely more than four to five meters thick. Where sandstone beds are greater than five meters thick, they are not easily correlated between adjacent wells, appear to have sharp lower and upper contacts, and appear to have both fining- and coarsening-upwards trends. The top of the sub-unit is marked by a shale package that is three to six meters thick capping the top of the coarsening-upwards trend of interbedded siliciclastics.

Gross thickness trends of sub-unit 322 are illustrated in Figure 6.21, which shows gradual thickening to the north. Thickening over the Graben is due in part to increased displacement along the Jinker Fault as well as the northern portion of the Mauzy Fault. There is also thickening over the Far East along the northern portion of the Prise Fault and minor displacement along the Doter Fault. Localized thinning and thickening through the study area is likely due to the unconformable nature with overlying sub-unit 324, which has similar depositional character to sub-unit 322, as well as the laterally discontinuous nature of sub-unit 322. Percent-sandstone trends of sub-unit 322 are

illustrated in Figure 6.22. Abundant shale deposition along the western edge of the study area suggests the basin depocentre was towards the west. The area to the northeast shows forty to fifty percent-sandstone deposition suggesting the northeastern siliciclastic sediment source present in sub-unit 320 was still influential during the onset of the Upper Hibernia Member. However, the primary siliciclastic sediment source was from the south and southeast, which has sandstone deposition in the range of fifty to eighty percent.

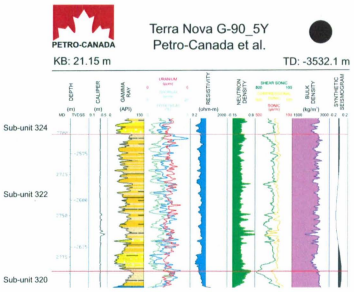


Figure 6.20: Type-section of Upper Hibernia Member sub-unit 322.

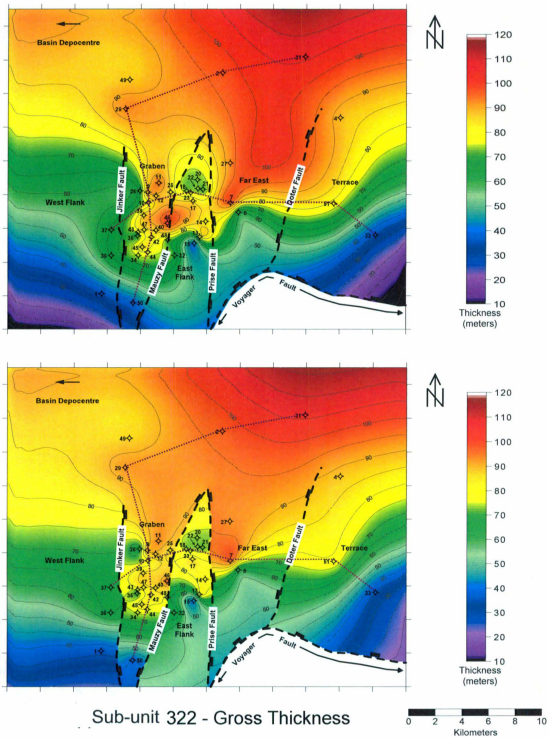


Figure 6.21: Gross thickness maps of Upper Hibernia Member sub-unit 322. Top map shows contouring without the influence of faulting. Bottom map shows contouring with the influence of faulting. Purple dotted lines show locations of Plate 3 (S-N/NE) and Plate 4 (W-E).

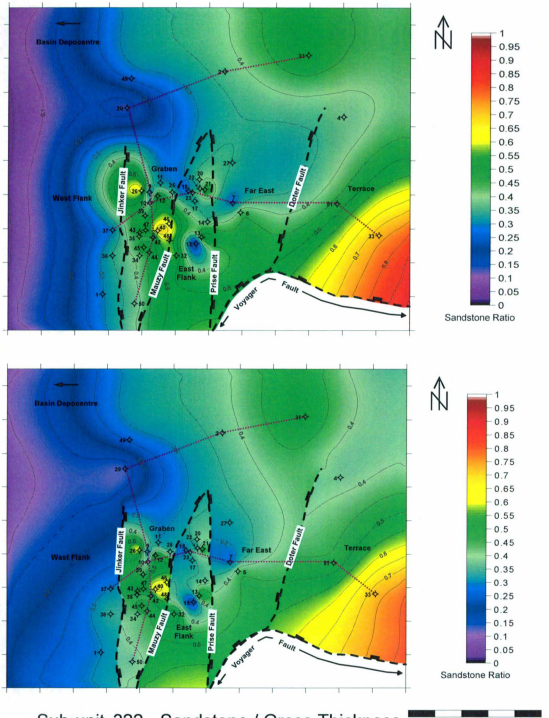


Figure 6.22: Percent-sandstone maps of Upper Hibernia Member sub-unit 322. Top map shows contouring without the influence of faulting. Bottom map shows contouring with the influence of faulting. Purple dotted lines show locations of Plate 3 (S-N/NE) and Plate 4 (W-E).

6.2.2.2 Upper Hibernia Member sub-unit 324

Upper Hibernia Member sub-unit 324 is similar to underlying sub-unit 322; however it is more sandstone-prone compared to the relatively high shale content of sub-unit 322. Well section considered to be typical of sub-unit 324 is shown in the Terra Nova G-90_5Y well (Figure 6.23). The base of sub-unit 324 is defined by the presence of three to six meters of a laterally continuous shale bed that overlies the coarsening-upwards trend of underlying sub-unit 322. Above the shale, the sub-unit generally exhibits a coarsening-upwards trend of interbedded sandstone, siltstone, and shale. Individual sandstone bed thicknesses are highly variable, ranging from less than two meters thick to greater than ten meters thick, and are generally not correlative with adjacent wells. The top of the sub-unit is defined as the base of a massive-appearing sandstone unit and is often marked by a thin (less than a meter) siltstone to shale bed that is present in most wells below the sandstone bed.

Gross thickness trends of sub-unit 324 are illustrated in Figure 6.24, which shows gradual thickening to the north. Greater preserved thickness over the Far East, compared to the Graben, suggests that the Prise and Doter faults were the predominant tectonically active faults at this time of deposition, in contrast with relationships observed in sub-unit 322, when the Jinker and Mauzy faults appear to have been most active. Some localized thickening of sub-unit 324 may represent areas of incision into the underlying sub-unit 322, which can be correlated to thinning of sub-unit 322 where sub-unit 324 thickens, such as at Terra Nova G-90_8. Percent-sandstone trends of sub-unit 324 are illustrated in Figure 6.25. Increased sandstone deposition from the south-southeast is evident as well as increased sandstone deposition in the north.

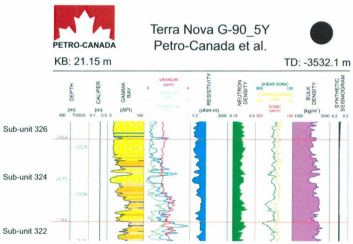


Figure 6.23: Type-section of Upper Hibernia Member sub-unit 324.

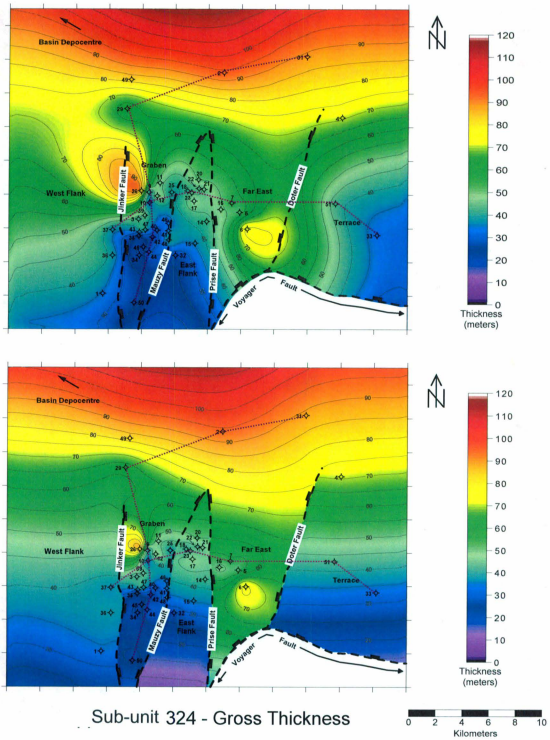


Figure 6.24: Gross thickness maps of Upper Hibernia Member sub-unit 324. Top map shows contouring without the influence of faulting. Bottom map shows contouring with the influence of faulting. Purple dotted lines show locations of Plate 3 (S-N/NE) and Plate 4 (W-E).

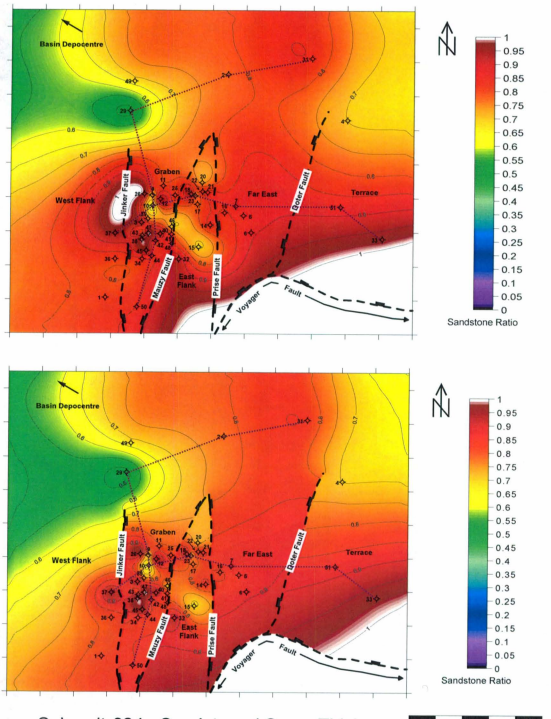


Figure 6.25: Percent-sandstone maps of Upper Hibernia Member sub-unit 324. Top map shows contouring without the influence of faulting. Bottom map shows contouring with the influence of faulting. Purple dotted lines show locations of Plate 3 (S-N/NE) and Plate 4 (W-E).

6.2.2.3 Upper Hibernia Member sub-unit 326

Upper Hibernia Member sub-unit 326 is almost entirely massive-appearing sandstone with little to no variation in petrophysical character except some very thin (less than a meter) shale to siltstone beds near the top of the sub-unit. Well section considered to be typical of sub-unit 326 is shown in the Terra Nova G-90_5Y well (Figure 6.26). The base of sub-unit 326 is defined as the top of a shale bed that is less than a meter thick, below thick, massive-appearing sandstone. The base of the sandstone coarsens-upward rapidly over five to ten meters, but can also be sharp-based. This thick, massive-appearing sandstone is very continuous laterally and marks the top of the overall coarsening-upwards trend of sub-units 322 and 324. The uppermost part of sub-unit 326 can display a fining-upwards pattern. In the southern half of the study area, the top of sub-unit 326 is marked by sharp truncation of the fining-upwards pattern by another package of thick massive-appearing sandstone. Moving northward, the top of sub-unit 326 is defined as the top of the fining-upwards pattern, when present, and base of a thick shale unit with rare sandstone deposition.

Gross thickness trends of sub-unit 326 are illustrated in Figure 6.27. Gradual thickening to the north is evident along with a northwest-trending increase in thickness across the south-central part of the study area. This thickening also suggests that the northern portions of the Jinker and possibly Mauzy faults experienced increased displacement during deposition of sub-unit 326; however, overall fault displacement in the study area seems to be minimal. Increased displacement along faults bounding the northern region of the Graben likely focused deposition in this region. Thinning in the southwest and across the Far East likely indicates regions of sediment bypass and minimal deposition. Percent-sandstone trends are illustrated in Figure 6.28. Across the

study area, sub-unit 326 has less than three percent shale content, further illustrating the clean character of this massive-appearing, widespread sandstone.

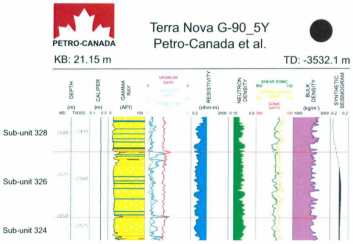


Figure 6.26: Type-section of Upper Hibernia Member sub-unit 326.

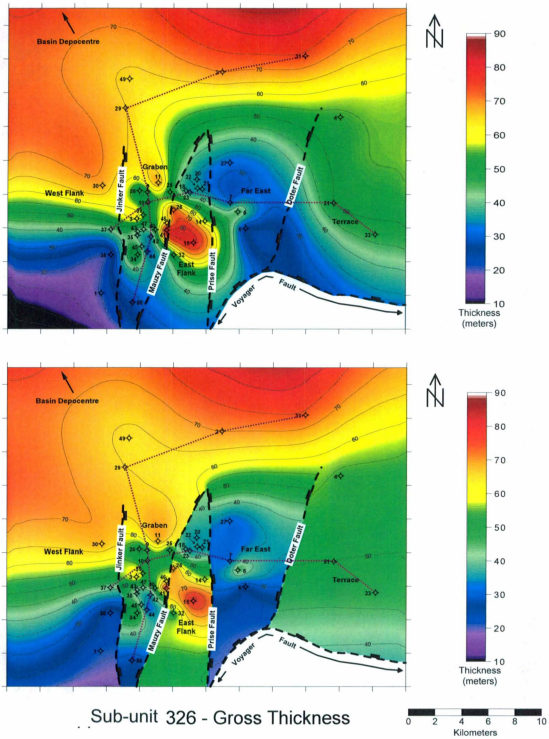


Figure 6.27 Gross thickness maps of Upper Hibernia Member sub-unit 326. Top map shows contouring without the influence of faulting. Bottom map shows contouring with the influence of faulting. Purple dotted lines show locations of Plate 3 (S-N/NE) and Plate 4 (W-E).

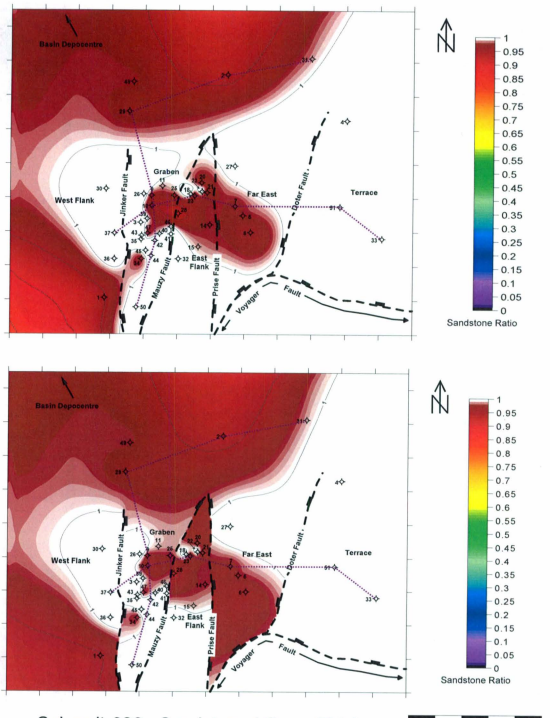


Figure 6.28: Percent-sandstone maps of Upper Hibernia Member sub-unit 326. Top map shows contouring without the influence of faulting. Bottom map shows contouring with the influence of faulting. Purple dotted lines show locations of Plate 3 (S-N/NE) and Plate 4 (W-E).

6.2.2.4 Upper Hibernia Member sub-unit 328

Upper Hibernia Member sub-unit 328 is composed of thick massive-appearing sandstone in the southern half of the study area with a sharp increase in shale content in the northern half. Well section considered to be typical of sub-unit 328 is shown in the Terra Nova G-90_5Y well (Figure 6.29). The base of sub-unit 328 is marked by sharp truncation of the fining-upwards pattern at the top of sub-unit 326 by clean, massive-appearing sandstone in the south. In the north, it is marked as the base of a thick shale package overlying the thick sandstone of sub-unit 326. Throughout the southern end of the study area, sub-unit 328 abruptly overlies sub-unit 326 and is characterized by thick sandstone with minimal shale bed occurrences. Shale beds are less than one meter in thickness when present and indicated by a thin zone of increased gamma ray (narrow "spike"). In the northern half of the study area, sub-unit 328 is characterized by a sharp increase in shale content above the thick sandstone of sub-unit 326 and shows thinning sandstone beds to the north. Gamma ray trends present at the northern wells suggest coarsening-upwards patterns from basal shale into sandstone beds. Individual sandstone beds vary in thickness from less than a meter to greater than twenty meters. The top of sub-unit 328 is marked by a shale bed, one to five meters thick, separating massive-appearing sandstone below from the thinner, massive-appearing sandstone above of sub-unit 330.

Gross thickness trends of sub-unit 328 are illustrated in Figure 6.30. Overall thickening to the north is evident, as well as thickening west of the Mauzy Fault and over the Far East. Increased displacement along the Mauzy Fault and northern region of the Jinker Fault created accommodation space across the Graben. Growth along the Prise and Doter faults provided accommodation space in the Far East, although it appears to

be to a lesser extent, particularly in the south. Percent-sandstone trends are illustrated in Figure 6.31. The thick, massive-appearing sandstone character of sub-unit 328 is evident by the high sandstone content across the southern half of the study area. The area to the north is marked by a rapid increase in the shale content of sub-unit 328. Comparing percent-sandstone maps with and without fault control clearly shows that faulting had minimal effect on sandstone distribution across the study area.

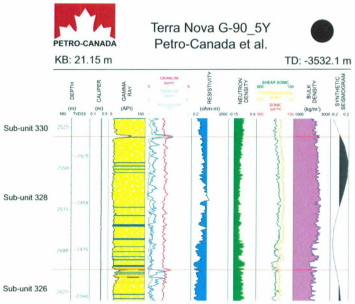


Figure 6.29: Type-section of Upper Hibernia Member sub-unit 328.

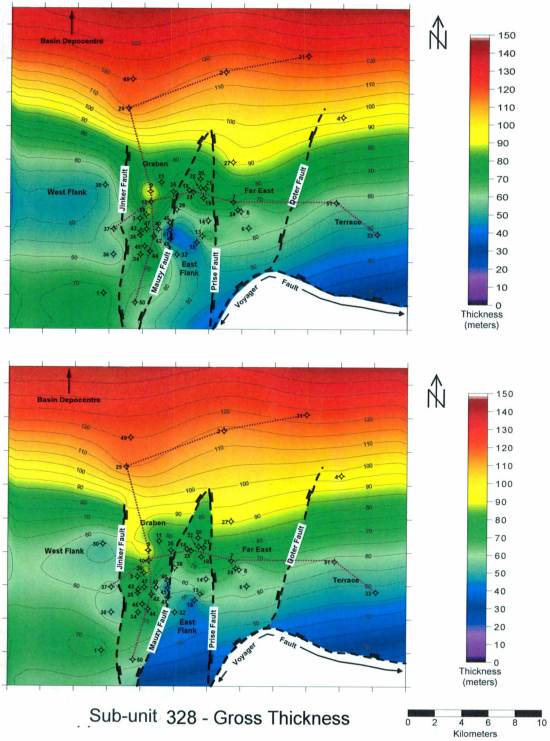


Figure 6.30: Gross thickness maps of Upper Hibernia Member sub-unit 328. Top map shows contouring without the influence of faulting. Bottom map shows contouring with the influence of faulting. Purple dotted lines show locations of Plate 3 (S-N/NE) and Plate 4 (W-E).

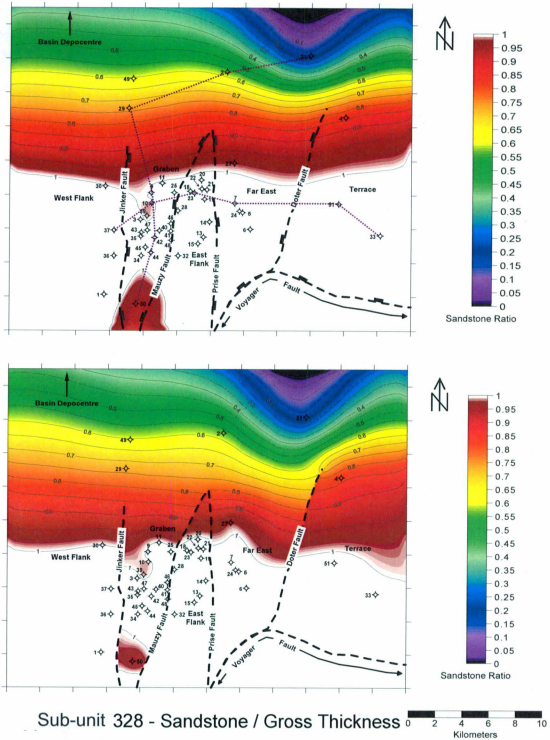


Figure 6.31: Percent-sandstone maps of Upper Hibernia Member sub-unit 328. Top map shows contouring without the influence of faulting. Bottom map shows contouring with the influence of faulting. Purple dotted lines show locations of Plate 3 (S-N/NE) and Plate 4 (W-E).

6.2.2.5 Upper Hibernia Member sub-unit 330

Upper Hibernia Member sub-unit 330 consists of massive-appearing sandstone in the south and has a coarsening-upwards pattern in the northern part of the study area. Well section considered to be typical of sub-unit 330 is shown in the Terra Nova G-90_5Y well (Figure 6.32). The base of sub-unit 330 is defined by the thin shale bed that is often present below the main sandstone package of sub-unit 330. The basal shale varies in thickness from near zero at the southern end of the study area to greater than five meters in the north where the boundary between basal shale and overlying sandstone bed appears gradational. The top of sub-unit 330 is marked by the distinct change in lithology from siliciclastics below to carbonates above. This boundary is easily identified in petrophysical logs by the sharp increase in resistivity above sub-unit 330 in conjunction with the increase in bulk density and decrease in transit time of the sonic log for the carbonate cap.

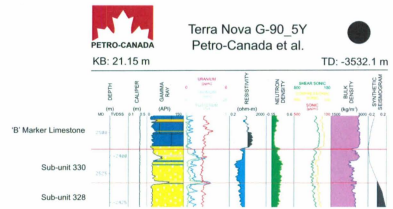


Figure 6.32: Type-section of Upper Hibernia Member sub-unit 330.

Gross thickness trends of sub-unit 330 are illustrated in Figure 6.33. Gradual increase in thickness to the north is shown with minimal changes along the main fault traces, suggesting decreased fault activity. There is, however, some displacement along the Jinker and Doter faults creating a depositional low through the centre of the study area. Percent-sandstone trends of sub-unit 330 are illustrated in Figure 6.34. Sandstone deposition decreases to the north and northeast, with a rapid transition to shale deposition in the northeast. The one hundred percent sandstone contour also retreats southward between the Jinker and Doter Faults, which correlates with increased thickness in the same region. The relatively small thickness of sub-unit 330, typically less than twenty meters of sandstone, combined with decreased influence of faulting on the depositional nature, marks the end of siliciclastic sediment input and tectonic activity of the Jeanne d'Arc Basin during the North Atlantic Rifting Phase before deposition of the 'B' Marker limestone.

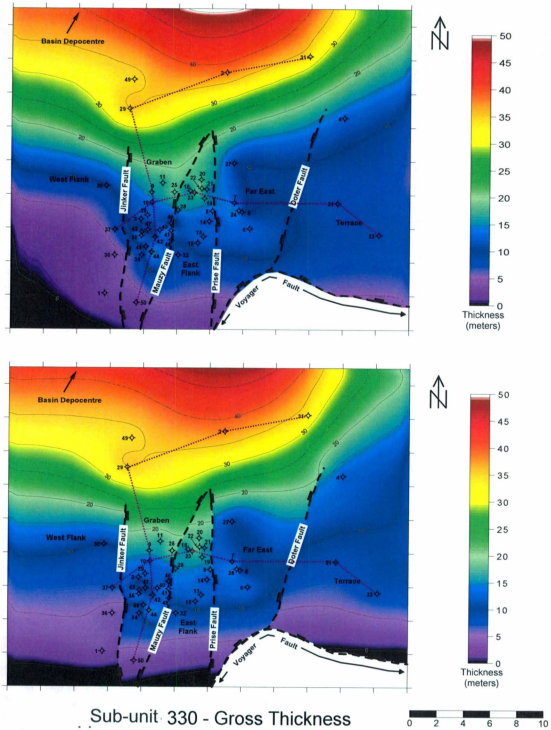


Figure 6.33: Gross thickness maps of Upper Hibernia Member sub-unit 330. Top map shows contouring without the influence of faulting. Bottom map shows contouring with the influence of faulting. Purple dotted lines show locations of Plate 3 (S-N/NE) and Plate 4 (W-E).

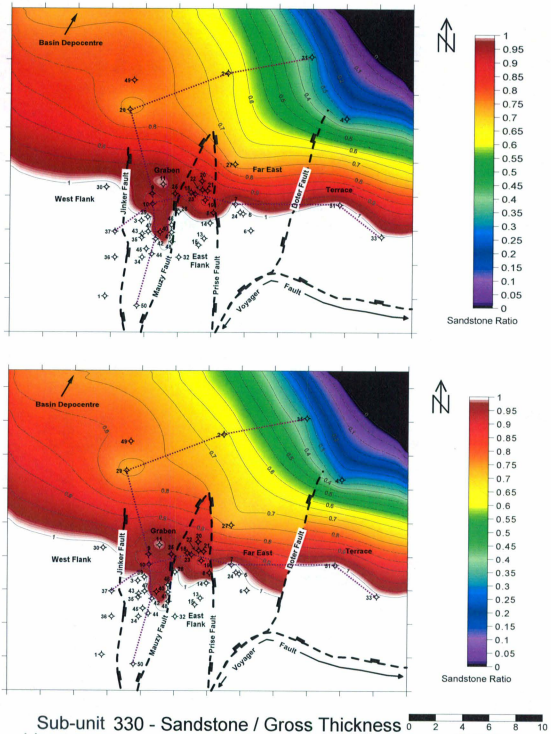


Figure 6.34: Percent-sandstone maps of Upper Hibernia Member sub-unit 330. Top map shows contouring without the influence of faulting. Bottom map shows contouring with the influence of faulting. Purple dotted lines show locations of Plate 3 (S-N/NE) and Plate 4 (W-E).

6.3 Discussion

The Lower Hibernia Member marks the onset of coarse clastic sedimentation potentially due to renewed tectonic activity following marine shale deposition of the Fortune Bay Formation. Based on gross thickness and percent-sandstone maps of the Lower Hibernia Member, the primary focus of deposition during this period is the Far East half-graben block, (Figures 6.1 and 6.2); however sandstone deposition is generally widespread across the majority of the study area. The Upper Hibernia Member gradationally overlies the Lower Hibernia Member; however it has significantly different depositional characteristics. Coarse siliciclastic content is higher and individual sub-units suggest a clockwise rotation in depositional direction (progradation direction) from westward to northeastward. Thickness variations of the Upper Hibernia Member suggest faults within the study area experienced significant syn-sedimentary displacement (Figure 6.18). Percent-sandstone maps indicate the local source direction was generally from the southeast and shale deposition progressively increases to the north and northwest (Figure 6.19).

For the purpose of summarizing the evolution of the Hibernia Formation a series of simplified maps is presented below. These maps highlight key percent-sandstone contours taken from maps of Section 6.2 and illustrate general shifts in contour locations between subsequent sub-units. Changes in contour locations and gradients are interpreted as representing periods of transgression and regression of the paleo-shoreline in conjunction with changes in depositional slope. To compare changes in contour locations, the seventy percent contour is taken to represent the approximate location of the paleo-shoreline and zero percent could represent the limit of fully marine conditions.

The Lower Hibernia Member had siliciclastic input from the south for sub-units 306 through 312, changing to a possible eastern source in sub-unit 320. The prolonged southern sediment source direction during Lower Hibernia Member deposition allowed development of an approximately east-west trending shoreline that recorded four distinct periods of transgression and regression. Figure 6.35 shows the location of the key percent sandstone contours for each of the Lower Hibernia Member sub-units, which are contrasted with the underlying sub-unit to establish a relative paleo-shoreline migration direction. Maximum progradation shoreline shifts between subsequent sub-units can be more than six kilometers, as shown between sub-units 306 and 308, or nearly zero, as shown between sub-units 310 and 312. Overall, the paleo-shoreline was positioned across the center of the study area until deposition of sub-unit 320 when the shoreline shifted north of the study area or became submerged and a new shoreline developed in the northeast due to a new sediment source in the study area (prograding westward to southwestward).

Figure 6.35A highlights key percent-sandstone contours for sub-unit 306. The east-west trend of the seventy percent contour (paleo-shoreline trend) is consistent with northward progradation along the basin rift axis. Increased displacement along the Doter and Prise faults helped focus sandstone deposition along the Far East half graben where the depositional slope was likely the greatest. The southwestern region of decreased sandstone deposition could represent coastal plain shales as coarse-grained sediment was transported further northward to an east-west paleo-shoreline running across the study area. The gradient from seventy percent to zero percent-sandstone nearly doubles toward the east, consistent with a steep, fault-controlled depositional slope closer to the basin-bounding Voyager Fault System.

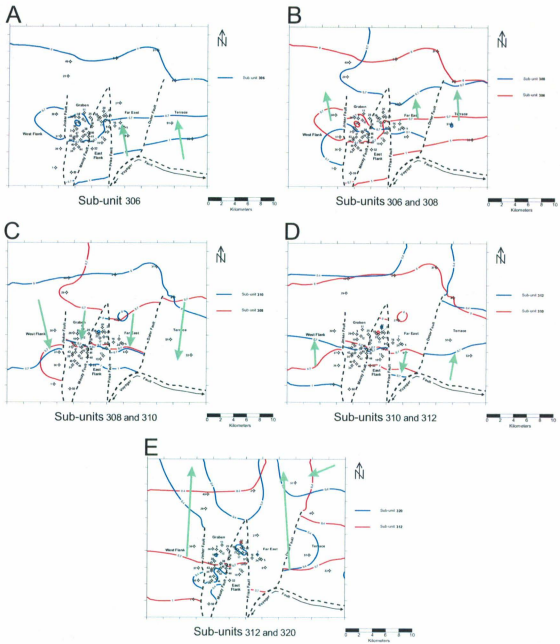


Figure 6.35: Series of simplified percent sandstone maps with key contours shown for each unit to illustrate relative shifts in the paleo-shoreline of the Lower Hibernia Member. Blue contours represent the younger sub-unit, while red contours represent the older sub-unit. Arrows illustrate lateral migration trends of the paleo-shoreline between successive sub-units (red to blue contours).

Sub-unit 308 characterizes a subsequent prograding coarse clastic deposit that rapidly thickens in the north, suggesting tectonic activity was further basinward. Therefore, displacements along faults within the study area are considered to be fairly minimal and sandstone distribution patterns are considered to be depositional in nature. Figure 6.35B highlights changes in key percent-sandstone contour locations for sub-unit 308 compared with sub-unit 306. Progradation of the paleo-shoreline is represented by the northward shift of the seventy percent contour of sub-unit 308. The east-west trend across the study area is still evident suggesting northward progradation along the basin rift axis; however the rapid transition to shale in the north (sub-unit 306) is no longer present and a thick sandstone interval was deposited across the northern region of the study area. If tectonic activity was focused north of the study area, as mentioned previously, sub-unit 308 could represent sediment infill and shallowing of the depositional slope across the northern region of the study area.

Sub-unit 310 is characterized by a relatively thin lobate deposit across the southern half of the study area that changes to shale in the north. Figure 6.35C highlights changes in key percent-sandstone contour locations for sub-unit 310 compared to sub-unit 308. Relative to sub-unit 308, sandstone deposition is significantly reduced across the northern part of the study area, illustrated by the southerly shift of the seventy percent contour representing back-stepping of the paleo-shoreline within the study area.

Sub-unit 312 is a thick, northward-prograding clastic succession. Figure 6.35D highlights changes in key percent-sandstone contour locations for sub-unit 312, compared to sub-unit 310. Slight variations in the position and shape of the shoreline are evident, suggesting a period of overall aggradation with respect to the seventy

percent sandstone contour. For example, progradation across the West Flank is offset by retrogradation across the Far East. However, overall progradation of sub-unit 312 is shown by increased sandstone deposition in the north, compared to predominantly shale deposition in the north of sub-unit 310. This reduced gradient from shoreline to fully marine shale deposition in sub-unit 312, compared to sub-unit 310, suggests reduction of the depositional slope and/or increased coarse-grained siliciclastic sediment input. Northward progradation is evident by the similar east-west trend as seen in previous sub-units suggesting a similar sediment provenance and depositional direction between sub-units 306 to 312.

Sub-unit 320 suggests a period of accommodation space creation and possibly increased sedimentation, forcing the shoreline to retreat outside the study area either to the north or south as noted by the decreased sandstone deposition across the study area (Figure 6.17). If sedimentation was greater than accommodation space creation then the paleo-shoreline may have migrated north of the study area representing a period of progradation. However, if sedimentation was less than accommodation space creation then the paleo-shoreline may have migrated south of the study area representing a period of retrogradation. Figure 6.35E highlights changes in key percent-sandstone contour locations for sub-unit 320, compared to sub-unit 312. It is possible that sedimentation outpaced the creation of accommodation space forcing the paleo-shoreline to prograde northward into the basin. The high shale content of sub-unit 320 could represent coastal plain shales as some of the sandstone beds resemble channel sandstone profiles, where thick enough, with a sharp base and fining-upwards top (see sandstone bed in Terra Nova F-100_4 at ~2920 m TVDSS, Plate 1). Higher sandstone deposition in the northeast is evident in the vicinity of Ben Nevis I-45 (well 31, Figure

6.35E), representing the northern shift of paleo-shoreline progradation and possible introduction of a northeastern siliciclastic sediment source into the study area. The correlative sandstone deposit marking the top of sub-unit 320 likely represents a period when sedimentation is outpaced by accommodation space creation, possibly through relative sea-level rise and/or increased fault activity, forcing the paleo-shoreline, and sandstone deposition, to rapidly shift southward. This sandstone package marks the top of sub-unit 320 and subsequently the top of the Lower Hibernia Member, as above sub-unit 320 the depositional character changes as the progradational direction shifts from north-south to east-west above the maximum flooding surface.

The Upper Hibernia Member records varying degrees of coarse-grained siliciclastic input from the southeast to south into the study area, which caused a clockwise rotation in depositional direction from westward to northeastward. Figure 6.36 highlights the constantly shifting nature of Upper Hibernia Member shorelines, represented by the seventy percent-sandstone contours. The paleo-shoreline of sub-unit 326 is located north to northwest of the study area since sub-unit 326 is greater than ninety-five percent-sandstone across the study area and represents maximum progradation of the Upper Hibernia Member. Position of the paleo-shoreline changes by tens of kilometers between sub-units 322 to 326 and is relatively stabilized through sub-units 328 and 330 trending approximately east-west. The Upper Hibernia Member represents a period of high coarse-grained siliciclastic sediment input and rapid accommodation space creation via fault displacement and tectonic subsidence.

Figure 6.36A highlights changes in key percent-sandstone contour locations for sub-unit 322, compared to sub-unit 320. Establishment of an eastern to southeastern coarse-grained sediment source is suggested by emplacement of the paleo-shoreline

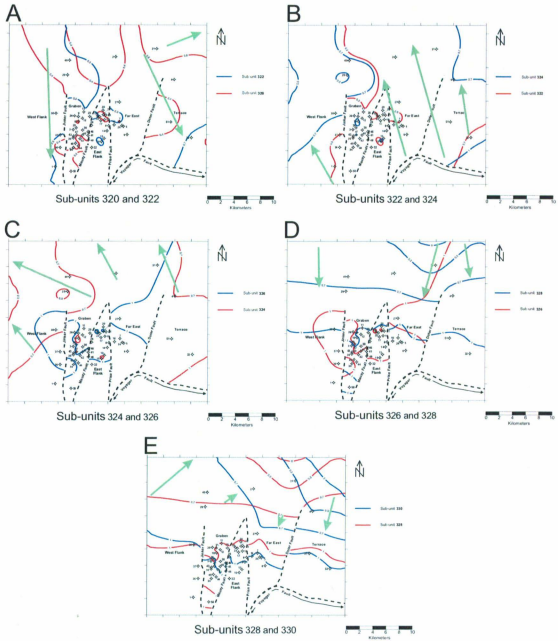


Figure 6.36: Series of simplified percent sandstone maps with key contours shown for each unit to illustrate relative shifts in the paleo-shoreline of the Upper Hibernia Member. Blue contours represent the younger sub-unit, while red contours represent the older sub-unit. Arrows illustrate lateral migration trends of the paleo-shoreline between successive sub-units (red to blue contours).

across the Terrace and north-south to northeast-southwest trend of the percent-sandstone contours. Sediment input was potentially reduced as a result of shifting source provenances and could represent a coarse-grained sediment hiatus, further forcing back-stepping of the paleo-shoreline to the southeast.

Figure 6.36B highlights changes in key percent-sandstone contour locations for sub-unit 324, compared to sub-unit 322. Progradation of the paleo-shoreline to the northwest is evident as much of the study area is greater than seventy percent-sandstone. Transportation of coarse-grained sediment tens of kilometers from the basin's boundaries likely represents shallowing of the depositional slope through rapid sedimentation, which allowed the paleo-shoreline to prograde towards the basin depocentre.

Fault activity appears to have decreased across the study area during deposition of sub-unit 326; however, displacement along the Jinker and Mauzy faults provided accommodation space to the northwest. Thickening across the southern half of the East Flank, a paleo-high, could represent incision into underlying sub-unit 324, which created a paleo-valley acting as a sediment conduit across the East Flank into the northwest region of the study area. Figure 6.36C highlights changes in key percent-sandstone contour locations for sub-unit 326, compared to sub-unit 324. Sandstone deposition across the entire study area exceeds ninety percent and the paleo-shoreline migrated north and west of the study area. Sub-unit 326 represents maximum progradation of coarse-grained clastic deposition across the study area suggesting the depositional slope was minimized.

Sub-unit 328 is thick high percent-sandstone across the south with a sharp increase in shale content northward. Onset of shale deposition also appears to closely

correlate to the seventy to eighty meter thick contour, north of which shale deposition rapidly increases. Figure 6.36D highlights changes in key percent-sandstone contour locations for sub-unit 328, compared to sub-unit 326. Significant back-stepping of the paleo-shoreline is seen across the study as the seventy percent-sandstone contour is established across the central region of the study area. East-west trending contours suggest depositional strike was re-established in an east-west trend with the main source of coarse-grained sediment shifting back to southerly from the southeasterly direction as seen in sub-units 322 to 326. Rapid lateral transition from sandstone to shale also suggests coarse-grained input is decreasing, although still high, and/or wave re-working is minimizing lateral distribution of sandstone.

Sub-unit 330 represents the final stage of deposition of the Upper Hibernia Member and subsequently the Hibernia Formation. Figure 6.36E highlights changes in key percent-sandstone contour locations for sub-unit 330, compared to sub-unit 328. Continued clockwise rotation of the depositional strike is suggested by forward-stepping of the paleo-shoreline in the west and back-stepping of the paleo-shoreline in the east, compared to sub-unit 328. Increased sandstone deposition across the northwestern region of the study area in conjunction with minimal changes in the one hundred percent sandstone contour location, compared to sub-unit 328, suggests shallowing of the depositional slope through basinward progradation of sandstone deposition. It could also indicate a westward lateral shift in the coarse-grained sediment input while maintaining a north-south depositional direction. Siliciclastic sedimentation across the study area ceases with deposition of sub-unit 330, representing the end of major tectonic activity and primary onset of thermal subsidence allowing the subsequent 'B' Marker Limestone to be deposited overtop the Hibernia Formation.

6.4 CONCLUSION

Petrophysical log data provide the best vertical resolution of the Hibernia Formation and allow a much greater understanding of possible depositional trends. The Hibernia Formation appears to be a series of coarsening-upwards deposits that prograded across the study area where accommodation space was available and were distributed to reduce the depositional slope. When fault activity increased, the depositional slope seems to have been steepened, forcing periods of shoreline back-stepping, that reflect periods when coarse-grained clastic input was outpaced by accommodation space creation. Siliciclastic sediment was sourced from along the basin margins to the south and east and throughout the history of the Hibernia Formation the two sources displayed varying degrees of influence. Occasionally, the eastern sediment source appears to have outpaced the southern source and east-west trending depositional directions are evident in several sub-units. Depositional trends were also controlled by tectonic activity and subsequent accommodation space that was created determined the dominant area of deposition and often resulted in both greater shale deposition and increased overall thickness of the zone.

Petrophysical log data provide depositional patterns (well log shapes) that characterize individual sub-units. However, the scale of these patterns is on the tens of centimeters to meters scale. The finer details that would ultimately determine the depositional environment of the Hibernia Formation are best recorded in recovered core. However, core coverage in the study area is extremely limited, and the characteristic features observed (e.g. sedimentary structures, smaller-scale grain-size trends, trace fossils) can not be easily extrapolated across the entire study area. In the next chapter the various data are integrated into a depositional model of the Hibernia Formation.

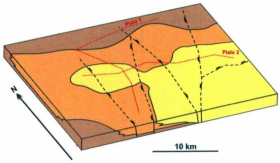
CHAPTER 7 – CONCLUDING SUMMARY

7.1 GEOLOGICAL MODEL

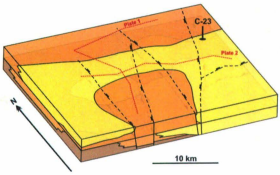
The Hibernia Formation in the study area can be characterized by two distinct periods of coarse-grained siliciclastic deposition, separated by a hiatus of diminished sediment supply and widespread flooding. Initial coarse-grained sedimentation is represented by the Lower Hibernia Member, which records multiple forward- and back-stepping coarsening-upward intervals that filled the basin from the south and southeast. A widespread flooding event, possibly due to abundant tectonic activity and relative sea-level rise, is correlable across the study area and is present in all wells, except when faulted out. Final coarse-grained sedimentation is represented by the Upper Hibernia Member, which records stacked forward-stepping coarsening-upwards intervals suggesting rapid sedimentation and progradation towards the basin depocentre. Towards the top of the Upper Hibernia Member sedimentation appears to have slowed and shows a shift towards higher shale deposition and relative stability in paleo-shoreline position. The following summarizes individual depositional events comprising the Hibernia Formation and its depositional history.

Figure 7.1 summarizes the depositional history of the Hibernia Formation through a series of schematic diagrams based on average percent-sandstone maps for each sub-unit presented in Chapter 6. It is important to remember that these average percent-sandstone maps are representative of a significant interval within any given well. Thick shale beds can be found in areas of greater than seventy percent-sandstone, and conversely, thick sandstone beds can be found in areas of less than thirty percent-sandstone. Interpretation of depositional environments is also based on cored intervals,

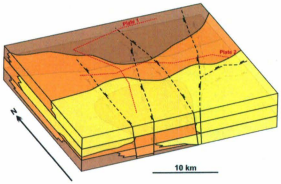
A - Sub-unit 306



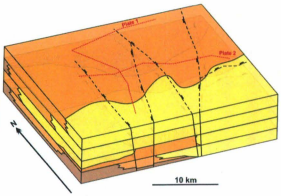
B - Sub-unit 308



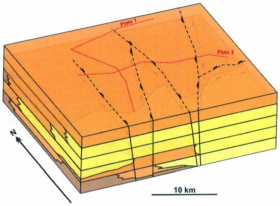
C - Sub-unit 310



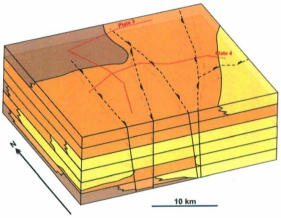
D - Sub-unit 312



E - Sub-unit 320



F - Sub-unit 322



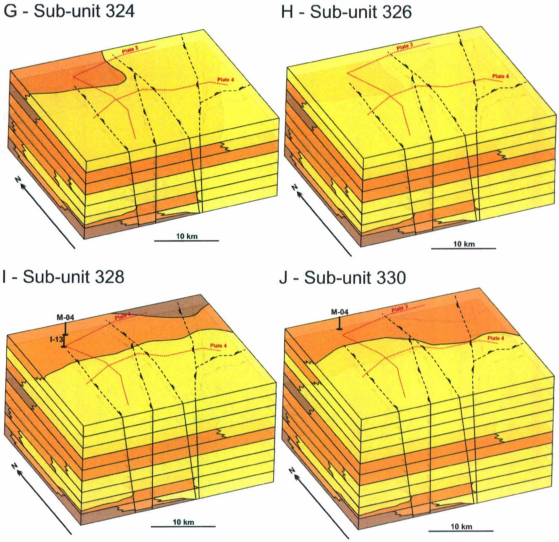


Figure 7.1: Schematic model of the Hibernia Formation. The yellow areas represent the delta plain to delta front facies of the Hibernia Formation (characterized by >70% sandstone deposition). The orange areas represent the upper- to mid-shoreface facies of the Hibernia Formation (characterized by 20-70% sandstone). The brown areas represent the lower shoreface to marine facies of the Hibernia Formation (characterized by 0-20% sandstone). Figure 7.1 consists of ten images progressing from **A** illustrating the depositional setting of the Lower Hibernia Member sub-unit 306 through the depositional history to **J** illustrating the depositional setting of the Upper Hibernia Member sub-unit 330.

which are recovered from portions of the Upper and Lower Hibernia Members (Chapter 5). These interpretations are applied to adjacent sub-units, where core is not available and petrophysical signatures are similar, on the assumption that depositional environments are relatively unchanged between sub-units, hence the differences between maps emphasize changes in sediment distribution patterns.

Following deposition of the Fortune Bay Formation marine shales, renewed tectonic activity gradually provided additional accommodation space and uplifted sediment source areas (to the south and southeast) to initiate deposition of the Hibernia Formation. Increased displacement along the Voyager, Doter and Prise faults during deposition of sub-unit 306 focused sandstone deposition along the southeastern margin of the basin, the Voyager Fault System (Figure 7.1A). Sub-unit 306 represents northwest progradation of sandstone into the Jeanne d'Arc Basin, due to increased coarse-clastic sedimentation from the southeast, across a steepened depositional slope. A somewhat protected embayment or lagoon may have been present in the southwest as an east-west trending shoreline prograded north to northwestward. The area could also represent a coastal plain setting with deposition of fluvial sandstones and mudstones; however Beothuk M-05 (Plate 1) shows a rather uniform coarsening-upwards pattern suggesting progradation of shoreface sandstones not fining-upwards sandstone beds to support coastal plain channel deposition.

Further progradation occurs during deposition of sub-unit 308 as the paleo-shoreline (represented by the transition from yellow to orange) moved north, partly outside the study area in the northwest (Figure 7.1B). Note that the overall east-west trend of the paleo-shoreline is maintained but shifted further north. The area in the south-central portion of the study area likely represents a zone of sediment bypass as

coarse-grained sediment is transported further north and could represent a lagoon to back-barrier depositional setting due to thin episodic sandstone bedsets that are evident in the region. It is also possible that this region represents coastal plain deposits and the thin sandstone beds could represent channel deposits encased in fluvial mudstones. Recovered core from the West Bonne Bay C-23 well suggests a wave-influenced upper shoreface to foreshore depositional setting for the thick sandstone deposit that can be correlated across the northern region of the study area (refer to Section 5.2). Bimodal dip directions can be taken to suggest possible flood and ebb tidal deposits, which together with coarse-grained, possibly storm-induced overwash deposits found within fine-grained, bioturbated deposits, could support a lagoon to back-barrier setting to the south. Note, that this interpretation is highly uncertain due to the large lateral distance between overwash deposits seen in core and the south-central region of the study area. Overall, deposits of sub-unit 308 appear to have experienced minimal fault-induced deposition and represent a period of high coarse-grained siliciclastic deposition to the northwest that reduced the depositional slope. However, recovered core from the top of sub-unit 308 in West Bonne Bay C-23 suggests decreasing sedimentation and likely represents redirection of coarse-grained sediment away from the study area or a rise in relative sea-level, possibly due to renewed subsidence and faulting activity.

Increased subsidence and tectonic activity to the north may have caused the paleo-shoreline to move southward (back-step) during deposition of sub-unit 310, leading to higher shale deposition in the north (Figure 7.1C). The thin nature of sub-unit 310 suggests accommodation space and/or sediment input was minimal and coarse-grained clastic deposition may have shifted south of the study area following deposition of sub-unit 308. However, increased fault activity north of the study area may have

begun to increase the depositional slope and sub-unit 310 represents partial re-establishment of coarse-grained clastic deposition into the study area from the south. Note that the east-west trend of the paleo-shoreline is still persistent suggesting progradation is still to the north along the basin's rift axis. If coarse-grained siliciclastic deposition was partially diverted away from the study area between deposition of sub-units 308 and 310 this could explain the rapid lateral transition to shale in the north across a steepening depositional slope.

Compared to sub-unit 310, fault activity was similar or slightly higher across the study area during deposition of sub-unit 312, which shows minimal lateral changes in the paleo-shoreline (Figure 7.1D). Increased sandstone deposition in the northeast (primarily recorded at the Ben Nevis I-45 well) may indicate introduction of a coarse-grained sediment source northeast of the study area, but no firm data suggest a new sediment provenance. The relative rapid lateral transition from sandstone to shale deposition may represent progradation of the paleo-shoreline into relatively deep water with the seafloor below wave base (a steep depositional slope). The slope would have been reduced through deposition of sub-unit 310, allowing sandstone deposition to shift further basinward during deposition of sub-unit 312.

Increased displacement along the Doter, Prise and Jinker faults created abundant accommodation space across the study area, forming a north-south oriented paleo-valley, during deposition of sub-unit 320 (Figure 7.1E). Abundant accommodation space was possibly filled with coastal plain shales and channel sandstones which transported coarse-grained siliciclastic sediment further north, representing a forward-stepping shoreline, relative to sub-unit 312. Here it is important to note that the orange area in Figure 7.1E represents the interbedded sandstone and shale of coastal plain

deposits rather than upper to mid-shoreface deposits. Near the end of deposition of sub-unit 320, sedimentation rates may have been reduced or tectonic activity increased forcing the paleo-shoreline to backstep to the south, which is recorded by the widespread sandstone bed at the top of sub-unit 320. This increase in tectonic activity (faulting) may represent a relative rise in sea-level. This regional flooding surface marks the top of the Lower Hibernia Member and separates it from the overlying Upper Hibernia Member.

Increased displacement along the major faults in the study area continued through deposition of sub-unit 322, which further steepened the depositional slope and prohibited any major progradation of coarse-grained clastic deposition into the basin, restricting it to the basin margins (Figure 7.1F). Increased shale deposition in the west also suggests a steepened depositional slope (seafloor below wave base) combined with decreased coarse-grained clastic input. The paleo-shoreline of sub-unit 322 was restricted to the southeast corner of the study area and suggests the predominant sediment provenance was to the southeast, possibly from the platform east of the Voyager Fault System. Overall the progradation direction appears to be from east to west based on the north-south trending percent sandstone contours.

Dominantly northwest progradation of the siliciclastic paleo-shoreline was established during deposition of sub-unit 324 as coarse-grained sedimentation increased and reduced the depositional slope allowing coarse-grained clastic sediment to be transported further westward (Figure 7.1G). Displacement along the major faults continued during deposition of sub-unit 324, however, the rate of accommodation space generated was less than sediment flux allowing the siliciclastic paleo-shoreline to prograde to the northwest by tens of kilometers.

Maximum progradation of the siliciclastic paleo-shoreline occurred during deposition of sub-unit 326 as a thick unit of high percent sandstone was deposited across the entire study area (Figure 7.1H). Thickness variations across the major faults are minimal and possibly masked by incision of sub-unit 326 into the underlying sub-unit 324 across most of the East Flank and Graben, which is suggested by anomalously thick deposits of sub-unit 326 in regions that correspond to areas of thin deposition of sub-unit 324. This incision may have been initiated by increased displacement along the northern regions of the Jinker and Mauzy faults, which may have uplifted the East Flank region allowing erosion of sub-unit 324 and infill with sub-unit 326 during subsequent deposition.

It was near this time that tectonic activity likely began to cease, albeit not entirely, initiating the waning of the North Atlantic Rifting Phase (see Chapter 3) and gradual shift to basin stability and post-rift sedimentation. Coarse-grained siliciclastic input began to diminish during deposition of sub-unit 328 (Figure 7.1I) causing back-stepping of the paleo-shoreline to the south. Further clockwise rotation of the shoreline orientation is noted as the percent sandstone contours have an east-west trend suggesting sandstone progradation to the north (ninety degree shift from sub-unit 322). Recovered core from the Hebron I-13 and M-04 wells record the distal depositional history for sub-unit 328 in detail, as these wells are located north of the paleo-shoreline. Waning fault activity and coarse-grained sedimentation is supported through the sedimentary structures and trace fossil assemblages present in these cores. Well-sorted, low-angle cross-laminated, sandstones support a strong wave-influence in the re-working of deposits, which are punctuated by sharp-based grainstone beds, likely the result of storm events. Grainstone beds are composed of serpulid and mollusc shell fragments possbily sourced

from shell-serpulid banks along the margins of tidal inlets or channels, which are damaged or destroyed during storm events. Sharp-based coarse-grained sandstone beds (two to six centimeters thick) within an overall fining-upwards sequence suggest discrete influxes of coarse sediment possibly caused by storms or minor fault activity in the region. These beds become less abundant up-section representing the waning stages of fault activity. Conversely, grainstone beds become increasingly more common up-section supporting the decreasing siliciclastic input and gradual shift towards carbonate deposition.

The transition continues through deposition of sub-unit 330 (Figure 7.1J), which marks the final depositional stage of the Upper Hibernia Member, at the top of the Hibernia Formation. Depositional slope was at a minimum during deposition of sub-unit 330 and siliciclastic deposition was nearing an end, which is supported by the thin nature of sub-unit 330 when compared to sub-unit 328. Shoreline orientation rotates slightly clockwise as the western paleo-shoreline forward-steps north of the study area, while the eastern paleo-shoreline back-steps slightly to the south. This could be due to minor changes in subsidence patterns as the rate of sedimentation outpaces accommodation space in the west and vice versa towards the east, possibly due to increased displacement along the northern regions of the Prise and Doter faults.

Following deposition of the Upper Hibernia Member, siliciclastic sedimentation ceased and shifted to widespread carbonate deposition of the 'B' Marker limestone. Post-rift deposition is marked by this limestone, which suggests a period of basin stability without siliciclastic deposition. Deposition of sub-units 328 and 330 record the gradual shift from syn-rift to post-rift deposition. This gradual change in tectonic environments is best recorded in the Hebron M-04 core (Chapter 5) which recovered

continuous core across the 'B' Marker limestone and Upper Hibernia Member contact. Multiple beds of grainstone and rudstone carbonate deposits exist throughout sub-units 328 and 330 that contain clasts up to thirty centimeters in diameter. These large clasts could not have been transported over long distances and therefore likely represent storm deposits or renewed siliciclastic deposition following a short-period of basin stability in which localized carbonate banks were beginning to develop north of the siliciclastic paleo-shoreline. These carbonate beds become more common up-section and suggest the waning of the North Atlantic Rifting Phase and increasing basin stability. Deposition of the 'B' Marker limestone marks the end of siliciclastic deposition and prolonged onset of post-rift thermal subsidence and subsequent carbonate deposition across the study area and entire Jeanne d'Arc Basin.

7.2 FUTURE WORK

To further enhance the interpretation of the existing three-dimensional seismic dataset, seismic inversion for reservoir parameters is likely the most effective method to extract additional information. The high quality seismic that was recorded could also be improved through new methods of processing made available in the past twelve years since the seismic was acquired (i.e. improved depth migration or pre-stack time migration). For the purpose of this thesis the seismic dataset was used primarily to determine the structural setting of the Hibernia Formation and look for gross geometrical relationships. Petrophysical well data and core data could be combined with the seismic dataset to produce a working statistical reservoir model that could further predict the reservoir parameters of the individual sub-units across the study area. This model would contain the structural information of the seismic dataset and would allow determination

of potential hydrocarbon accumulations based on modern-day structure and fault juxtaposition of reservoirs. Available core data across the study area is very limited and much better coverage is required, particularly in the southern region of the study area where no cored intervals exist. The only cored intervals are sub-unit 308 (West Bonne Bay C-23), sub-unit 328 (Hebron I-13 and M-04) and sub-unit 330 (Hebron M-04), therefore additional cores should target the intervals that have not been cored. This would allow refining of the depositional model, reduce the uncertainty of extrapolations from presently cored wells, and better constrain sandstone distribution patterns, in- and outside the study area. Finally, detailed interpretation and mapping of sedimentary log facies to possibly further sub-divide the Hibernia Formation into correlative sub-units, must also be calibrated with additional cored intervals.

REFERENCES:

Note: C-NLOPB represents Canada-Newfoundland and Labrador Offshore Petroleum Board.

Adams, J.A.S. and Weaver, C.E., 1958, Thorium to Uranium ratios as indicators of sedimentary processes: Example of the concept of geochemical facies. American Association of Petroleum Geologists, Bulletin 42, pp. 387-430.

Angelier, J., 1985, Extension and rifting: the Zeit region, Gulf of Suez. Journal of Structural Geology, v. 7, pp. 605-612.

Brown, D.M., 1985, Sedimentology of the Upper Jurassic – Lower Cretaceous Hibernia Member of the Missisauga Formation in the Hibernia Oil Field, Jeanne d'Arc Basin. M.Sc. Thesis, Carleton University, 78 pp. C-NLOPB Project Number: 8934-C121-1E.

Brown, D.M., McAlpine, K.D., and Yole, R.W., 1989, Sedimentology and sandstone diagenesis of Hibernia formation in Hibernia oil field, Grand Banks of Newfoundland. American Association of Petroleum Geologists, Bulletin 73, pp. 557–575.

Canada-Newfoundland and Labrador Offshore Petroleum Board (C-NLOPB), 2005, Offshore Schedule of Wells. St John's, NL. http://www.cnlopb.nl.ca/.

Crimes, T.P., Goldring, R., Homewood, P., van Stuijvenberg, J. and Winkler, W., 1981, Trace fossil assemblages of deep-sea fan deposits, Grunigel and Schlieren flysch (Cretaceous-Eocene, Switzerland). Ecolgae Geologicae Helvetiae, v. 74, pp. 953-995.

Enachescu, M.E., 1987, Tectonic and structural framework of the northeast Newfoundland continental margin. *In:* Sedimentary Basins and Basin-forming Mechanisms, C. Beaumont and A.J. Tankard (eds.). Canadian Society of Petroleum Geologists, Memoir 12, pp. 117-146.

Enachescu, M.E., 1988, Extended basement beneath the intracratonic rifted basins of the Grand Banks of Newfoundland. Canadian Journal of Exploration Geophysics, v. 24, pp. 48-65.

Enachescu, M.E. 1992, Basement extension on the Newfoundland continental margin (Canadian east coast). *In:* Basement Tectonics 7, R. Mason (ed.). Kluwer Academic Publishers, Netherlands, pp. 227-256.

Enachescu, M. and Fagan, P., 2004, Newfoundland and Labrador Call for Bids NF04-01. Government of Newfoundland and Labrador, Department of Natural Resources, 35 pp. http://www.nr.gov.nl.ca/mines&en/oil/call_for_bids_nf04_01.stm

Fitzgerald, C.E., 1987, Deposition and diagenesis of the Hibernia Member, Jeanne d'Arc Basin, offshore Newfoundland. M.Sc. Thesis, Dalhousie University, 140 pp. C-NLOPB Project Number: 8934-D14-1E.

Gibbs. A.D., 1983, Balanced cross-section construction from seismic sections in areas of extensional tectonics: Journal of Structural Geology, v. 5, pp. 153-160.

Gibbs, A.D., 1984, Structural evolution of extensional basin margins. Journal of Geological Society of London, v. 141, pp. 609-620.

Gower, S., 1988, Hibernia Formation in the Jeanne d'Arc Basin. C-NLOPB Released Geophysical and Geological Reports: GL-CNOPB-1988-05, 48 pp.

Grant, A.C. and McAlpine, K.D., 1990, The continental margin around Newfoundland. *In*: Geology of the Continental Margins of Eastern Canada, M.J. Keen and G.L. Williams (eds.). Geological Survey of Canada, Geology of Canada, no. 2, pp. 239-292.

Grant, A.C., McAlpine, K.D., and Wade, J.A., 1986, The continental margin of eastern Canada – Geological framework and petroleum potential. *In:* Future Petroleum Provinces of the World, M.T. Halbouty (ed.). American Association of Petroleum Geologists, Memoir 40, pp. 177-206.

Jansa, L.F. and Pe-Piper, G., 1986, Geology and Geochemistry of middle Jurassic and early Cretaceous igneous rocks on the eastern North American continental shelf. Geological Survey of Canada, Open File Report No. 1351, 104p.

Ma, X.Q. and Kusznir, N.J., 1993, Modelling of near-field subsurface displacements for generalized faults and fault arrays. Journal of Structural Geology, v.15, pp. 1471-1484.

McAlpine, K.D., 1990, Mesozoic stratigraphy, sedimentary evolution, and petroleum potential of the Jeanne d'Arc Basin, Grand Banks of Newfoundland. Geological Survey of Canada Paper 89-17, 50 pp.

NACSN (North American Commission on Stratigraphic Nomenclature), 2005, North American Stratigraphic Code. American Association of Petroleum Geologists, Bulletin 89, pp. 1547-1591.

Pemberton, S.G., Spila, M., Pulham, A.J., Saunders, T., MacEachern, J.A., Robbins, D. and Sinclair, I.K., 2001, Ichnology and Sedimentology of Shallow to Marginal Marine Systems: Ben Nevis & Avalon Reservoirs, Jeanne d'Arc Basin. Geological Association of Canada, Short Course Notes 15, St. John's, Canada, 343 pp.

Ricker, N., 1953, The Form and Laws of Propagation of Seismic Wavelets. Geophysics, v. 18, pp. 10-40.

Rider, M., 1996, The Geological Interpretation of Well Logs. Gulf Publishing Company, Houston, 280 pp.

Saito, Y., 2005, Beach Stratigraphy. *In:* Encyclopedia of Coastal Science, Schwartz, M. (ed.), Springer, pp. 179-181.

Sinclair, I.K., 1988, Evolution of Mesozoic-Cenozoic sedimentary basins in the Grand Banks area of Newfoundland and comparison with Falvey's (1974) rift model. Canadian Society of Petroleum Geologists, Bulletin 36, pp. 255-273.

Sinclair, I.K. 1993. Tectonism: the dominant factor in mid-Cretaceous deposition in the Jeanne d'Arc Basin, Grand Banks. Marine and Petroleum Geologists, v. 10, pp. 530-549.

Sinclair, I.K., 1995a, Sequence stratigraphic response to Aptian-Albian rifting in conjugate margin basins: a comparison of the Jeanne d'Arc Basin, offshore Newfoundland and the Porcupine Basin, offshore Ireland. *In:* The Tectonics, Sedimentation and Palaeoceanography of the North Atlantic Region, R.A. Scrutton, M.S. Stoker, G.B. Shimmeld and A.W. Tudhope (eds.). Geological Society of London, Special Publication 90, pp. 29-49.

Sinclair, I.K., 1995b, Transpressional inversion due to episodic rotation of extensional stresses in the Jeanne d'Arc Basin, offshore Newfoundland. *In:* Basin Inversion, J.G. Buchanan and P.G. Buchanan (eds.). Geological Society of London, Special Publication 88, pp. 249-271.

Sinclair, I.K., Churchill, I.D. and Mclean, J.J., 2005, Oblique deformation during rifting in the Jeanne d'Arc Basin: examples and timing. CSPG/GAC-MAC Conference, Abstract.

Tankard, A.J., 1990, Extensional basin styles in exploration. Grand Banks of Newfoundland (Eastern Canada), The potential of deep seismic profiling for hydrocarbon exploration, pp. 219-223.

Tankard, A.J. and Welsink, H.J., 1987, Extensional tectonics and stratigraphy of Hibernia oilfield, Grand Banks, Newfoundland. American Association of Petroleum Geologists, Bulletin 71, pp. 1210-1232.

Tankard, A.J. and Welsink, H.J., 1988, Extensional tectonics and stratigraphy of the Mesozoic Grand Banks of Newfoundland. *In:* Triassic-Jurassic Rifting: Continental Breakup and the Origin of the Atlantic Ocean and Passive Margins, Part A, W. Manspeizer (ed.). Developments in Geotectonics 22, Elsevier, Amsterdam, pp. 129-165.

Walsh, J.J. and Watterson, J., 1988, Analysis of the relationship between displacements and dimensions of faults. Journal of Structural Geology, v.10, pp. 239-247.

Watterson, J., 1986, Fault dimensions, displacement, and growth. Pure and Applied Geophysics, v.124, pp. 365-373.

Wernicke. B., 1981, Low-angle normal faults in the Basin and Range Province: nappe tectonics in an extending orogen. Nature, v. 291, pp. 645-648.

Williamson, M.A., 1992, The subsidence, compaction, thermal and maturation history of the Egret Member source rock, Jeanne d'Arc Basin, offshore Newfoundland. Canadian Society of Petroleum Geologists, Bulletin 40, pp. 136-150.

APPENDIX A

Detailed Core Log and Core Photos

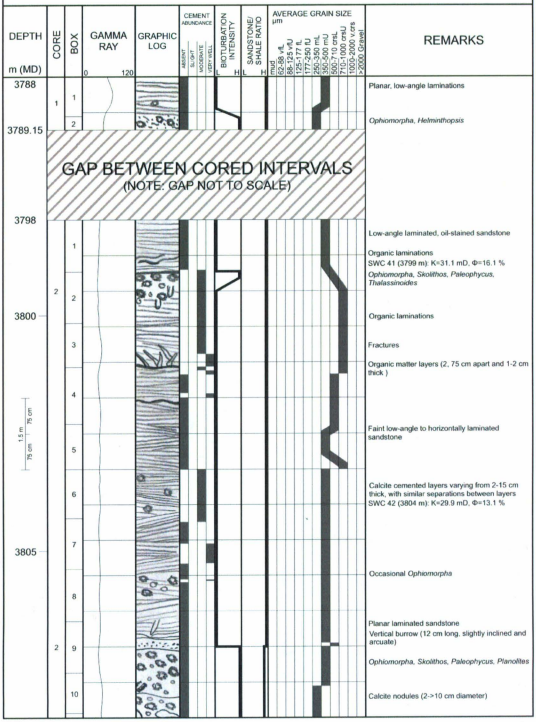
Amoco et al. West Bonne Bay C-23 Well

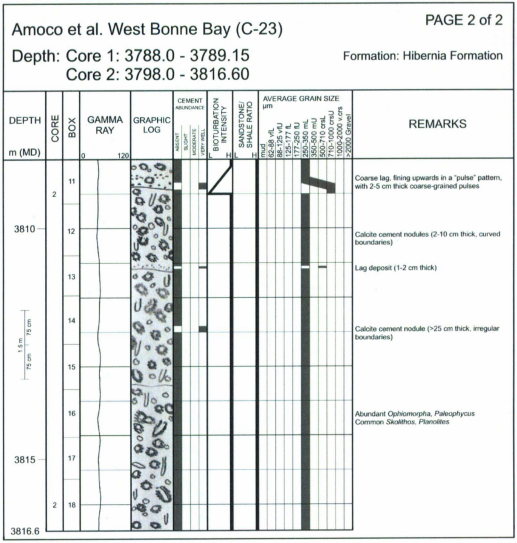
Detailed Core Log

Amoco et al. West Bonne Bay (C-23)

Depth: Core 1: 3788.0 - 3789.15
Core 2: 3798.0 - 3816.60

Formation: Hibernia Formation





Detailed log of the Amoco et al. West Bonne Bay (C-23) well core recovered over the Hibernia Formation. Depth is measured depth in meters. Graphic log is NOT to scale and is a series of photographs chosen to represent the present facies or depositional or structural characteristics that are visible in the core. Cement abundance refers to the amount of calcite cement that is found in the core and has been tested with HCl acid. Bioturbation Intensity refers to the relative abundance of trace fossils and the extent to which the sedimentary structures have been preserved ranging from a low to high relative intensity. Low intensity refers to none or rarely present trace fossils in which the sedimentary structures are easily recognizable where present. High intensity refers to the presence of an abundance of trace fossils in which the sedimentary structures are no longer distinguishable. Sandstone/shale ratio refers to the relative ratio of sandstone and shale ranging from a low sandstone abundance to a high sandstone abundance. Average grain size is the average or predominant grain size that is present in the core. Remarks are short descriptions of characteristic properties of the core that are irrelevant to the preceding columns of information. These will include present sedimentary structures, types of trace fossils, details of Sidewall Core (SWC) analysis, and other diagnostic properties of the core. The detailed facies description and interpretation of depositional environments can be found in Chapter 5.

Core Photographs

Note: The core photographs are presented from top to bottom. The West Bonne Bay C-23 core is approximately 9 centimeters wide. Each photograph has top of core in the upper right and bottom of core in lower left.



Core 1: Box 1 (right) and Box 2 (left)



Core 2: Box 1 (right) and Box 2 (left)



Core 2: Box 3 (right) and Box 4 (left)



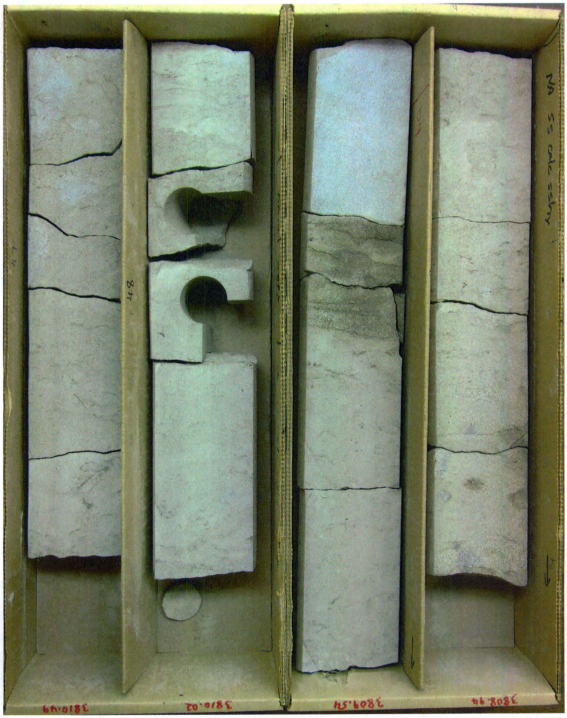
Core 2: Box 5 (right) and Box 6 (left)



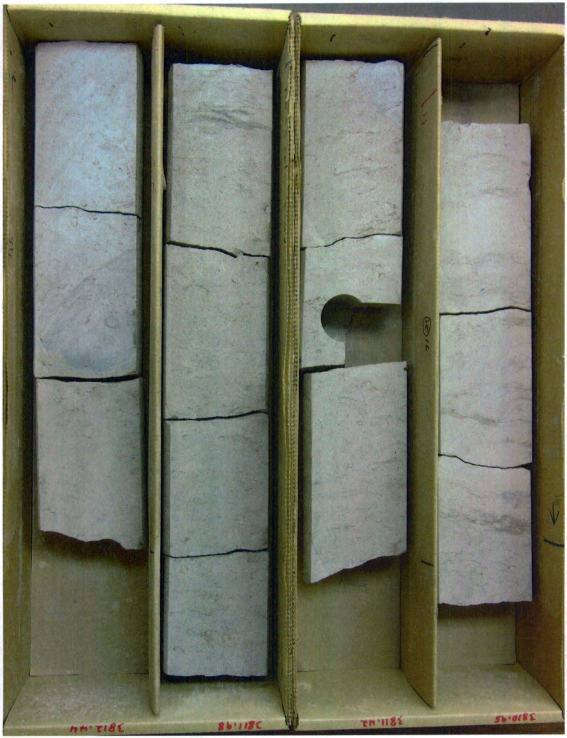
Core 2: Box 7 (right) and Box 8 (left)



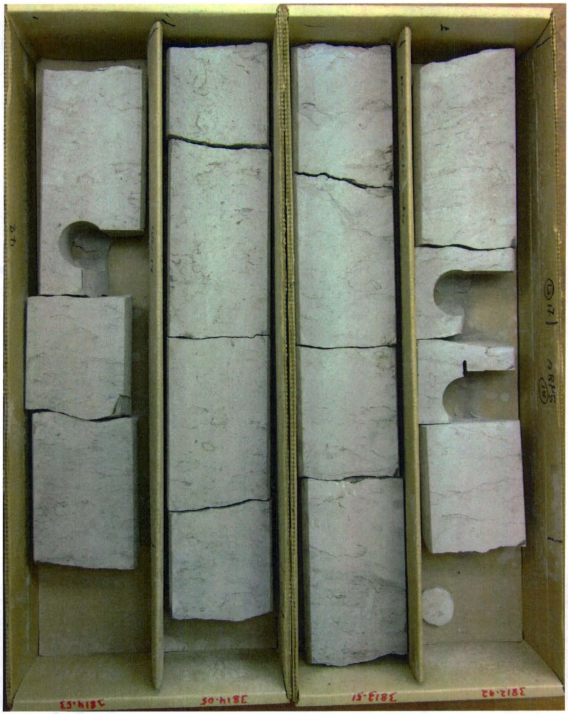
Core 2: Box 9 (right) and Box 10 (left)



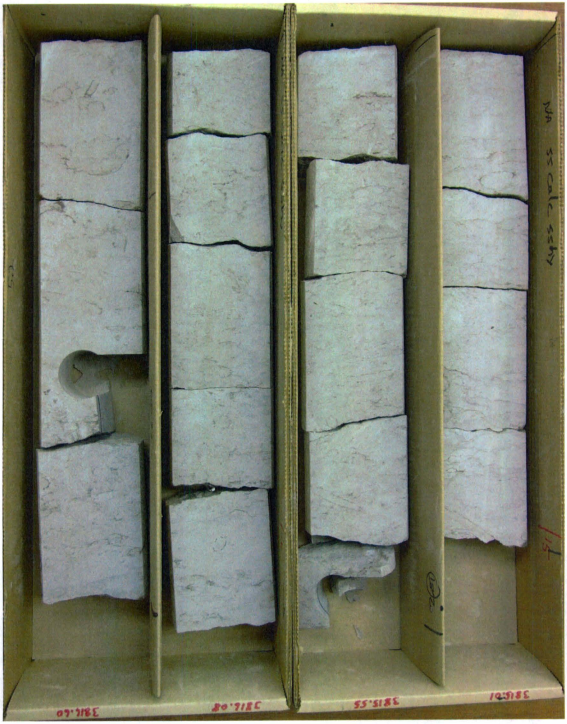
Core 2: Box 11 (right) and Box 12 (left)



Core 2: Box 13 (right) and Box 14 (left)



Core 2: Box 15 (right) and Box 16 (left)



Core 2: Box 17 (right) and Box 18 (left)

APPENDIX B

Detailed Core Log and Core Photos

Mobil et al. Hebron I-13 Well

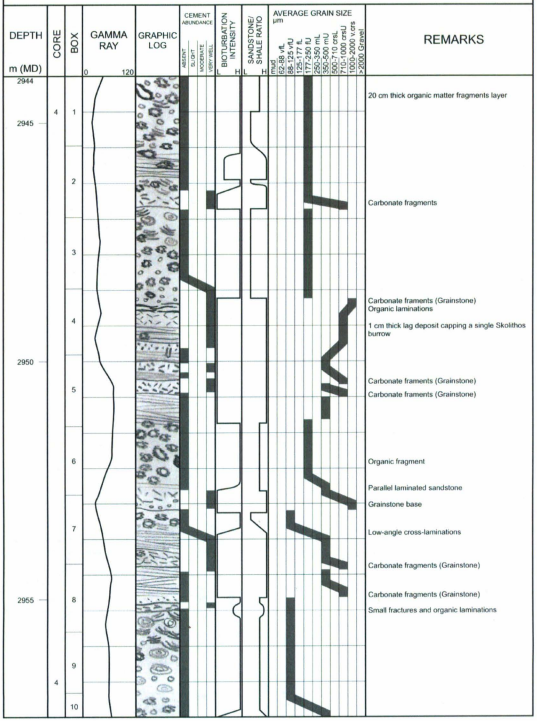
Detailed Core Log

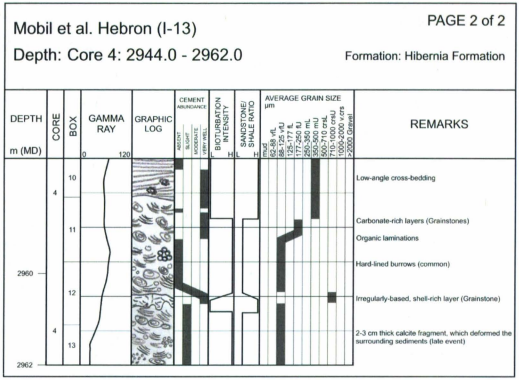
Mobil et al. Hebron (I-13)

PAGE 1 of 2

Depth: Core 4: 2944.0 - 2962.0

Formation: Hibernia Formation





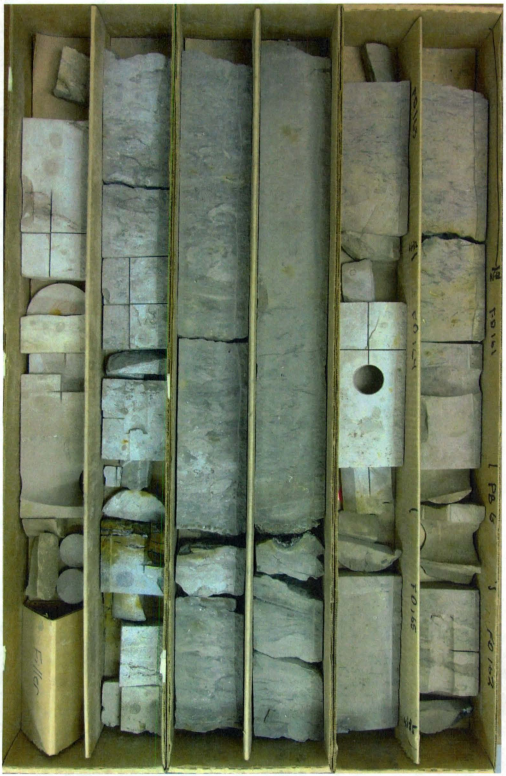
Detailed log of the Mobil et al. Hebron (I-13) well core recovered over the Hibernia Formation. Depth is measured depth in meters. Graphic log is NOT to scale and is a series of photographs chosen to represent the present facies or depositional or structural characteristics that are visible in the core. Cement abundance refers to the amount of calcite cement that is found in the core and has been tested with HCl acid. Bioturbation Intensity refers to the relative abundance of trace fossils and the extent to which the sedimentary structures have been preserved ranging from a low to high relative intensity. Low intensity refers to none or rarely present trace fossils in which the sedimentary structures are easily recognizable where present. High intensity refers to the presence of an abundance of trace fossils in which the sedimentary structures are no longer distinguishable. Sandstone/shale ratio refers to the relative ratio of sandstone and shale ranging from a low sandstone abundance to a high sandstone abundance. Average grain size is the average or predominant grain size that is present in the core. Remarks are short descriptions of characteristic properties of the core that are irrelevant to the preceding columns of information. These will include present sedimentary structures, types of trace fossils, details of Sidewall Core (SWC) analysis, and other diagnostic properties of the core. The detailed facies description and interpretation of depositional environments can be found in Chapter 5.

Core Photographs

Note: The core photographs are presented from top to bottom. The Hebron 1-13 core is approximately 6.5 centimeters wide. Each photograph has top of core in the upper right and bottom of core in lower left.



Core 4: Box 1



Core 4: Box 2 (right), Box 3 (center), and Box 4 (left)



Core 4: Box 5 (right), Box 6 (center), and Box 7 (left)



Core 4: Box 8 (right), Box 9 (center), and Box 10 (left)



Core 4: Box 11 (right), Box 12 (center), and Box 13 (left)

APPENDIX C

Detailed Core Log and Core Photos

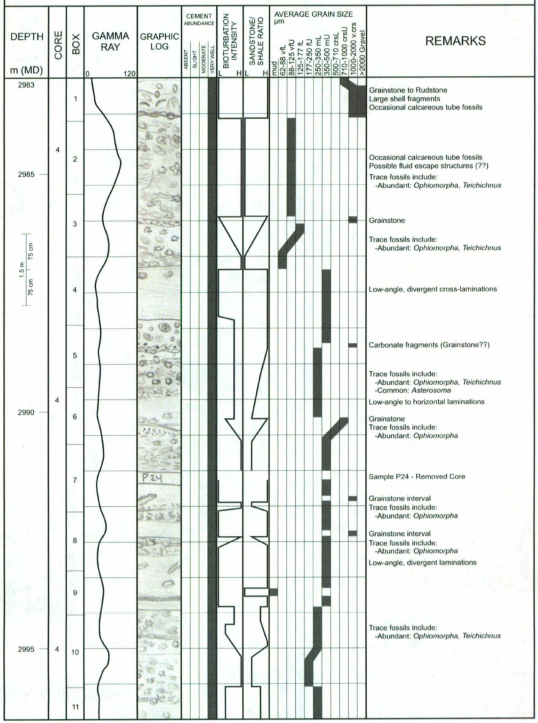
Chevron et al. Hebron M-04 Well

Detailed Core Log

Chevron et al. Hebron (M-04)

Depth: Core 3: 2983.0 - 3093.60

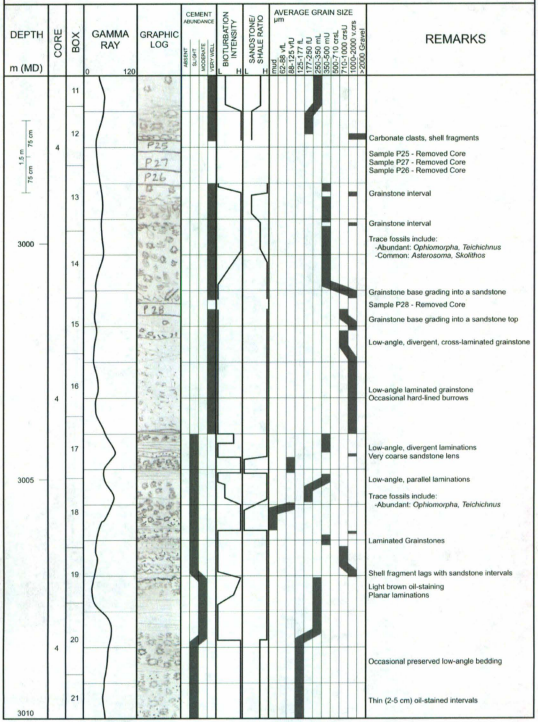
Formations: Catalina Formation (<2991 m MD)
Hibernia Formation (>2991 m MD)



Chevron et al. Hebron (M-04)

Depth: Core 3: 2983.0 - 3093.60

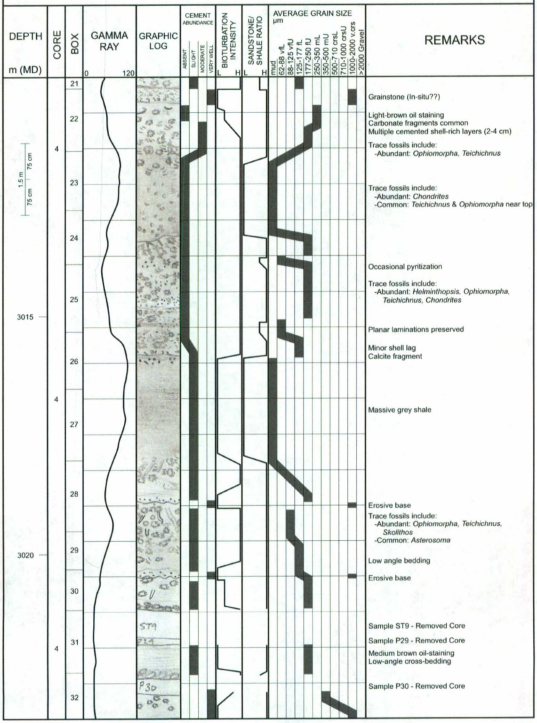
Formations: Catalina Formation (<2991 m MD)
Hibernia Formation (>2991 m MD)



Chevron et al. Hebron (M-04)

Depth: Core 3: 2983.0 - 3093.60

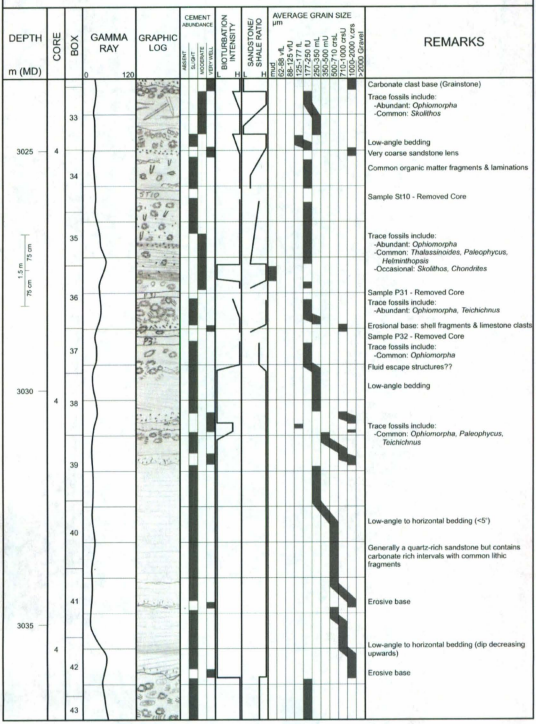
Formations: Catalina Formation (<2991 m MD)
Hibernia Formation (>2991 m MD)



Chevron et al. Hebron (M-04)

Depth: Core 3: 2983.0 - 3093.60

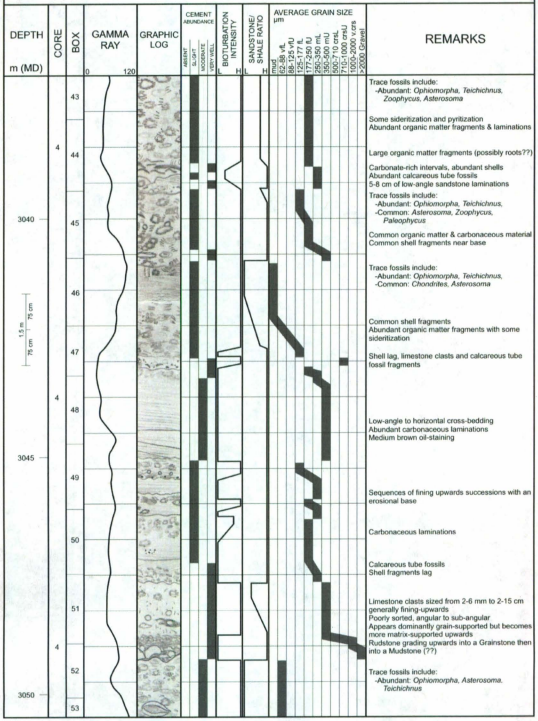
Formations: Catalina Formation (<2991 m MD)
Hibernia Formation (>2991 m MD)



Chevron et al. Hebron (M-04)

Depth: Core 3: 2983.0 - 3093.60

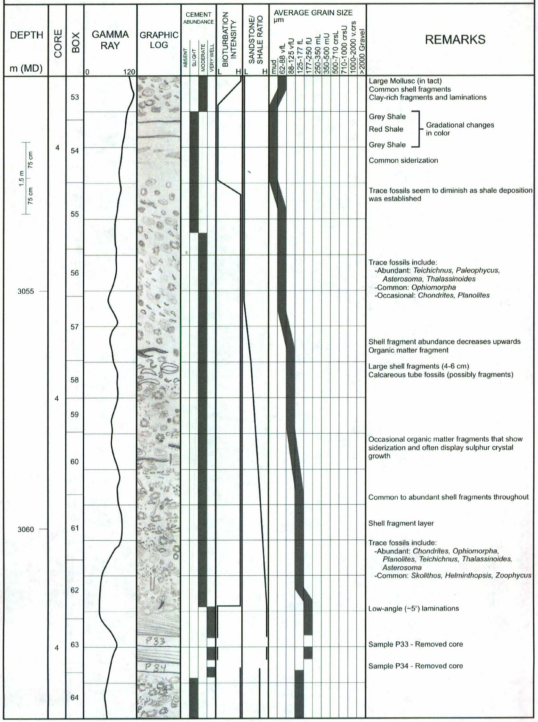
Formations: Catalina Formation (<2991 m MD)
Hibernia Formation (>2991 m MD)



Chevron et al. Hebron (M-04)

Depth: Core 3: 2983.0 - 3093.60

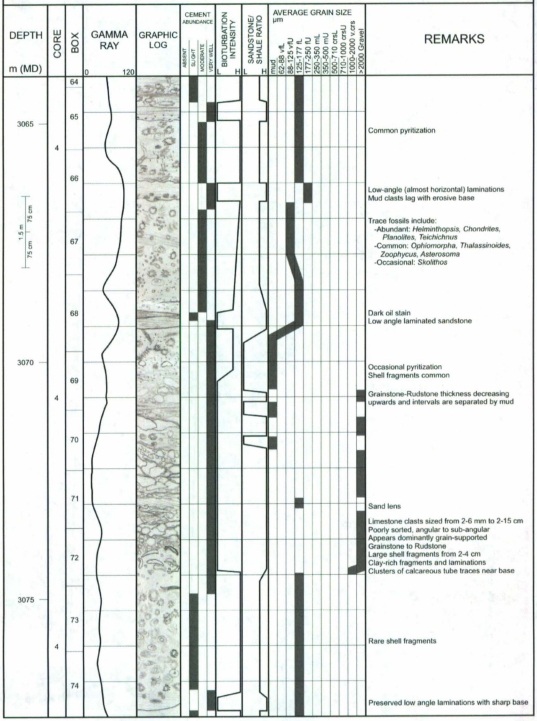
Formations: Catalina Formation (<2991 m MD)
Hibernia Formation (>2991 m MD)



Chevron et al. Hebron (M-04)

Depth: Core 3: 2983.0 - 3093.60

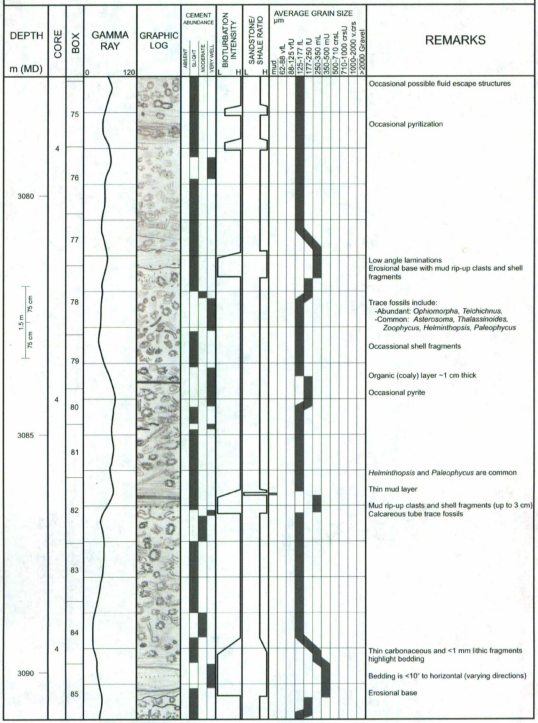
Formations: Catalina Formation (<2991 m MD)
Hibernia Formation (>2991 m MD)

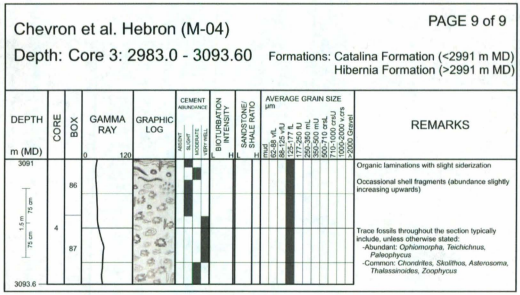


Chevron et al. Hebron (M-04)

Depth: Core 3: 2983.0 - 3093.60

Formations: Catalina Formation (<2991 m MD)
Hibernia Formation (>2991 m MD)

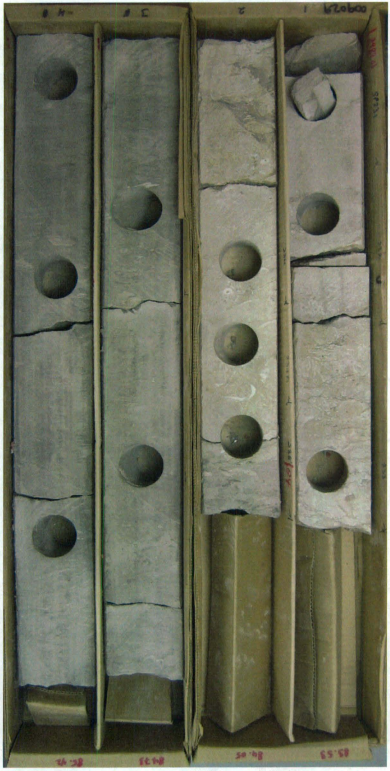




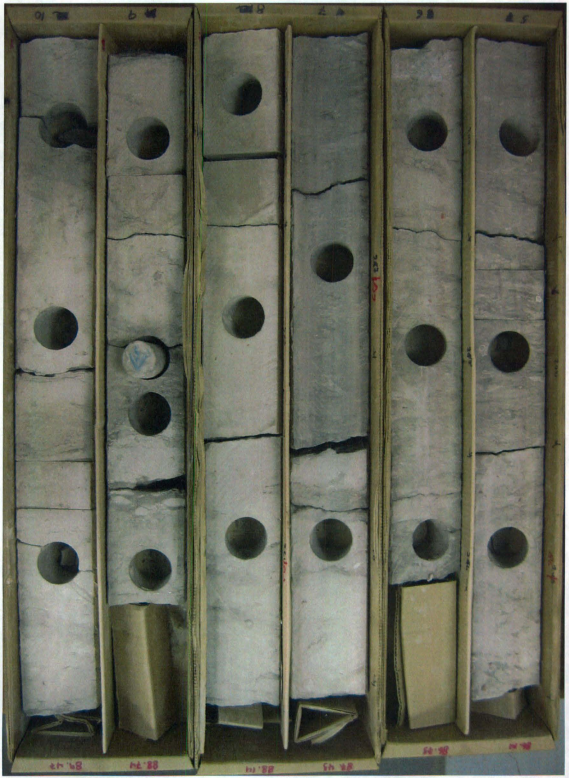
Detailed log of the Chevron et al. Heborn (M-04) well core recovered over the Hibernia Formation. Depth is measured depth in meters. Graphic log is NOT to scale and is a series of photographs chosen to represent the present facies or depositional or structural characteristics that are visible in the core. Cement abundance refers to the amount of calcite cement that is found in the core and has been tested with HCl acid. Bioturbation Intensity refers to the relative abundance of trace fossils and the extent to which the sedimentary structures have been preserved ranging from a low to high relative intensity. Low intensity refers to none or rarely present trace fossils in which the sedimentary structures are easily recognizable where present. High intensity refers to the presence of an abundance of trace fossils in which the sedimentary structures are no longer distinguishable. Sandstone/shale ratio refers to the relative ratio of sandstone and shale ranging from a low sandstone abundance to a high sandstone abundance. Average grain size is the average or predominant grain size that is present in the core. Remarks are short descriptions of characteristic properties of the core that are irrelevant to the preceding columns of information. These will include present sedimentary structures, types of trace fossils, details of Sidewall Core (SWC) analysis, and other diagnostic properties of the core. The detailed facies description and interpretation of depositional environments can be found in Chapter 5.

Core Photographs

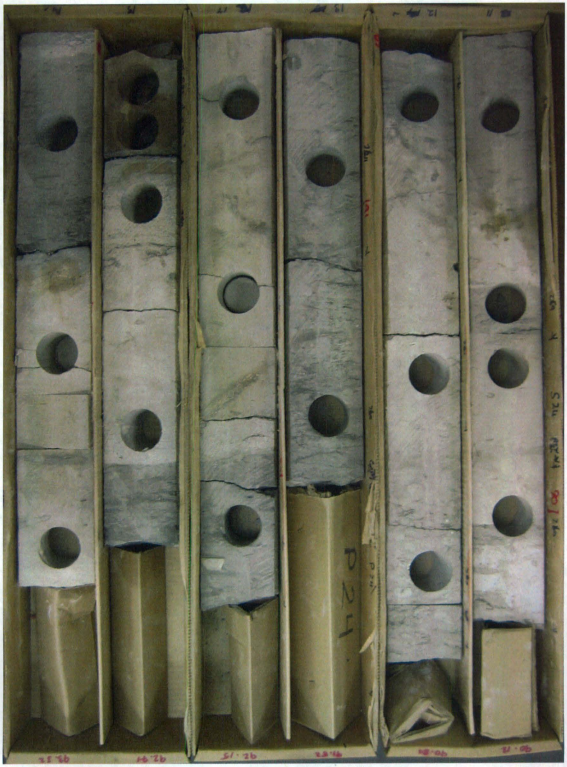
Note: The core photographs are presented from top to bottom. The Hebron M-04 core is approximately 8 centimeters wide. Each photograph has top of core in the upper right and bottom of core in lower left.



Core 3: Box 1 (right) and Box 2 (left)



Core 3: Box 3 (right), Box 4 (center), and Box 5 (left)



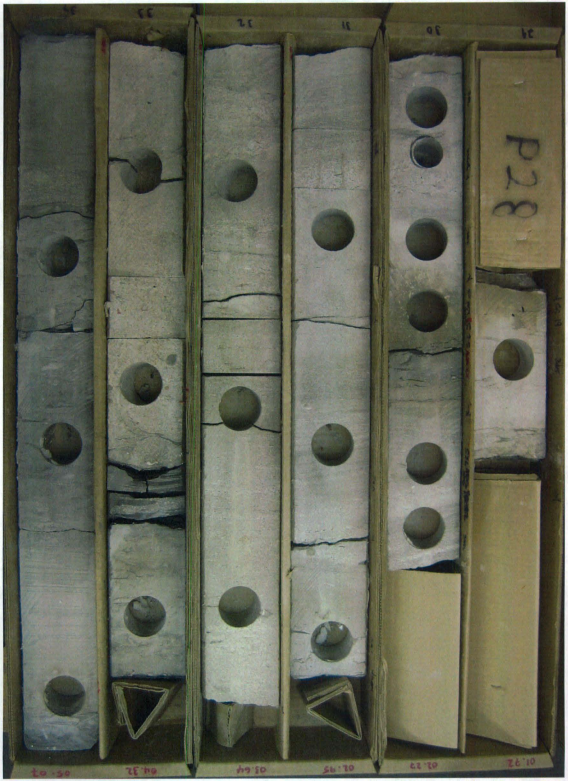
Core 3: Box 6 (right), Box 7 (center), and Box 8 (left)



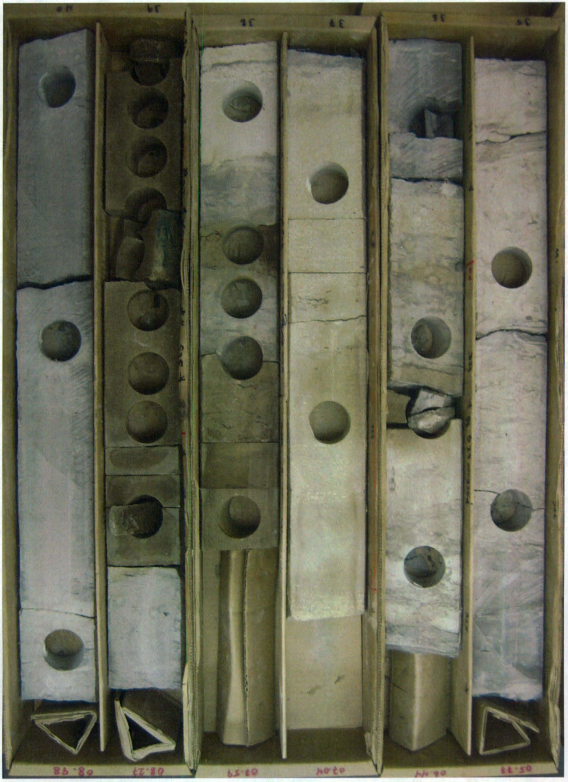
Core 3: Box 9 (right), Box 10 (center), and Box 11 (left)



Core 3: Box 12 (right), Box 13 (center), and Box 14 (left)



Core 3: Box 15 (right), Box 16 (center), and Box 17 (left)



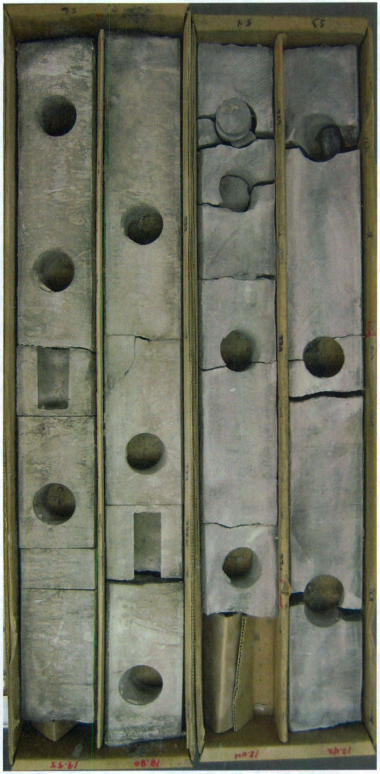
Core 3: Box 18 (right), Box 19 (center), and Box 20 (left)



Core 3: Box 21 (right), Box 22 (center), and Box 23 (left)



Core 3: Box 24 (right), Box 25 (center), and Box 26 (left)



Core 3: Box 27 (right), Box 28 (left)



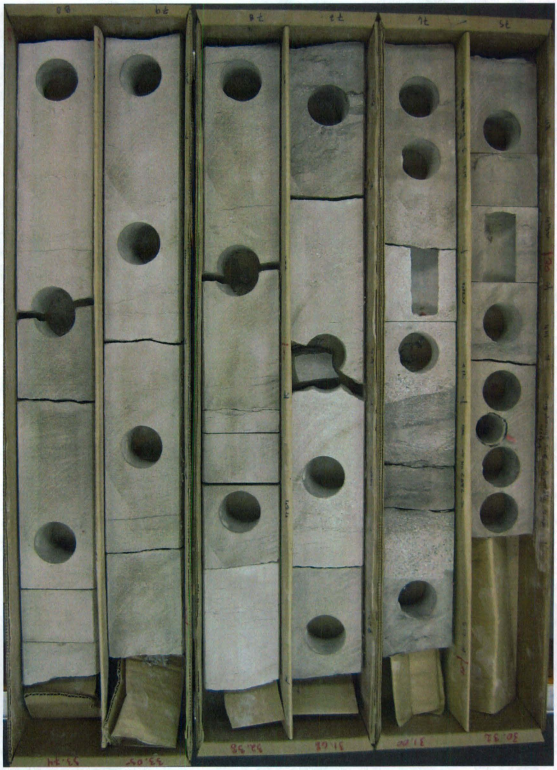
Core 3: Box 29 (right), Box 30 (center), and Box 31 (left)



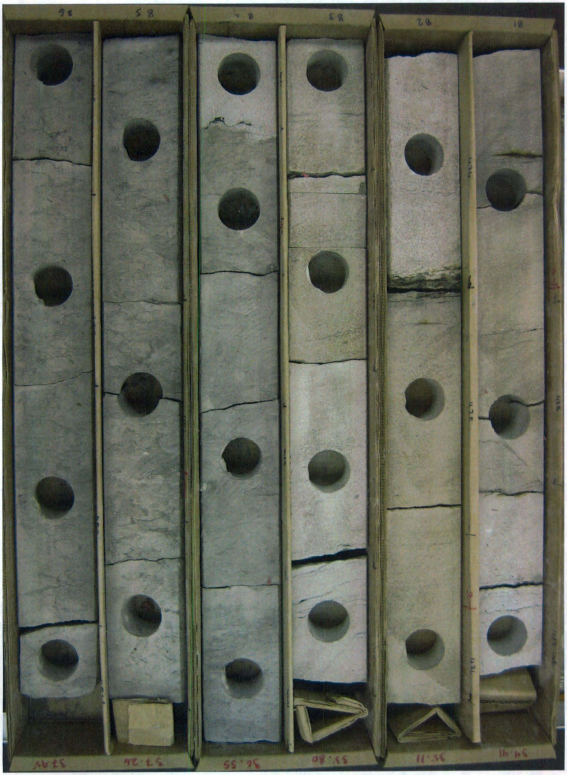
Core 3: Box 32 (right), Box 33 (center), and Box 34 (left)



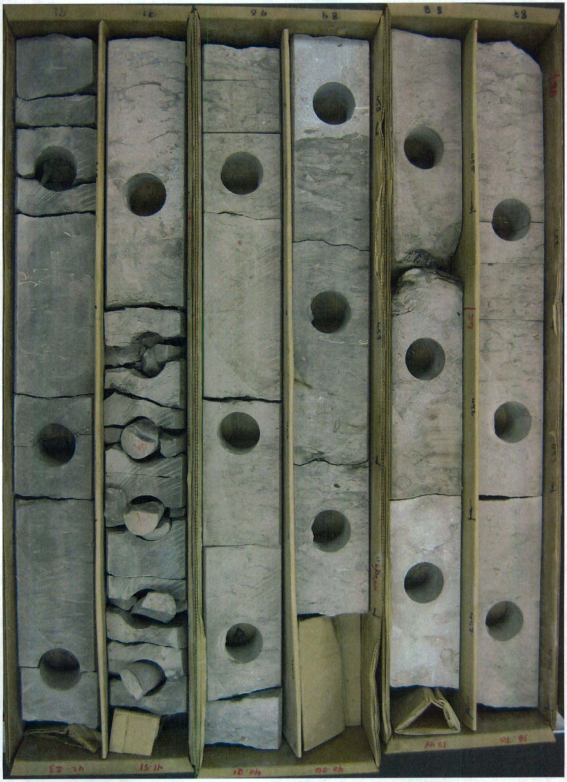
Core 3: Box 35 (right), Box 36 (center), and Box 37 (left)



Core 3: Box 38 (right), Box 39 (center), and Box 40 (left)



Core 3: Box 41 (right), Box 42 (center), and Box 43 (left)



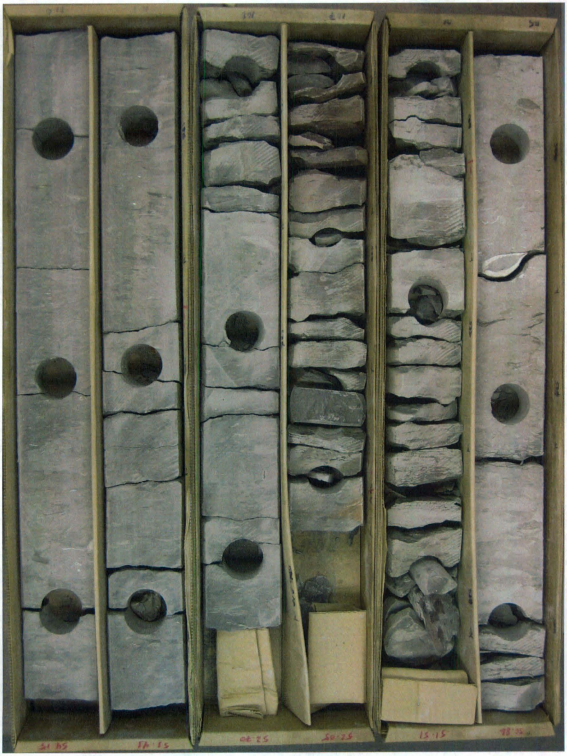
Core 3: Box 44 (right), Box 45 (center), and Box 46 (left)



Core 3: Box 47 (right), Box 48 (center), and Box 49 (left)



Core 3: Box 50 (right), Box 51 (center), and Box 52 (left)



Core 3: Box 53 (right), Box 54 (center), and Box 55 (left)



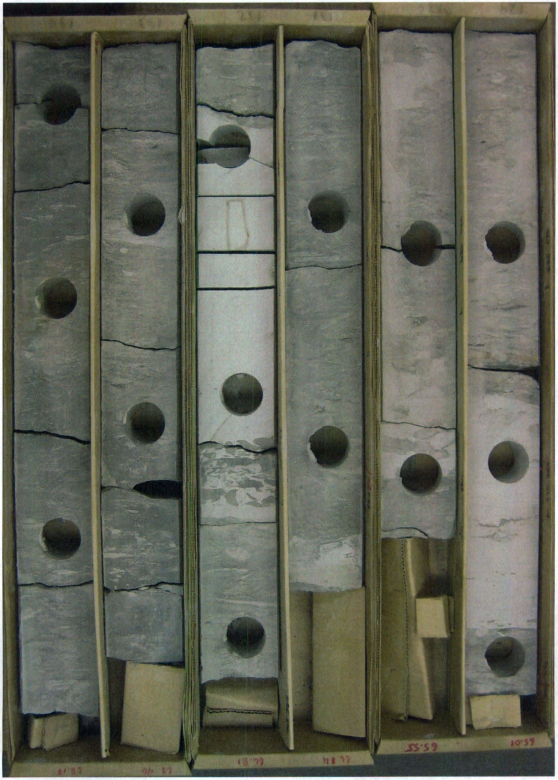
Core 3: Box 56 (right), Box 57 (center), and Box 58 (left)



Core 3: Box 59 (right), Box 60 (center), and Box 61 (left)



Core 3: Box 62 (right), Box 63 (center), and Box 64 (left)



Core 3: Box 65 (right), Box 66 (center), and Box 67 (left)



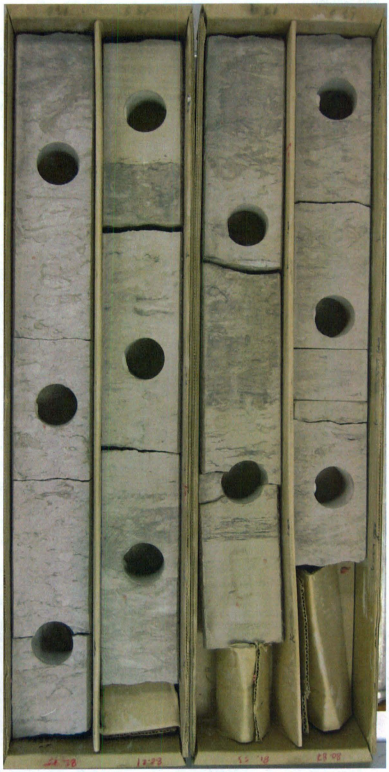
Core 3: Box 68 (right), Box 69 (center), and Box 70 (left)



Core 3: Box 71 (right), Box 72 (center), and Box 73 (left)



Core 3: Box 74 (right), Box 75 (center), and Box 76 (left)



Core 3: Box 77 (right), Box 78 (left)



Core 3: Box 79 (right), Box 80 (center), and Box 81 (left)



Core 3: Box 82 (right), Box 83 (center), and Box 84 (left)



Core 3: Box 85 (right), Box 86 (center), and Box 87 (left)